Development of a Spread Spectrum Based Wireless LAN

A Thesis Submitted to the College of

Graduate Studies and Research

in Partial Fulfillment of the Requirements

for the Degree of

Master of Science

in the

Department of Electrical Engineering

University of Saskatchewan

Saskatoon, Saskatchewan

by

Kirupairaj Asirvatham

Spring 2001

Permission To Use

In presenting this thesis in partial fulfillment of the requirements for a Post-graduate degree from the University of Saskatchewan, I agree that the Libraries of this University may make it freely available for inspection. I further agree that permission for copying of this thesis in any manner, in whole or in part, for scholarly purposes may be granted by the professor or professors who supervised my thesis work or, in their absence, by the Head of the Department or the Dean of the College in which my thesis work was done. It is understood that any copying or publication or use of this thesis or parts thereof for financial gain shall not be allowed without my written permission. It is also understood that due recognition shall be given to me and to the University of Saskatchewan in any scholarly use which may be made of any material in my thesis.

Requests for permission to copy or to make other use of material in this thesis in whole or part should be addressed to:

Head of the Department of Electrical Engineering
University of Saskatchewan
Saskatoon, Saskatchewan, Canada
S7N 0W0

Acknowledgements

I wish to express my sincerest gratitude to Prof. Surinder Kumar for his valuable guidance, supervision and support throughout the course of the work. The technical discussions and guidance were mainly reasons for the successful completion of the thesis.

I will like to take this opportunity to thank Prof. Hugh Wood for his encouragement and positive criticism, which are mainly responsible for the success of the work presented in this thesis.

I wish to acknowledge the technical advice and assistance provided by Prof. Charbel Tannous. I will like to thank I. J. Macphedran for his help and support with the computing facilities. I will like to express my gratitude to the University of Saskatchewan for providing me with the graduate scholarhip.

I will like to thank my family and friends for their encouragement and moral support throughout the course of the Masters program.

Abstract

Wireless LAN products are gaining momentum in the market due to recent technological innovations in circuit devices and packaging, the availability of license–free frequency bands, and the new end–user needs for communication with portable computers. In addition to providing secure communication, long battery life, and ease of management, the wireless LAN devices should be designed to operate in a robust manner. The indoor environment is particularly hostile to radio frequency communication, because of mutipath fading, spatial loss (or distance loss) and shadowing of the receiver. A design of the RF transmitter and receiver should take the deleterious indoor channel into consideration to build a robust wireless LAN product.

The goal of this work was to design a robust transmitter and receiver for wireless LAN products which operate in the indoor environment in the 2.4GHz ISM frequency band. The thesis consisted of two phases. The first phase focused on the study of the wireless LAN products to understand the application and then the indoor environment and analyzed the performance of the optimal receiver. This sets up the background for the design requirements of a robust transceiver design.

The second phase explored the spatial and vertical polarization techniques to achieve diversity reception. The key contribution of the thesis is in the proposal of a neural network based diversity combiner. Simulations studies were conducted which showed that a multilayer feedforward neural network performs close to the optimal receiver for a diversity combiner.

Table Of Contents

List of Figures

List of Abbreviations

AP Access Point

ARQ Automatic Repeat Request

BER Bit Error Rate

BPSK Binary Phase Shift Keying

BSS Basic Service Set

CRC Cyclic Redundancy Check

CSMA/CA Carrier Sense Multiple Access/Collision Avoidance

CSMA/CD Carrier Sense Multiple Access/Collision Detect

CTS Clear To Send

DBPSK Differential Binary Phase Shift Keying

DCF Distributed Control Function

DS Distribution System

DSM Distribution System Medium

DSS Distribution Service Set

DQPSK Differential Quadrature Phase Shift Keying

DSSS Direct Sequence Spread Spectrum

ESS Extended Service Set

FCC Federal Communications Commission

FDM Frequency Division Multiplexing

FHSS Frequency Hopping Spread Spectrum

HP Horizontal Polarization

IEEE Institute of Electrical and Electronic Engineers

IR Infra-red

ISI Inter-Symbol Interference

ISM Industry Science and Medical

LAN Local Area Network

MAC Medium Access Layer

MFNN Multilayer Feed-forward Neural Network

MPDU MAC Protocol Data Unit

NNDC Neural Network Diversity Combiner

OSI Open Systems Interconnection

PCF Point Control Function

PLCP Physical Layer Convergence Procedure

PPDU Physical Protocol Data Unit

RF Radio Frequency

RTS Request To Send

SS Station Services

STA Station

SNR Signal to Noise Ratio

SYNC Synchronization

VP Vertical Polarization

WLAN Wireless Local Area Network

XPD Cross-Polarization Discrimination

Chapter 1

Introduction

1.1 Wireless Local Area Network

A LAN (Local Area Network) is a network of computers, which are linked together with a small geographical area such as a department in a university or an office environment. The users of a LAN typically also share a file server, database server and print servers among others. The computers in a LAN are typically linked through coaxial cables using ethernet technology. Recent technological innovations in circuit devices and packaging, the availability of license–free frequency bands, and the new end–user needs for communication with portable computers have been key factors leading to the introduction of wireless LAN products [7]. The wireless LAN products are expected to alleviate the labour and material costs that are involved in wired networks, whether the medium is coaxial cable or fibre, whether it is for the initial installation or for subsequent re-wiring due to moves, adds, or changes [9] [14] [30]. All wireless LAN products communicate packets over the air, and their programming models and throughput are similar to those of wired LANs.

The purpose of a wireless LAN is the same as that of a wired or optical LAN: to convey packets of information among the devices attached to the LAN. The difference being, wireless LAN attaches portable devices, unlike the wired LAN. A wireless network must satisfy a number of requirements regarding its functionality, capacity, performance, and availability. The wireless LAN product requirements can be listed as follows:

- The portable products must be able to operate worldwide. This requires that the products be license–free.
- The wireless LAN adapters should minimize the drain of portable batteries.

- Wireless transmission uses an unsecured and interference–prone channel, and hence, transmission robustness and security needs should be met.
- The wireless LAN products should be easy to manage and to operate.
- The wireless LAN should be compatible with the wired network in terms of both physical and logical interfaces, functionality and operation.
- Wireless LANs is an emerging technology, and hence it should be flexible to accommodate future needs.

A wireless LAN product that meets the above requirements should lead to a plug–and–play approach that makes the life of the user easier.

Implementation of a wireless LAN under the above requirements requires changes in the data link layer and the physical layer of the open systems interconnection (OSI) reference model. The rest of the layers are left unchanged with the exception of the network layer. The network layer will require changes only if the terminal is moved outside the LAN. For a wireless LAN, the network layer is left unchanged. Before discussing the research objectives, it is instructive to briefly introduce the design choices in the network topology and medium access control (MAC) protocol, and the physical layer alternatives for the wireless LAN.

1.2 Network Topology and Medium Access Control

The function of medium access control is to permit multiple stations to access a shared channel with minimum interference and maximum performance. The available alternatives in access methods are closely related to the current techniques available for wired LANs. Wired LANs use a contention–based access method such as carrier sense multiple access with collision detect (CSMA/CD) or a deterministic access method such as Token–Ring. For a wireless LAN product, the access method can either be contention carrier sense multiple access (CSMA) and time multiplexing- time division multiple access (TDMA). Contention–based protocols allow all the stations in the wireless LAN the same right to access the network, so that the resulting network topology is a peer–to–peer network. With TDMA–based protocols, a base–station is required to assign different time intervals to the various members of the network. Such a topology is called a base–station/remote–station topology.

A base–station/remote–station topology has several advantages because it follows a deterministic access method. The coverage area of the network is deterministic and the presence of a base–station is advantageous for all control functions such as security management, network management, and configuration management. But for wireless networks operating in a strong fading environment, a completely deterministic TDMA access method is not feasible. A station that appears in a TDMA–based network must find an window in order to enter the wireless network. A CSMA–based network on the other hand, will allow the station, a side–door access to the network. CSMA–based network products can easily be implemented with an Ethernet chip set, as opposed to TDMA products, which require the use of a microprocessor. A CSMA–based network can also be formed anywhere without any network planning, as in a board meeting or conference. For these reasons, the IEEE 802 wireless LAN committee chose a peer–to–peer network topology, using CSMA–based access method, to be the standard. Since collisions cannot be detected in a wireless scenario as opposed to the wired scenario, a collision avoidance (CSMA/CA) system is used. In a collision avoidance system, the stations listen for a clear channel before transmitting. The unpredictability of the coverage of the peer–to–peer network topology can be reduced by using the CSMA/CA system with a four–way handshake.

1.3 Physical Layer

A critical question that arises in the implementation of the physical layer of a wireless LAN is the transmission medium to be used. There are two possible alternatives: infrared (IR) and radio frequency (RF) transmission [6]. The IEEE 802 wireless LAN committee has considered both IR and RF for the physical layer implementation. The technology of choice depends on a variety of factors:

- Penetration of the electro–magnetic energy through path obstacles,
- Sensitivity to the positioning of the surrounding objects,
- Multi–network co–existence,
- Ability to allow mobility,
- Regulatory constraints,
- Resistance to multipath propagation, and
- Cost.

A positive feature of IR as a medium technology is the absence of regulation, leading to a lower cost of IR–based products. Their use outdoors is difficult because of the extreme intensity of solar radiation. Their use indoors is also limited as many materials are opaque to IR radiation, leading to incomplete coverage as well as sensitivity to the positioning of nearby objects. IR technology is also limited by the fact that multi–network co–existence is not feasible. In comparison, RF as a medium technology, is unregulated (with some design constraints) when operating in the ISM (industry scientific and medical) frequency band with spread spectrum modulation. This is permissible because spectrum spreading disperses the signal energy over a wide band and different spread spectrum signals can coexist in the same band when orthogonal codes are used in spreading. Compared to IR, RF has better penetration and is less sensitive to the positioning of objects. A spread spectrum technology called the direct sequence spread spectrum permits the use of multipath diversity when multipath propagation occurs, as in an indoor channel.

Spread spectrum based wireless LAN has gained considerable market acceptance since its usage in the ISM band does not need regulatory urgency clearance, and because of its inherent multipath diversity feature, which permits the use of signals arriving from different path in an indoor channel [18] [30]. Hence the wireless modem, discussed in this thesis uses spread spectrum radio for wireless communication.

1.4 Research Objective

There has been considerable interest in the area of wireless LAN by both the research and the industrial communities [10]. The industry led by AT&T has come out with wireless LAN products since 1992 [30]. These products typically work at around 1 Mbps in the 900 MHz ISM band. The data rate has subsequently been extended to 2 Mbps with the radio operating in the higher 2.4 GHz ISM band. Although the data rate has been extended to 2 Mbps, the achievable data throughput is substantially less, because of the time–variant and fading characteristics of the indoor channel. An improved wireless modem that can achieve high data throughput in the harsh indoor environment is thus highly desirable.

In this thesis the IEEE 802 wireless LAN standard (IEEE 802.11) is adhered to [2]. The broad objective of the research was to investigate avenues of improvements in the design of the communication systems within the framework of this wireless LAN standard resulting in higher performance measured in terms of the system bit error rate. Researchers have traditionally used diversity reception and error

control coding to improve the performance. In this thesis the use of quad–diversity consisting of dual space and dual polarisation diversity is proposed and investigated.

The objectives of the research work reported in this thesis thus can be summarised as follows:

1. To study wireless LAN implementation with spread spectrum wireless modem and under the IEEE 802.11 specifications.

2. To model and investigate the impact of diversity reception on the system performance.

3. To study and investigate new implementations of the diversity combiner methods and compare their performance with the known methods.

1.5 Thesis Outline

The thesis is organised into seven chapters including this introductory chapter. In chapter 2, the wireless LAN, including the CSMA/CA multiple access protocol is described. The IEEE 802.11 standard is also described in context of a spread spectrum implementation of the communication system. In Chapter 3, the basics of the spread spectrum technology are reviewed, and the direct sequence spread spectrum technique is described. The indoor channel is also dealt in detail including the various parameters to be considered when designing an indoor wireless communication system. In Chapter 4, the design of the wireless modem radio is discussed and a system with the traditional combiner is analysed. In Chapter 5, the system design alternatives for diversity reception are discussed. A new proposed diversity combining method is described in this chapter. Various receiver models are considered for further evaluation. Chapter 6 contains performance evaluation studies of the wireless modem with the various receiver structures. The results are compared to the traditional diversity combiner. The overall performance of the communication systems is evaluated in terms of the bit error rate. The results obtained are then discussed. Conclusions are presented in Chapter 7.

Chapter 2

The Wireless LAN

In this chapter, the wireless LAN architecture as specified in the IEEE 802.11 standard is discussed. The medium access control (MAC) layer and the physical layer parts of the standard are then discussed in brief.

2.1 Wireless Vs. Wired LANs

Wireless networks have some fundamental characteristics that make them significantly different from the traditional wired LANs. Since one of the requirements of a wireless LAN is to allow mobility, the addressable unit, called a station is a message destination and is not, in general, a fixed location. This is the unlike wired LAN scenario, where an address is equivalent to a physical location. Thus, media (wired or wireless), impacts the design of a LAN in a fundamentally different manner [1] [2] [18] [1]:

1. In a wireless medium the boundary within which conformant transceivers can receive network frames is decided by the indoor channel. Since the indoor channel is dynamic and random, the boundary will change with time. Thus, the wireless medium has no readily observable boundaries. This is unlike the wired media, where, the boundary is well known such that repeaters can be placed strategically.

2. The wireless medium is unprotected from outside signals. Hence, interference, whether intentional or unintentional, is a criterion for the design. Another important consequence of unprotected media is that authentication of stations will be necessary for privacy.

3. The wireless medium is significantly less reliable than the wired medium, which is a consequence of the dynamic indoor channel with signal fades.

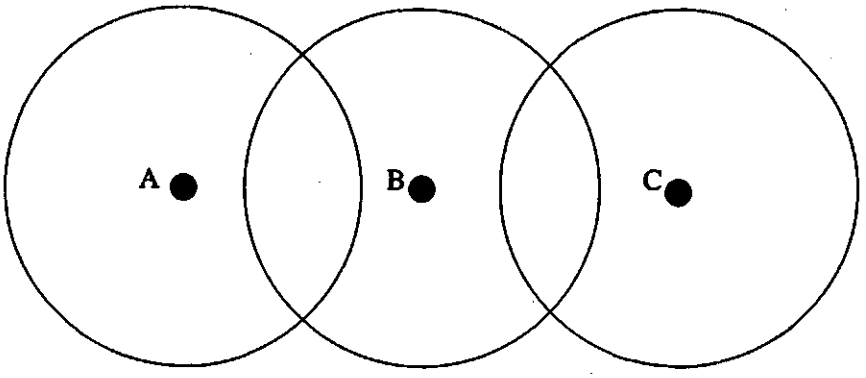

Figure 2.1: Station C might start transmitting when station A is transmitting (station C is hidden from station A).

4. The topology of the wireless medium is dynamic because stations are allowed freedom to move about within the network. Frequent signal fades might also force a station to switch its allegiance to another basic service set (BSS).

5. The wireless medium does not allow full connectivity. This means that every station may not hear every other station. For example, in Figure 2.1, if the circles approximately specify the range of communication for each station, then station C cannot hear station A, and it may start transmitting while A is also transmitting. In the wired medium, such situations led to collisions, which can be detected. In the wireless medium, this is not possible, and a collision avoidance system is needed.

The above characteristics of the wireless medium necessitates the need for a different medium access control (MAC) and physical layer specifications for the wireless LAN [9]. Accordingly, the IEEE 802 project formed a study group, 802.11, to establish an international standard for wireless LANs [2] that will support wireless data networking. The IEEE 802.11 standard discusses the wireless LAN architecture which is assumed for the MAC and the physical layer, which will be discussed in the next section.

2.2 The Wireless LAN Architecture

The basic building block of a wireless LAN as discussed in the IEEE 802.11 standard is the basic service set (BSS) [2]. A BSS is controlled by a single logical function which determines when a station operating within the BSS transmits and receives via the wireless medium. The coordination function at the BSS level consists of one point coordination function (PCF) and one distributed coordination function

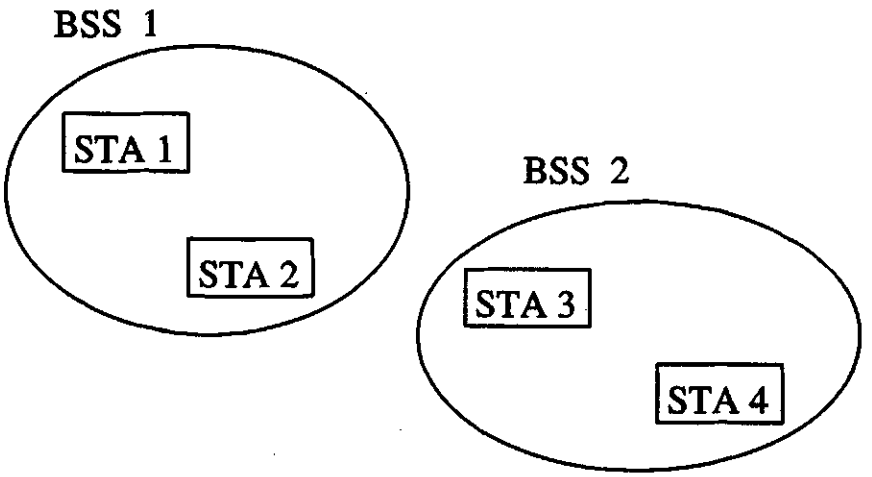

Figure 2.2: Basic service set 1 and basic service set 2 are controlled by two coordination functions.

(DCF). The PCF is active in only one station in a BSS at any given time the network is in operation, where as the DCF is active in every station in the BSS. For the transport of MAC frames between stations within a BSS, services known as station services are specified. Figure 2.2 shows two independent BSS. The ovals are used to depict logically, the coverage area within which the member stations of the BSS can remain in communication. If a station moves out of it's BSS, it can no longer directly communicate with other members of the BSS. An independent BSS can be formed without pre-planning, for only as long as the LAN is needed. Such a situation might arise in a board meeting or a conference, where the users might want to exchange data. The BSS thus formed is often referred to as an ad-hoc network.

The physical layer determines the direct station to station distance which can be supported within a BSS. For some networks, like ad-hoc networks, this distance is sufficient whereas other networks require increased coverage. Instead of existing independently, multiple BSSs can be interconnected to form an extended service set (ESS) as shown in Figure 2.3. Each BSS connects to a distribution system via an access point (AP). The distribution system is responsible for the transport of MAC frames between stations that are not in direct communication with each other (different BSS). For this purpose the distribution system provides services known as distribution system services (DSS). The key concept is that the ESS network appears the same to the logical data link layer as an independent BSS network. Mobile stations may move from one BSS to another inside an ESS, transparently to the data link layer. The BSSs in an ESS may partially overlap, be physically disjoint, or physically collocated (for redundancy). The medium used by the DS is

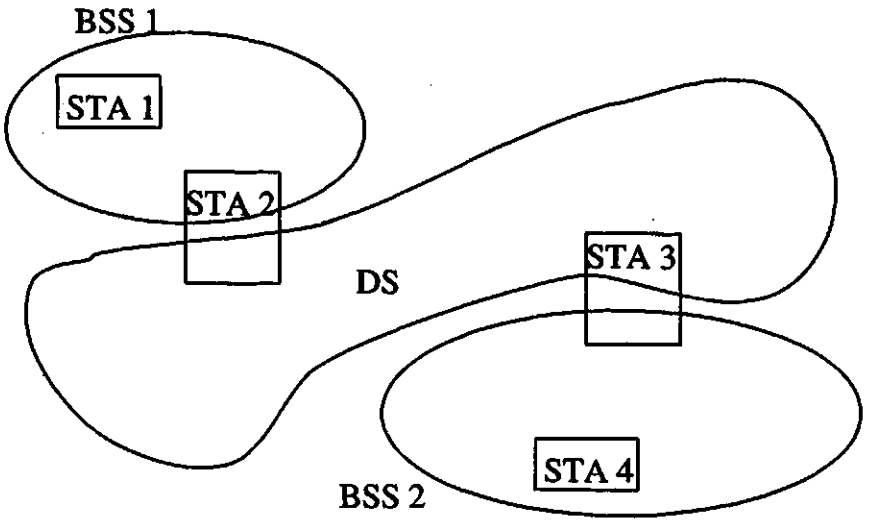

Figure 2.3: An extended service set (ESS) consisting of two independent BSS, which are interconnected by the distribution system (DS).

called the distribution system medium (DSM). In 802.11, the wireless medium is logically separated from the DSM to allow flexibility in the architecture.

To integrate the wireless LAN with a traditional wired LAN, a final logical architectural component is introduced called a portal. Data from the wired LAN enters the wireless LAN via the portal into the distribution system. Figure 2.4 shows the portal connecting to a wired LAN. The wireless LAN architecture specified in the 802.11 is flexible in that, it allows for the possibility that the wireless medium, the DSM, and the integrated wired LAN may all be different physical media. The transport of MAC frames within a wireless LAN is performed by services. These services are discussed in the next section.

2.3 The IEEE 802.11 Services

The IEEE 802.11 standard specifies services that are associated with different components of the architecture. The services can be categorized into, station services (SS) and distribution system services (DSS). Station services support the transport of MAC frames between stations within a BSS. Such services are present in every station in the wireless LAN. These services are classified into three groups, namely, authentication, deauthentication and privacy. The distribution station services are services provided by the distribution system. These services are invoked when the MAC frames need to cross media and address space logical boundaries. The DSS subsets are: association, disassociation, distribution, integration and reassociation.

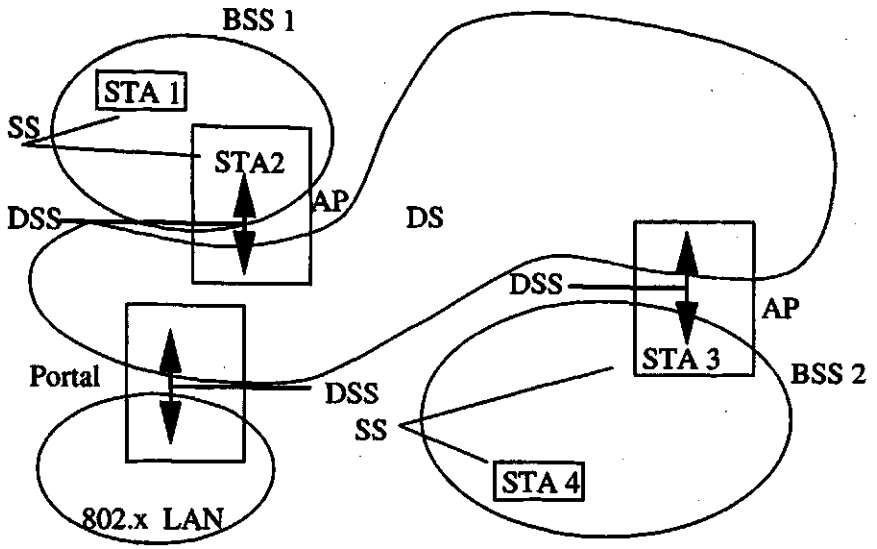

Figure 2.4: The wireless LAN shown connected to the wired LAN via the portal

An overview of all the services (DSS & SS) is presented below:

1. **Distribution**: This the primary service used by 802.11 stations and is invoked by every data message to or from an 802.11 station operating within an ESS. In Figure 2.4, an instance when a message is to sent from STA 1 to STA 4, is considered. The message sent from STA 1 is first received by STA 2 (the input AP). The AP gives the message to the distribution service of the distribution system. The function of the distribution service is to deliver the message within the distribution system such that it arrives at the destination system. Thus the message is distributed to the STA 3 (the output AP) which uses the wireless medium to send the message to STA 4, the intended destination.

2. **Integration**: This service enables delivery of MAC frames between the DS and an existing network. If the distribution service determines that the intended recipient of a message is a member of an integrated LAN, the *output* point of the DS would be a portal instead of an AP. In such a case, it invokes the integration service, which is responsible for accomplishing whatever is needed to deliver a message from the DSM to the integrated LAN medium.

3. **Association**: Before a data message can be handled by the distribution service, a station must be associated. To deliver a message within a DS, the distribution service needs to know which AP to access for the given station. Since the station is allowed to be mobile, three degrees of mobility is defined by 802.11:

(a) No-transition: Static or local movement within the BSS.

(b) BSS-transition: Movement from one BSS in a ESS to another within the same ESS.

(c) ESS-transition: Movement from one BSS in one ESS to a BSS in an independent ESS.

The act of being associated invokes the association service which provides the station to AP mapping to the DS. The DS uses this information to accomplish it's message distribution service. The following possibilities could arise:

- At any given instant an station may be associated with no more than one AP.
- An AP may be associated with many stations at one time.
- A station learns what APs are present and then requests to establish an association by invoking the association service.
- Association is always initiated by the mobile station.

4. **Reassociation**: During the process of communication, an station may traverse another BSS, in which case it needs to establish Association (of the station) to be transferred from one AP to another AP (within an ESS). This keeps the DS informed of the current mapping between AP and the station as the station moves from BSS to BSS within an ESS. Reassociation is always initiated by the mobile station.

5. **Disassociation**: This service voids an existing Association, and is a notification rather than a request. In an ESS, this informs the DS to avoid an existing association information. Attempts to send messages to a disassociated station will be unsuccessful. The following situations are possible:

   - The disassociation service can be invoked by either party to an Association (station or AP).
   - APs might need to disassociate stations to enable the AP to be removed from a network for service or for other reasons (for example, security)
   - Stations are encouraged to disassociate whenever they leave a network, but the MAC protocol protects itself against stations which simply die or go away.

6. **Authentication**: This service is used to establish the identity of the stations to each other. In a wired LAN, physical connection conveys the authority to connect to the LAN. This is not a valid assumption for a wireless LAN. To control LAN access, the stations have to use this service to establish their identity.

7. **Deauthentication**: In an ESS, since authentication is a prerequisite for association, the act of deauthentication causes an explicit disassociation.

8. **Privacy**: This service is used to prevent the contents of messages from being read by stations other than the intended recipient. This service along with authentication is specified to bring the security of the wireless LAN up to the level assumed by the wired LAN design.

2.4 Medium Access Control

In a wired LAN, carrier sense multiple access (CSMA) with collision detect CSMA/CD has been used because of the ease of sensing the carrier by measuring the signal in the cable. But as shown in Figure 2.1, due to the hidden node problem, where station C could start transmitting when station A is transmitting, reliable carrier sensing is extremely difficult [11]. To alleviate the hidden node problem and to increase reliability, CSMA with collision avoidance (CSMA/CA) along with a four–way handshaking has been accepted as a standard by the IEEE 802.11 committee [3] [6].

The CSMA/CA with four–way handshaking is shown in Figure 2.5. An originating station that wants to send a packet to a destination station sends a request–to–transmit (RTS) to the destination station. When the destination station gets an RTS from a user, it polls that originating station by sending a clear–to–send (CTS). The originating station then sends its packet to the destination station. After correctly receiving the packet, the destination station sends a positive acknowledgement (ACK) to the originating station. Apart from the physical mechanism of performing carrier sense, the hidden node problem has been resolved by a virtual mechanism of carrier sensing. The virtual carrier sensing is achieved by distributing the medium busy information through an exchange of RTS and CTS, where both these frames contain the duration field that defines the period of time that the medium is to be reserved to transmit the actual data frame and the returning ACK. This information is distributed to all stations within range of both the transmitter and the receiver, so also to stations that are possibly hidden from the transmitter but not from the

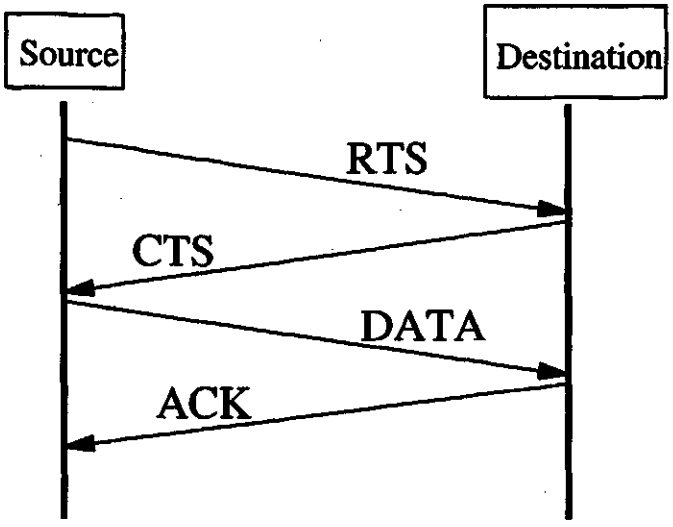

Figure 2.5: Collision avoidance system with four-way handshaking. (RTS: Request to send, CTS: Clear to send, ACK: Acknowledgement)

receiver. Handshaking in wireless LANs differs from that in the wired LAN because of the fact that there is no need to acknowledge every data frame. Another important difference being, that data frames in the wireless LAN need to have a CRC field to check for errors and retransmit if it is not able to correct. In the case of wired LAN, retransmission is done by the network layer.

Stations desiring to initiate transfer of asynchronous MAC frames utilise the carrier sense function to determine the state of the medium. If the medium is busy, the station defers until after a DIFS (DCF intra frame space) gap is detected. It then generates a random backoff period for an additional deferral time before transmitting. This process resolves contention between multiple stations that have been deferring to the same MAC frames occupying the medium. The contention window (CW) is doubled at every retry until it reaches a maximum value and will take the maximum value for the remaining of the retries.

The backoff procedure is shown in Figure 2.6. The frame, shown in Figure 2.6 is a combination of the RTS–CTS–DATA–ACK frames. In this case, stations B, C and D want to use the medium when station A is still using the medium. In such a case, stations B, C and D will defer and go into a randomly set backoff time. Once station A has completed its usage of the medium for the duration of the frame, the backoff timers of stations B, C and D start decrementing. The station with the lowest random backoff will win the contention. In this case, station C captures the medium first because of its smaller backoff time. The backoff timers of stations B

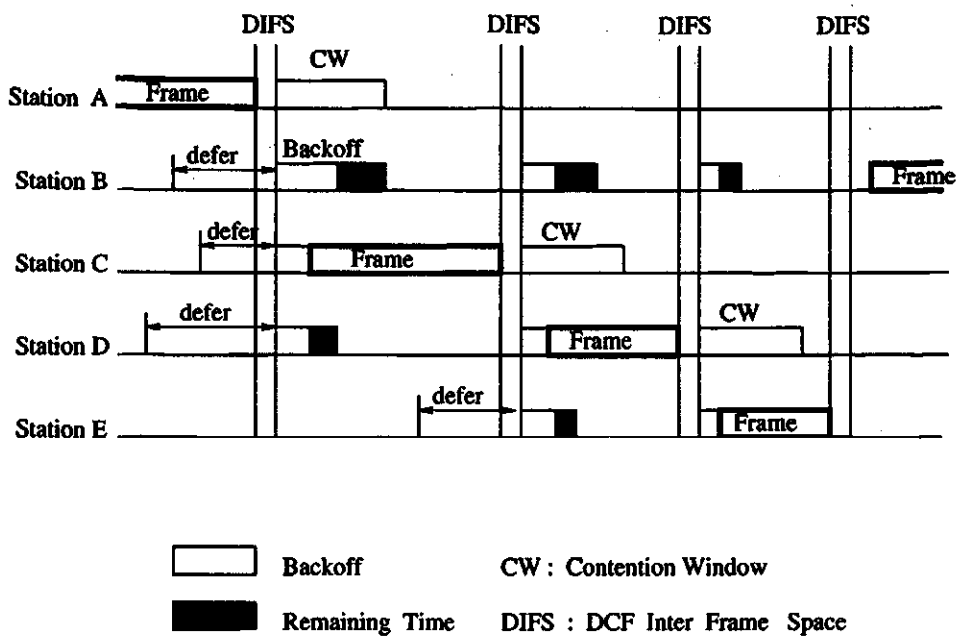

Figure 2.6: The backoff procedure

and D are then frozen for the period that the medium is busy and they resume decrementing, after the frame duration as demanded by station C. A station which has just used the medium will have to perform the backoff procedure which produces the level of fairness of access amongst the stations to the medium.

2.5 Physical Layer

The IEEE 802.11 standard specifies physical layer standards for infrared (IR), frequency hopped (FHSS) and direct sequence (DSSS) spread spectrum. Of the three industry, scientific and medical (ISM) bands, at 900 MHz, 2.4 GHz and 5.7 GHz, the 2.4 GHz band was chosen because it is the only band among the ISM bands to be available world-wide. Another important reason for using this band is that cheaper silicon integrated circuits could be used for front end processing instead of the costlier gallium arsenide integrated circuits. Since this thesis deals with the DSSS technique for the wireless modem implementation, only the 2.4 GHz ISM band, DSSS physical layer specifications are discussed.

The physical layer specifications for the DSSS implementation require the use of additional headers. The frame which is then transmitted over the wireless medium is called the physical protocol data unit (PPDU). Figure 2.7 shows the PPDU for the DSSS system. The PPDU is logically divided into a 144 bit physical layer convergence procedure (PLCP) preamble and a 48 bit PLCP header. The PLCP

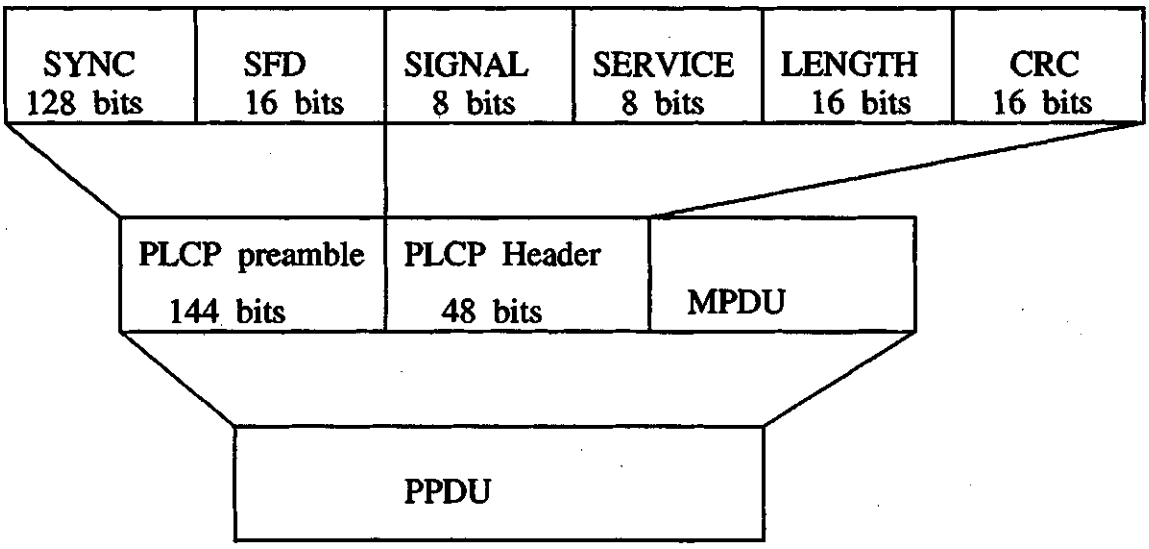

Figure 2.7: The physical layer protocol data unit (PPDU) for the direct sequence spread spectrum based physical layer. (SFD: Start frame delimiter, CRC: Cyclic redundancy check, PLCP: Physical layer control protocol, MPDU: Multi protocol data unit)

defines a method of mapping the MAC frames into a framing format suitable for transmiting and receiving frames over the associated physical layer. The PLCP preamble has two fields, the first consisting of 128 bits for the necessary operations of synchronization (SYNC) and the second field, a 16 bit start frame delimiter (SFD) field, to indicate the start of the physical layer dependent parameters. The PLCP header consists of the signal, service, length and CRC fields. The 8 bit signal field indicates the modulation scheme which will be used for transmission of the MAC frame. The service field of 8 bits is left for future use. The 16 bit length specifies the number of octets to be transmitted in the MAC frame. A 16 bit cyclic redundancy check (CRC) field protects the signal, service and length fields. The length of the MAC protocol data unit (MPDU) is between 64 to 1536 bytes.

The DSSS system under IEEE 802.11 standard provides for both 1 Mbps and 2 Mbps data payload communication capability. According to the FCC regulations, the DSSS system needs to employ a minimum processing gain of 10 dB. This is accomplished by using an 11-chip length spreading code known as the Barker sequence. The Barker sequence is known to have excellent autocorrelation properties important for robust multipath reception. The 11-chip Barker sequence specified in IEEE 802.11 standard is

$$\{+1, -1, +1, +1, -1, +1, +1, +1, -1, -1, -1\}$$

The DSSS system uses baseband modulations of differential binary phase shift keying (DBPSK) and differential quadrature phase shift keying (DQPSK) to provide 1 and 2 Mbps data rates, respectively. Thus the transmitted signal will have a null-to-null bandwidth of 22 MHz for both the modulation schemes. In a multiple cell network topology, adjacent cells will experience interference, since the same spreading code is used throughout the network. For adjacent cells to operate without interference, the distance between the centre frequencies has to be at least 30 MHz. This is possible since the allocated ISM band at 2.4 GHz has a span of of 83.5 MHz (2.4 to 2.4835 GHz). The FCC allows specific channel center frequencies, each separated by 5 MHz, starting from 2412 MHz to 2462 MHz. The channel center frequency is decided in advance for transmission and reception. The carrier sense (energy detection) required by the CSMA/CA is done by using an energy detection threshold which is specified in the IEEE 802.11 standard.

2.6 Summary

In this chapter, the characteristics of the wireless medium as opposed to the wired medium were discussed; this required that the medium access method and physical layer be addressed. The wireless LAN architecture as discussed in the IEEE 802.11 standard was then presented and the various services which need to be offered for reliable transmission of the MAC frames was briefly discussed. The MAC layer and the physical layer specifications were also described. The following chapter addresses the various issues concerning the design of the wireless modem.

Chapter 3

Indoor Spread Spectrum Systems

The need for a wireless modem, the wireless LAN architecture and the IEEE 802.11 standards were discussed in Chapter 1 and Chapter 2. Before proceeding to the design of the direct sequence spread spectrum, ISM band radio LAN, it is instructive to discuss the digital modulation scheme, the direct sequence spread spectrum (DSSS) technique, and the indoor channel in some detail. These issues form the subject of this chapter.

3.1 Digital Modulation

Digital modulation is a process by which digital symbols are transformed into analog signal waveforms that are compatible with the characteristics of the channel. In a bandpass system, the information signal modulates a sinusoid signal called a carrier. Bandpass systems with a high frequency carrier use a realizable antenna to convert the signal into electro-magnetic field for propagation to the desired destination.

Bandpass modulation results in other important benefits in signal transmission like allowing more than one signal to utilise a single channel by using frequency division multiplexing (FDM). It can also be used to ease design requirements by placing an information signal appropriately in a frequency band. The choice of a modulation technique is influenced by requirements like, compact output spectrum, good probability of error (P_e) performance and one leading to a simpler implementation of the receiver.

A digital modulation technique that meets the requirements and has subsequently been chosen as the IEEE 802.11 standard is differential quadrature phase shift keying (DQPSK). The DQPSK modulation technique is described in the following section.

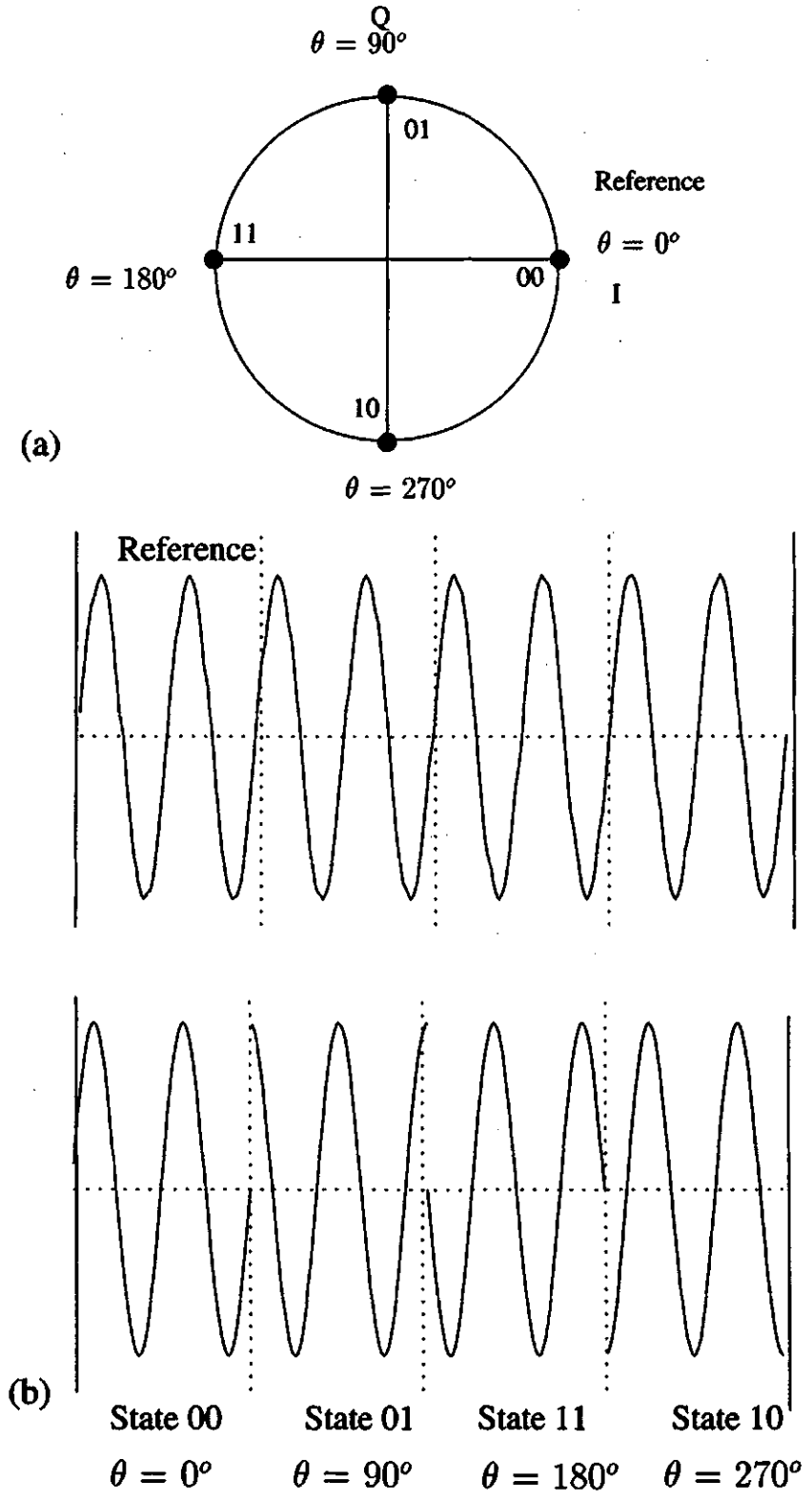

Figure 3.1: (a) I–Q diagram of QPSK modulation. (b) QPSK timing diagram.

3.1.1 Differential Quadrature Phase Shift Keying (DQPSK)

The differential quadrature phase shift keying (DQPSK) modulation technique along with the differential binary phase shift keying (DBPSK) modulation technique has been specified by the IEEE 802.11 standard for use with the direct sequence spread spectrum technique to provide 2 Mbps and 1 Mbps data rate respectively. Differential modulation techniques simplify the receiver design by precluding the necessity for an absolute phase reference for demodulation. This thesis uses DQPSK as the modulation technique as it provides a higher data rate than DBPSK. In the subsequent section, the DQPSK modulation format is described. To understand DQPSK modulation, it is instructive to consider various blocks of a typical digital modulation scheme.

The quadrature modulated signal has two components, called inphase (I) and quadrature (Q) phase. The representation of the signal in the I–Q coordinate system presents the magnitude and phase of the signal. The length of the vector from the origin being the magnitude and the angle with respect to the positive I– axis being the phase of the signal. To determine the phase and magnitude of the modulation signal, a reference is used. At the transmitter side, it is the local oscillator, and at the receiver, it is derived from the incoming phase-modulated signal.

The DQPSK is a modification of quadrature phase shift keying (QPSK). The QPSK modulation is a multilevel modulation technique that represents a data symbol (formed by a data bit pair) by one of the four phase states. Thus two bits are transmitted during each signalling interval. An I–Q diagram of QPSK is shown in Figure 3.1. Determining the phase relationships and the corresponding digital bit patterns requires a known phase reference for comparison. DQPSK also uses four phase states, which requires two bits per data symbol. The modification is that the phase states are defined relative to the last phase state. Table 3.1.1 shows the phase transitions defined for the corresponding symbols. Based on these definitions, symbols arriving in the order as shown in Table 3.1.1 will have the associated phase states, assuming an initial state of θ^o.

This method of modulation alleviates the need for an absolute phase reference as the phase of the current symbol is determined from its relative phase difference with the phase state of the previous symbol. Thus, DQPSK modulation leads to noncoherent detection. The price paid towards a simple receiver is performance. DQPSK has worse bit error rate (BER) performance than the coherent QPSK modulation.

Symbol	DQPSK Phase Transition
00	0^o
01	90^o
10	-90^o
11	180^o

Table 3.1: Phase transition of DQPSK

Arrival Time	Symbol	New Phase State
t	00	0^o
t+1	01	90^o
t+2	11	-90^o
t+3	00	-90^o

Table 3.2: Phase states at different time instants

3.2 Spread Spectrum Communications System

Most radio communication systems are narrowband, and the systems are designed to be minimum power and minimum bandwidth. This is a good strategy to use where the major source of performance degradation is thermal noise. In spread spectrum communication systems, the information signal is spread over a bandwidth much wider than that required to achieve reliable communication. A formal definition for spread spectrum can be given as [43]:

> Spread spectrum is a means of transmission in which the signal occupies a bandwidth much in excess of the minimum necessary to send the information; the spreading is accomplished by means of a code which is independent of data. Synchronized reception with the code at the receiver is used for despreading and subsequent data recovery.

Spread spectrum communication systems were initially developed for military applications. Recently applications of spread spectrum communications have grown into the areas of commercial applications, including wireless LANs, personal communication networks, and digital cellular radios. Spread spectrum modulation has gained considerable acceptance as a good alternative to narrowband communication systems [27] [35] [30]. The burgeoning number of applications have led to the U.S. Federal Communications Commission (FCC) providing deregulated frequency

bands, called industry scientific medical (ISM) bands, for spread spectrum communications. There are three such bands presently allowed, 900 MHz, 2.4 GHz and the 5.7 GHz.

Spread spectrum technology comes in two flavors: direct–sequence spread spectrum (DSSS) and frequency–hopping spread spectrum (FHSS). In an FHSS system, the total bandwidth is split into a set of channels of equal bandwidth. Both transmitter and receiver dwell on one channel for a period of time, and then "hop" from that channel to another. The pattern of channel usage is referred to as an hopping sequence, which can either be random or deterministic (pseudo–random). The time spent on each channel is called a chip. The ratio between the chipping rate (hopping rate) and the data rate differentiates two modes of FHSS: when the chipping rate is higher that the data rate, then the system is known as a fast FHSS; when the chipping rate is lower than the data rate, then the system is known as a slow FHSS. Although fast FHSS provide higher data rates, they are costly and power hungry, relative to slow FHSS. As the transmitter and the receiver must hop together, slow FHSS systems provide relaxed tolerances on the degree of synchronization. The IEEE 802.11 specifies the use of slow FHSS. In a DSSS system, a pseudo–random binary sequence is used to modulate the transmitted signal. The relative rate between the pseudo–random sequence and the user data is typically between 10 and 100 for commercial systems. This ratio is called the spreading factor. In DSSS systems the receiver sequence and the transmitter sequence must be in phase for reliable communications.

In this thesis, the DSSS technique was preferred over FHSS technique for the following reasons. FHSS has a better performance than DSSS in the presence of interference because of its resistance to a partial band jammer. FHSS has worse performance than DSSS in a time dispersive multipath channel, because it has no delay resolution capability (this can be done only by a fast FHSS) [30]. Though, fast FHSS has frequency diversity, which can be exploited with the application of interleaving and coding, it is not easy to implement such techniques with the slow FHSS systems because the interleaving must be performed across many hops or packets which would introduce excessive delays. Consequently, performance of the slow FHSS systems over a time dispersive channel is no better than the narrowband communication system. The maximum tolerable normalized delay spread of the DSSS systems is greater than 0.4, as compared to 0.1 for FHSS systems and this allows DSSS systems to provide higher data rates than FHSS systems. Moreover, the FHSS systems are slightly more costlier compared to DSSS systems because

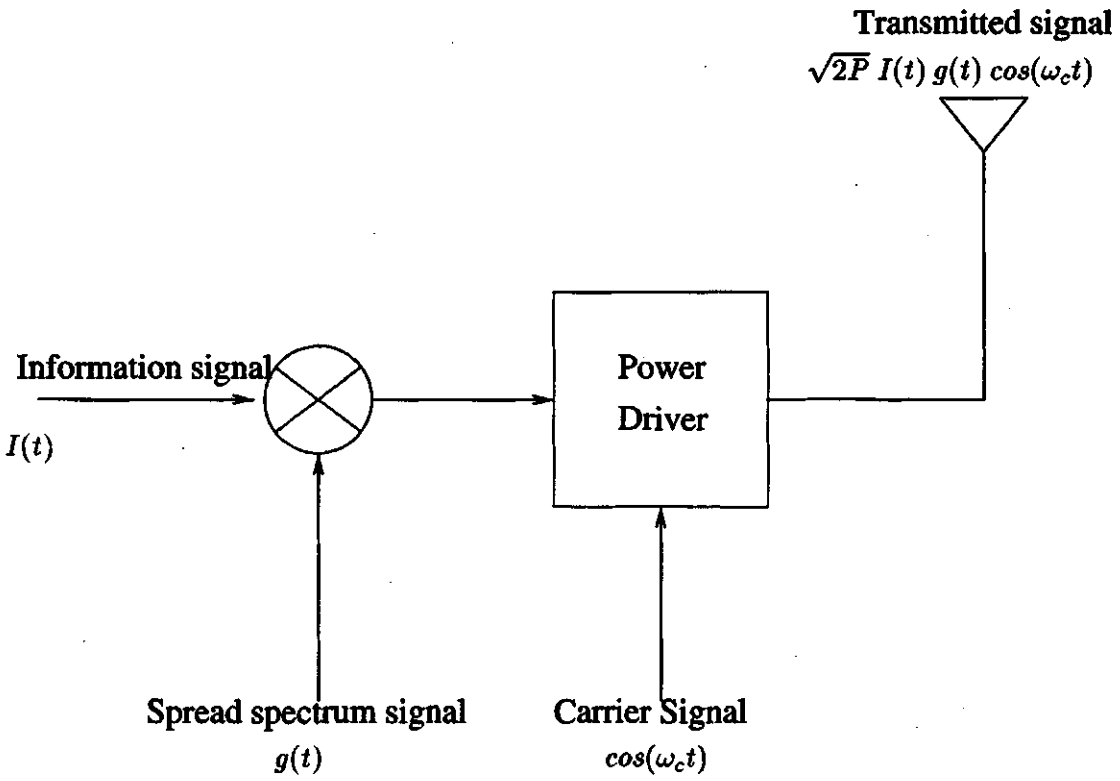

Figure 3.2: Simplified DSSS transmitter

the radio transceiver requires high–stability frequency–determining components and high–selectivity filters [6]. Therefore, DSSS was chosen as the preferred spread spectrum technique.

In the subsequent section, the direct sequence spread spectrum technology is discussed.

3.2.1 Direct Sequence Spread Spectrum (DSSS)

Direct sequence spread spectrum (DSSS) is a technique which allows the information signal $I(t)$ to be spread (widened) in the frequency domain by multiplying it with a pseudo–noise (PN) code $g(t)$ [27]. The transmitted signal is given by

$$s(t) = \sqrt{2P}\ I(t)\ g(t)\ cos(\omega_c t)\ , \tag{3.1}$$

where P is the power of the carrier signal and ω_c is the carrier frequency. This process is shown in Figure 3.2.

The bandwidth occupied by $s(t)$ is much larger than the bandwidth of the information signal $I(t)$, assuming that the bandwidth of the spreading signal $g(t)$ is

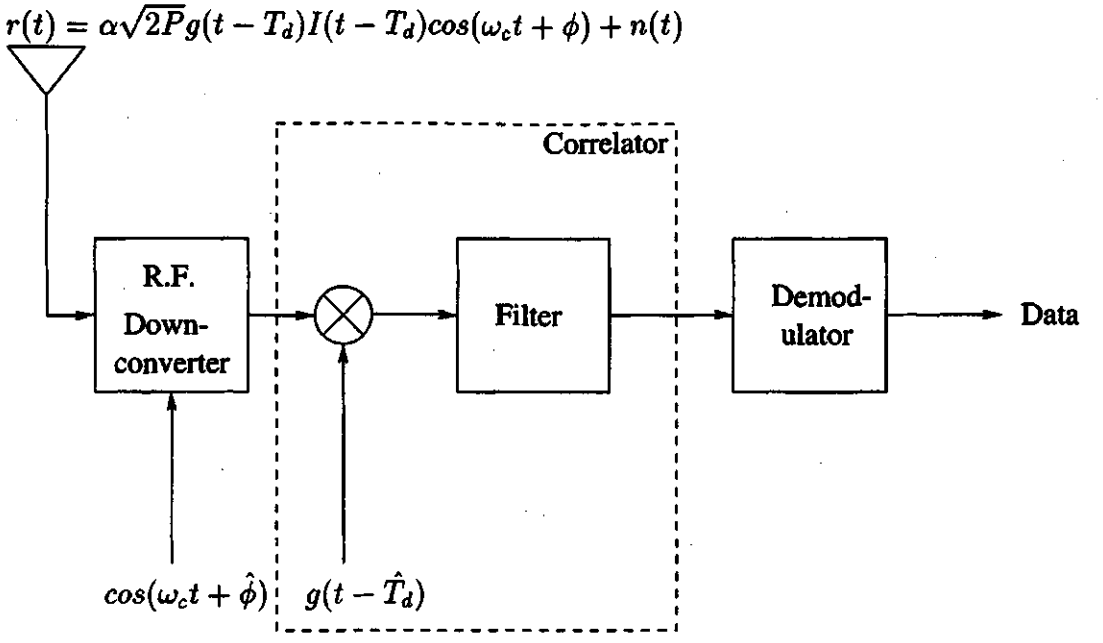

Figure 3.3: Simplified DSSS receiver

much larger that the bandwidth of the information signal $I(t)$. The bandwidth expansion factor $B_c = W/B$, where W represents the null–to–null bandwidth of the information signal after spreading and B represents the null–to–null bandwidth of the information signal $I(t)$, is also called the processing gain of the direct sequence spread spectrum system. It represents the advantage gained over another signal using the same RF channel.

If there is only one user in the channel, for a simple channel that introduces a transmission delay T_d, and attenuates the signal, the received signal $r(t)$ is given by

$$r(t) = \alpha\sqrt{2P}I(t-T_d)g(t-T_d)cos(\omega_c t+\phi)+n(t)\,, \tag{3.2}$$

where α is the attenuation in the channel, $\phi = \omega_c T_d + \psi$ (ψ is the random phase distortion by the channel), and $n(t)$ is white Gaussian noise. The received signal is then down converted to baseband by multiplying the RF signal by a locally generated signal $cos(\omega_c t+\hat{\phi})$, where $\hat{\phi}$ is an estimation of ϕ. The baseband signal is then despread by a correlator–type matched filter. The matched filter uses a local replica of $g(t-\hat{T}_d)$, where $\hat{T}_d$ is an estimate of T_d. Figure 3.3 shows the simplified spread spectrum receiver. The despread signal, is then an estimate of the transmitted information signal, which when demodulated provides the detected data output. Figure 3.4 illustrates the spectrum of the signals at various points in the spread spectrum communication process. It may be noted that the narrow spectrum of the informa-

tion signal is spread over a wide bandwidth by spread spectrum modulation. At the receiver the signal is despread or the spectrum is collapsed to the narrow information signal bandwidth. This results in any intentional or unintentional interference to be spread over a wide bandwidth which can then be filtered out.

3.3 The Indoor Channel

The indoor environment is particularly hostile to radio frequency signals [28]. In an indoor wireless LAN, according to the IEEE 802.11 standard, the medium access control allows only one user to occupy the channel at any given time. Figure 3.5 shows the indoor communication system operating in an indoor environment. A typical indoor environment consists of numerous scatterers, and reflectors, which are characterized by the structure of the building, objects in the vicinity, and motion of people. Thus, there may be many different propagation paths between the transmitter and the receiver. These paths may not include a line of sight path. The multiple paths can be of varying lengths and may experience significantly different phase shifts and attenuations. At the receiver, the signals arriving from multipath are added constructively or destructively. Destructive addition leads to the phenomena called signal fading, and as it is a consequence of multipath channel, it is termed multipath fading. In addition to mutipath fading, shadowing of the receiver causes slower power variations and is caused by physical structures blocking the transmission path of the signal. Fading and shadowing are time varying phenomena, which arise from the motion of the transmitter and the receiver. These may also be caused by the motion of people even when the transmitter and receiver are stationary. In addition to fading and shadowing, spatial loss or distance loss is also a factor.

3.3.1 Indoor Channel Impulse Response

Measurements made in the indoor environment have shown that the complicated random and time–varying indoor radio propagation channel can be modelled as a linear time–varying filter for each point in three–dimensional space [15] [19] [23]. The impulse response at a given point in space may be written as:

$$h(t,\tau) = \sum_{l=0}^{L(\tau)-1} a_l(t)\delta(\tau - \tau_l)e^{j\theta_l(t)}\,, \tag{3.3}$$

where t and τ are the observation time and application time of the impulse respectively. $L(\tau)$ represents the number of multipath components; $a_k(t)$, $\tau_k(t)$ and $\theta_k(t)$ are the random time–varying amplitude, arrival–time, and phase sequences

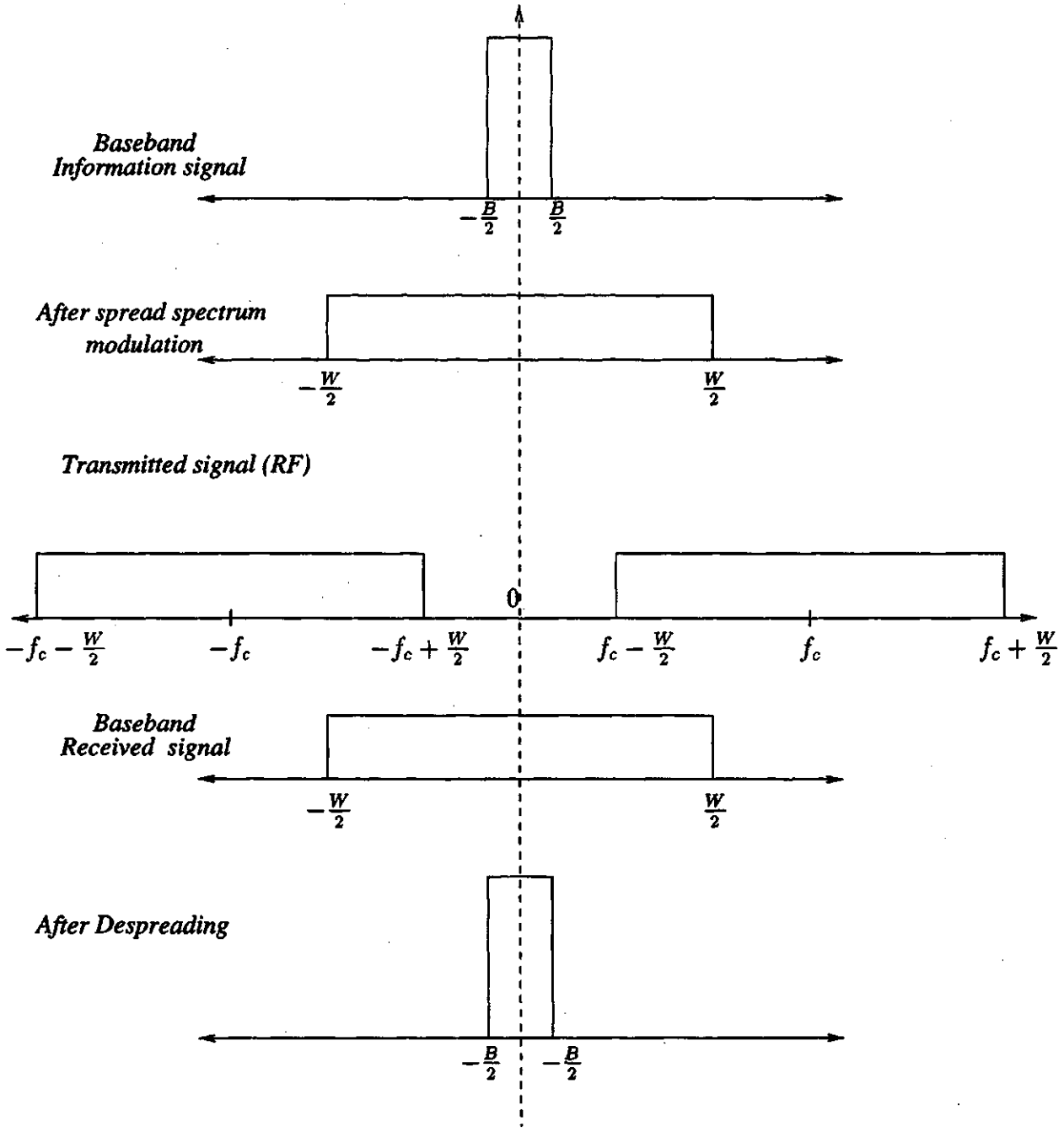

Figure 3.4: The spectrum of the various signals in the DSSS communication system

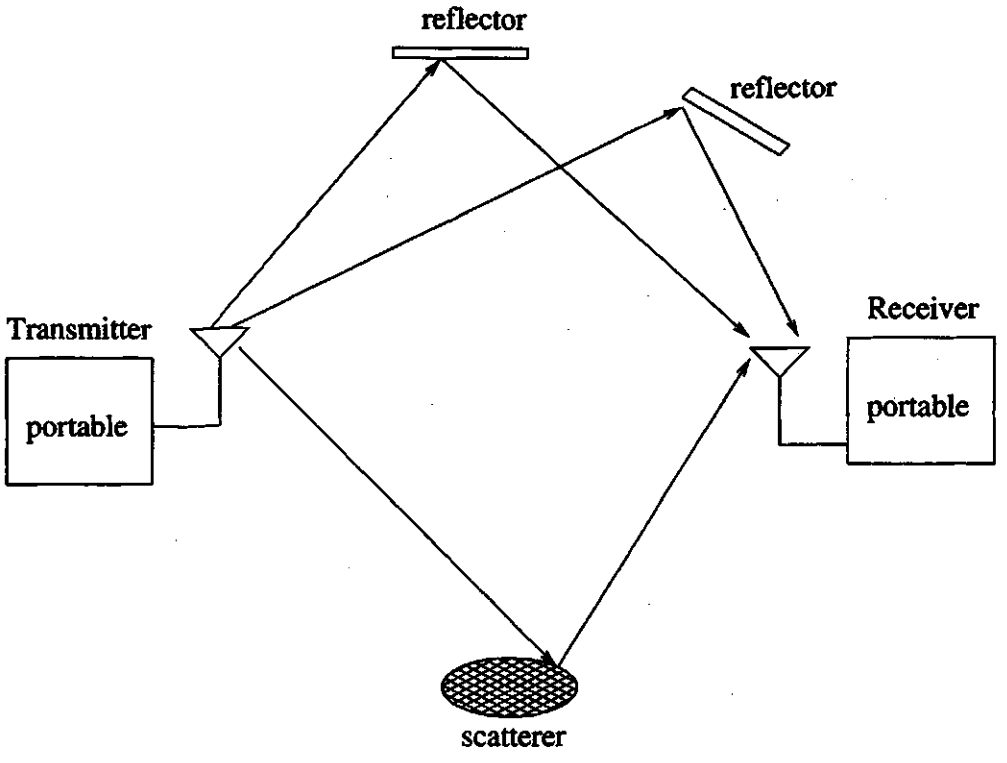

Figure 3.5: Indoor multipath environment

respectively. The channel is completely characterized by these path variables. This mathematical model is illustrated in Figure 3.6.

The indoor channel will, according to this model, make a transmitted impulse to be received as a series of $L(\tau)$ impulses. As the paths have different lengths, and attenuations, each of the received pulses will arrive at different times with different amplitudes as shown in Figure 3.7. Because of the motion of other portables and scatterers, the channel is in general time–variant. Measurements have shown that in a typical office environment, the channel changes its characteristics after a period of about 100 ms, in the 2.4 GHz frequency band [24]. For this period of time, the parameters which characterize the indoor channel may be considered to be constant.

For the stationary (time–invariant) channel, Equation 3.3 may be simplified to,

$$h(t) = \sum_{l=0}^{L-1} a_l \delta(t - \tau_l) e^{j\theta_l} \ . \tag{3.4}$$

The output $y(t)$ of the channel in response to the transmitted signal $s(t)$ is therefore given by

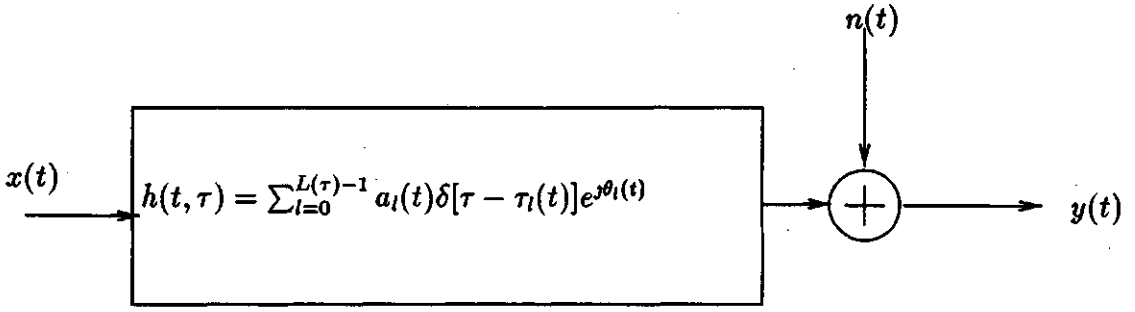

Figure 3.6: Mathematical model of the channel

$$y(t) = \int_{-\infty}^{\infty} s(\tau)h(t-\tau)d\tau + n(t)\,, \tag{3.5}$$

where $n(t)$ is low–pass, complex–valued, additive, Gaussian noise.

If a signal $x(t) = Re\{s(t)exp[j\omega_c t]\}$, where $s(t)$ is any low–pass signal and ω_c is the radian carrier frequency, is transmitted, the output of the channel $y(t)$ is given by $y(t) = Re\{\rho(t)exp[j\omega_c t]\}$ where,

$$\rho(t) = \sum_{l=0}^{L-1} a_l s(t-t_l)e^{j\theta_l} + n(t)\,. \tag{3.6}$$

When an unmodulated carrier is transmitted, then $s(t) = 1$ and Equation 3.6 simplifies to

$$\rho(t) = \sum_{l=0}^{L-1} a_l e^{j\theta_l}\,. \tag{3.7}$$

The low–pass equivalent signal $\rho(t)$ is, thus, a vector sum of L vectors with phase θ_k and amplitude a_k. The phase of each multipath component depends upon the path delay and the carrier frequency. At high carrier frequencies, the phase θ_k

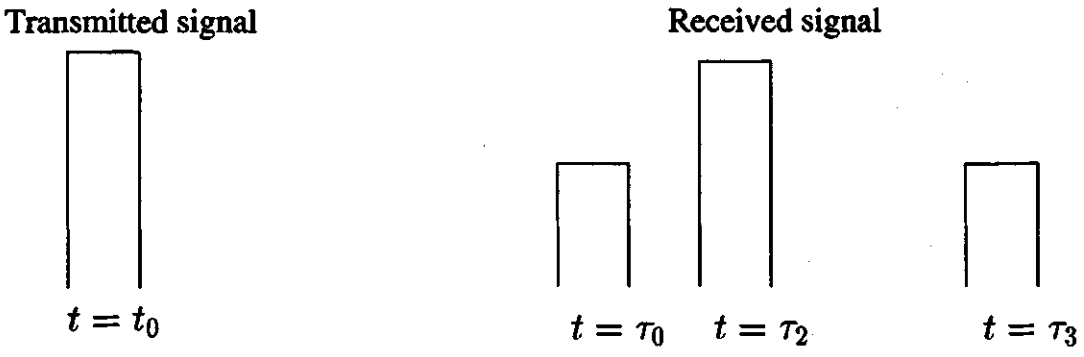

Figure 3.7: Impulse response of the channel

can change by 2π radians with small changes in the path length. Therefore, the vectors might add constructively or destructively to give rise to a strong or a weak signal respectively. With a large number of paths, the central limit theorem can be applied, and $\rho(t)$ can be modelled as a zero–mean, complex–valued, Gaussian random process. The envelope of which, $r(t) =\mid \rho(t) \mid$, has a well known Rayleigh probability density function given by

$$f(r) = \frac{r}{\alpha^2} e^{-\frac{r}{2\alpha^2}} U(t) \,, \tag{3.8}$$

where α^2 is the variance and $U(t)$ is the unit step function. A multipath channel that can be modelled by a zero–mean, complex–valued, Gaussian random process is said to exhibit Rayleigh fading.

In order to decide on the number of resolvable paths, the time variance of the channel, there are a number of parameters which need to be discussed. This is done in subsequent sections.

3.3.2 Delay Spread

Due to multipath propagation, signals arrive at the destination with different time delays [26]. The range of values over which the measured power is above a certain threshold value is called the multipath delay spread of the channel. A measure of this delay spread is needed to ascertain the limits on digital transmission rates possible over such radio channels. The parameter commonly used to describe the overall characteristics of the mutipath profile is the root mean square (rms) delay spread. The rms delay spread of τ_{rms} is given by,

$$\tau_{rms} = \sqrt{\frac{\sum_k (t_k - \tau_m - t_A)^2 a_k^2}{\sum_k a_k^2}} \,, \tag{3.9}$$

where t_A is the arrival time of the first path in a profile and $\tau_m$is the mean excess delay defined as,

$$\tau_m = \frac{\sum_k (t_k - t_A) a_k^2}{\sum_k a_k^2} \,. \tag{3.10}$$

Mean excess delay, τ_m, is the first moment of the power delay profiles $\mid h(t) \mid^2$ with respect to the first arriving path, and the rms delay spread τ_{rms} is the square root of the second moment of a power delay profile. The rms delay spread, τ_{rms}, gives an indication of the potential for intersymbol interference (ISI), and it has been shown that the performance of the communication system is very sensitive to

the value of τ_{rms} [19]. In order to avoid ISI, the width of the data symbol should be much larger than τ_{rms}. Therefore, the delay spread sets a limit on the transmission symbol rate in an indoor digital system.

3.3.3 Coherence Bandwidth

The channel in the frequency domain may be studied by taking the Fourier transform of the impulse response $h(t,\tau)$, to get

$$H(f,t) = \int_{-\infty}^{\infty} h(t,\tau)e^{-j2\pi f\tau}d\tau \ . \tag{3.11}$$

If the channel is wide sense stationary, then a spaced frequency, spaced time correlation function may be defined as [26],

$$\Phi_h(\Delta f,\Delta t) = \int_{-\infty}^{\infty} \phi_h(\tau,\Delta t)e^{-j2\pi\Delta f\tau}d\tau \ , \tag{3.12}$$

where, $\phi_h(\tau,\Delta t)$, is the autocorrelation function of $h(t,\tau)$, assuming $h(t,\tau)$ is wide sense stationary and the scattering is uncorrelated. Setting $\Delta t = 0$ in Equation 3.12 gives the spaced frequency correlation function which may be written as,

$$\Phi_h(\Delta f) = \int_{-\infty}^{\infty} \phi_h(\tau)e^{-j2\pi\Delta f\tau}d\tau \ . \tag{3.13}$$

This autocorrelation is a measure of the frequency coherence of the channel. One important measure of this function is the coherence bandwidth $(\Delta f)_c$ which is approximately the reciprocal of the multipath delay spread,

$$(\Delta f)_c \approx \frac{1}{\tau_{rms}} \ . \tag{3.14}$$

Coherence bandwidth is the width of frequencies in a channel over which the signal experiences approximately the same fading. In other words, two sinusoids with frequency separation greater than the coherence bandwidth are affected differently by the channel. The channel is called frequency–selective if the signal bandwidth is small in comparison to the coherence bandwidth. Otherwise, the channel is called frequency–nonselective. Spread spectrum systems are generally designed such that the channel behaves as a frequency–selective channel. In this case, the multipath components can be resolved in time, with a time resolution equal to the reciprocal of the signal bandwidth. As each path is independently affected by the channel, these paths can be combined to improve the signal–to–noise ratio at the receiver. This form of diversity reception is called multipath diversity, or spread spectrum diversity.

3.3.4 Doppler Spread and Coherence Time

In a mobile communication environment, due to the relative motion of the portables and reflectors, the radio transmissions are frequency shifted. The time variation in the channel results in Doppler broadening of the transmitted spectrum. Doppler shift affects all the propagation paths, some of which may exhibit a positive shift and others a negative shift at the same instant. This shift introduces random frequency modulation in the received signal. A relation between Doppler shift and time variations of the channel may be found by defining the Fourier transform of the spaced frequency, spaced time correlation function, $\Phi_h(\Delta f, \Delta t)$, defined in Equation 3.12. This transform is given by

$$S_h(\Delta f, \lambda) = \int_{-\infty}^{\infty} \Phi_h(\Delta f, \Delta t) e^{-j2\pi\Delta t} d\Delta t \,. \tag{3.15}$$

The Doppler spectrum, $S_h(\lambda)$, is defined by setting Δf to zero in Equation 3.15,

$$S_h(\lambda) = \int_{-\infty}^{\infty} \Phi_h(\Delta t) e^{-j2\pi\Delta t} d\Delta t \,. \tag{3.16}$$

The range of values over which $S_h(\lambda)$ is non–zero is called the Doppler spread, B_d, of the channel.

In an outdoor, land mobile channel, Doppler spreads can be as high as 100 Hz at a carrier frequency of 1.5 GHz. Where as in the indoor environment, the Doppler spread is significantly lower, at about 15 Hz, at the same carrier frequency.

The coherence time $(\Delta t)_c$ of the channel is defined approximately as the reciprocal of the Doppler spread of the channel.

$$(\Delta t)_c \approx \frac{1}{B_d} \,. \tag{3.17}$$

The channel is termed slowly fading if the signalling period is less than the channel's coherence time and the signal bandwidth is less than the coherence bandwidth. The channel impulse response may be considered to be invariant over the coherence time.

3.3.5 The Indoor Channel Model

The indoor environment, as discussed, changes with time, and hence the path gain, phase and the delay, which characterize the indoor channel impulse response, are constantly changing with time. An important consideration in a channel model is the rate of this change relative to the transmitted bit rate. A review of the literature

shows than it is reasonable to assume a stationary or quasi-static channel for a time span of a few seconds in residential buildings or office environments, where one doesn't expect a large degree of movement [19]. The situation is different in shopping malls and supermarkets, where there is constant movement of people. A measure of the channel's temporal variation is the width of its spectrum when a single sinusoid is transmitted. The largest Doppler spread reported in the literature for the indoor channel is 12.2 Hz [19]. This leads to a coherence time of about 82 ms. The largest MAC protocol data unit (MPDU) will take about 20 ms to transmit at the symbol period of $1\mu s$. The channel, therefore, may be assumed to be time–invariant for the duration of the MPDU.

The channel is, thus, a quasi–static channel, which is given by,

$$h(t) = \sum_{l=1}^{L} g_l \delta(t - \tau_l) e^{j\theta_l} , \tag{3.18}$$

where t is the observation time, L is the number of paths and has a Bernoulli distribution [19] as given below

$$Pr[l = L] = \binom{N_\Delta}{L} P_b^L (1 - P_b)^{N_\Delta - L} , \tag{3.19}$$

where N_Δ is the number of bins that can be formed by dividing the maximum excess delay, Δ into intervals of one chip period such that $N_\Delta = \lfloor \frac{\Delta}{T_c} \rfloor$. The maximum possible value of L is N_Δ and $L \in 1, 2, \cdots, N_\Delta$. P_b is the probability that a path exists in any one of the bins.

Paths are counted as different paths only if

$$|\tau_k - \tau_l| > \frac{1}{W} , \tag{3.20}$$

for all $k \neq l$. This condition is called the resolvability condition, since in a system with a bandwidth of W, the maximum possible resolution is $\frac{1}{W}$. The unresolvable components present within a chip duration add vectorially to form a single resolvable path.

The ratio of the signal bandwidth to the coherence bandwidth of the channel indicates whether the channel is frequency–selective or not. The proposed system uses a 11-chip Barker sequence to spread a 1 M-symbols per second information signal. This indicates a null–to–null signal bandwidth of 11 MHz. The coherence bandwidth has been shown to be about 3 MHz. For an indoor channel at the 2.4

GHz ISM band, the value of the τ_{rms} varies from 100–150 ns, depending upon the indoor environment [15] [24]. For a chip period of 90.9 ns, a two path model is, thus, sufficient to represent the channel impulse response. Therefore, the channel used in the performance evaluation is a frequency–selective one with two independently fading paths.

The indoor channel model for 2.4 GHz is a two path model, each of which experiences independent Rayleigh fading. The phase associated with each of the paths is uniformly distributed. The channel impulse response may be assumed to be constant for the duration of the MPDU.

Intersymbol interference can be a limiting factor introduced by some channels, and generally dictates the largest bit rate which can be transmitted through the channel reliably. The ISI will affect the communication if the delay spread is comparable to the symbol period. The symbol period of the system presented here is $1\mu s$. The largest rms delay spread reported is about 150 ns, which is much smaller than the symbol period. Therefore, ISI will not be a significant problem and is therefore not considered in the model.

3.4 Summary

In this chapter, the various issues which affect wireless modem design were discussed. The DQPSK modulation technique was described, and the direct sequence spread spectrum technique was discussed. The indoor channel model for the 2.4 GHz ISM band was also discussed. The following chapter discusses the wireless modem design of the transmitter and the receiver, and analyzes the bit error rate performance of the wireless modem.

Chapter 4

The Indoor Wireless Modem

This chapter starts with a discussion of the transmitter and the receiver design for a indoor wireless modem and analyses bit error rate (BER) performance of the simple wireless modem. The BER analysis of an optimal receiver with a transversal filter diversity combiner is then discussed. The expression derived for such an optimal receiver will be useful in comparing against practical approaches to diversity combining receivers, which is the main contribution of this thesis.

4.1 The Wireless Modem

The design of the wireless modem includes the design of the transmitter and the receiver. The design specifications follow the IEEE 802.11 wireless LAN standard. The 2.4 GHz ISM band, direct sequence spread spectrum system uses the DQPSK modulation scheme. The system is designed to provide a data throughput of 2 Mbps. In the following sections, the design of the transmitter and receiver is discussed.

4.1.1 Transmitter

The transmitter of the indoor wireless modem is presented in Figure 4.1. As shown in the figure, the data source, which is the signal from the user's computer is split into two-bit segments by the data symbol mapping function. The differential phase encoder transforms the two-bit signal to four different phase states. This forms the information signal $I(t)$. The output of the data source is a 2 Mbps bit stream. As the information signal is formed by splitting the data stream into two-bit segments, the information signal has a rate of 1 M-symbols/s. The in–phase (I) and quadrature–phase (Q) components of the signal are individually modulated by the PN code (spread spectrum signal), which is then filtered, and combined for transmission by the power driver.

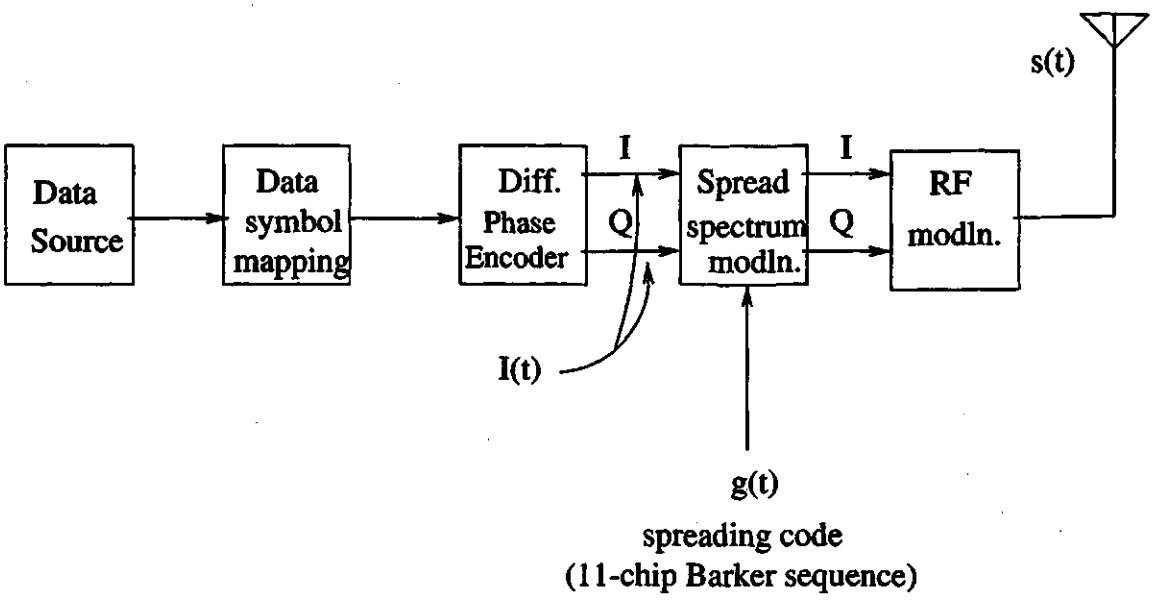

Figure 4.1: Modem Transmitter

The transmitted signal may be written as,

$$s(t) = Re\Big\{u(t)g(t)exp(j2\pi f_c t)\Big\}\,, \tag{4.1}$$

where $u(t)$ is the low pass complex envelope of the signal. This is also called the information signal, and is given by,

$$u(t) = \sum_n I_n.P_s(t - nT_s)\,, \tag{4.2}$$

where

T_s	=	the symbol period of the information signal,
$P_s(t)$	=	denotes a rectangular pulse of unit height and duration T_s, and
I_n	=	information vector, $exp(j\theta_n)$, with four phase states: $(\pi/4, -\pi/4, 3\pi/4, or\ -3\pi/4)$.

Equation 4.1 is composed of two components. I_n contains the complex information vector, and $g(t)$ is the spread spectrum modulating waveform. $g(t)$ contains the fast-time transitions needed for bandwidth expansion. The spread spectrum waveform, $g(t)$, is given by,

$$g(t) = \sum_k g_k P_c(t - kT_c)\,, \tag{4.3}$$

where,

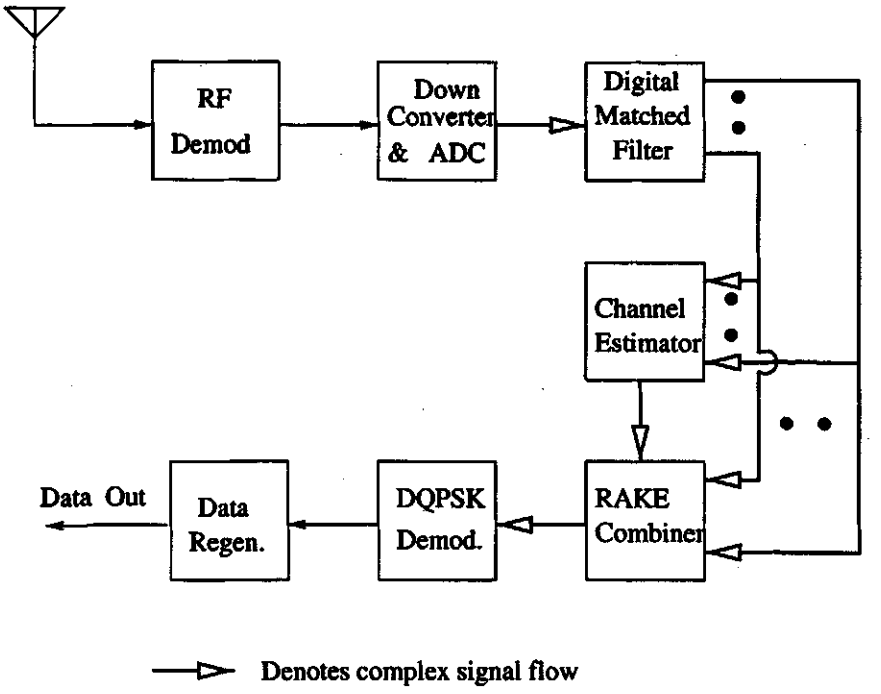

Figure 4.2: Modem Receiver

g_k = the spread spectrum impulse response,
T_c = the chip duration, and
$P_c(t)$ = denotes a rectangular pulse of unit height and duration T_c.

The Barker sequence has been shown to have excellent autocorrelation properties, important for robust multipath reception [42]. An 11–chip PN code is specified in the IEEE 802.11 standard to keep the processing gain greater than but close to 10, which is the minimum processing gain specified by the FCC. An added advantage of using a short spreading sequence is that inter–path interference is minimized when using codes with good autocorrelation properties such as the Barker sequence.

4.1.2 Receiver

The information signal is transmitted over the time-variant, multipath fading, indoor channel, and thus the receiver needs to be designed appropriately and is in general more complex than the transmitter. The receiver structure is shown in Figure 4.2. The receiver is a path combining diversity receiver, also known as a RAKE receiver.

The RF signal is first down converted to quadrature baseband signals to allow the implementation of the multipath combining receiver. The matched filter performs the cross–correlation between the spreading code (the 11–chip Barker code)

and the quadrature signals. For each received symbol, the matched filter output consists of a succession of correlation peaks. The number of such peaks depends upon the number of resolvable paths. The relative position of the peaks and their amplitude correspond to the delay, amplitude and phase of the resolvable paths for that symbol. The RAKE receiver implementation uses the RAKE–correlator and the RAKE –combiner, the combination of which deconvolves the transmitted signal from the channel impulse response. Such an implementation requires that the impulse response of the RAKE–correlator and combiner be the time reversal of the channel impulse response. The output of the RAKE–combiner is the estimate of the transmitted information signal. Demodulation of this output gives the detected data symbol.

In the following sections, the various blocks in the receiver structure are explained.

4.1.2.1 RF Demodulation

This stage is responsible for the down conversion of the RF signal to quadrature baseband signals.

With the channel impulse response as given by the Equation 3.4, the received signal $r(t)$ is given by

$$r(t) = Re\{\sum_{l=1}^{L-1} a_l(t)u(t-\tau_l)g(t-\tau_l)e^{(j\omega_c t+\theta_l)}\} + n_c(t)\cos\omega_c t - n_s(t)\sin\omega_c t\ , \quad (4.4)$$

where $n(t)$ has been expressed in terms of its lowpass equivalent components $n_s(t)$ and $n_c(t)$.

The low–pass signals $x(t)$ and $y(t)$ are defined as

$$x(t) = \sum_{l=1}^{L-1} a_l(t)u(t-\tau_l)g(t-\tau_l)\cos\theta_l + n_c(t)\ , and \quad (4.5)$$

$$y(t) = \sum_{l=1}^{L-1} a_l(t)u(t-\tau_l)g(t-\tau_l)\sin\theta_l + n_s(t)\ . \quad (4.6)$$

Thus, Equation 4.4 for the received signal $r(t)$ can be rewritten as,

$$r(t) = x(t)\cos\omega_c t - y(t)\sin\omega_c t\ . \quad (4.7)$$

$$\bar{r}(t) = x(t) + jy(t)\,. \tag{4.8}$$

The above equation is also the complex lowpass equivalent of the received signal $r(t)$. The complex baseband signal is then processed by the RAKE–correlator and combiner, which is described in the next section.

4.1.2.2 RAKE receiver

The RAKE receiver allows diversity combining in a fading multipath environment. The signals of paths with a propagation delay difference for more than the spreading code chip duration can be resolved in the receiver. And since these paths have independent fading patterns, their signals can be combined for diversity gain. The RAKE receiver is a combination of the matched filter or the RAKE–correlator and the RAKE–combiner. The function of the RAKE–correlator and combiner is to deconvolve the transmitted signal from the channel impulse response. Hence, its impulse response should approximate the time reversal of the channel impulse response.

RAKE–correlator

The RAKE–correlator performs a set of cross–correlations between the spreading code and the complex baseband signal. The number of cross–correlations or the number of arms of the RAKE–correlator is less than or equal to the number of resolvable multipaths. The functional diagram of a RAKE–correlator is shown in Figure 4.3

The RAKE–correlator consists of L (the number of resolvable paths) arms, and the complex baseband signal, $\bar{r}(t)$ is despread by multiplying by the delayed code signal $g(t-\tau_l)$. The output of each arm is integrated from $t = \tau_l$ to $t = T + \tau_l$.

The output of each arm is, thus, given by,

$$R_l = \int_{\tau_l}^{T+\tau_l} \bar{r}(t) \cdot g(t-\tau_l)dt\,, \tag{4.9}$$

$$= 2 \cdot E \cdot \bar{\gamma}_l \cdot u(t) + \bar{N}_l \tag{4.10}$$

where E is the transmitted signal energy, and $\bar{N}_l$ is the sampled Gaussian noise component. Note that in $\bar{x}$ the bar is used to denote that x is complex. The

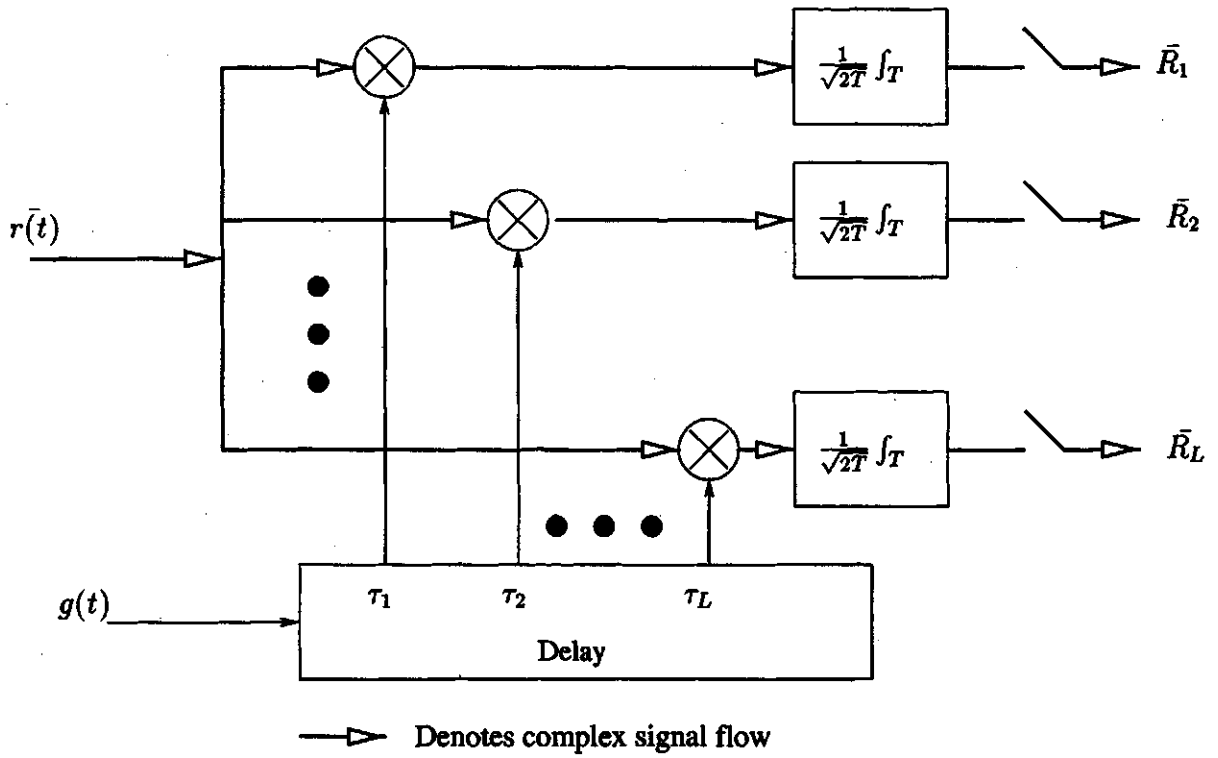

Figure 4.3: Functional block diagram of the RAKE–correlator

introduced l–th coefficient, $\bar{\gamma}_l = \gamma_l \cdot e^{j\theta_l}$, is given by

$$\bar{\gamma}_l = \int_{-\infty}^{\infty} R_{gg}(\xi - \tau_l) \cdot h(\xi) \cdot d\xi \,, \tag{4.11}$$

where $h(\xi)$ is the channel impulse response and the $R_{gg}(\xi)$ is the autocorrelation function of the spreading code $g(t)$. If $R_{gg}(\xi)$ has good autocorrelation properties, the $\bar{\gamma}_l$ will then be the corresponding path amplitude and phase, $\bar{\beta}_l = a_l e^{j\theta_l}$. The outputs R_l are then used by the RAKE–combiner to find a good estimate of the information signal.

RAKE–combiner

The output of the RAKE–correlator now consists of a succession of correlation peaks. The relative position of the peaks, amplitude and the phase correspond to the delay, amplitude and phase of received resolvable paths for that symbol, if the spreading code $g(t)$ has good autocorrelation properties. These peaks are then fed into the RAKE combiner which uses one of the following combining methods for diversity gain [8],

- Selection combining: The path with the largest signal power is selected and paths with weaker signals are discarded
- Equal gain combining: Signals of all received paths are treated on par and are added equally.
- Maximal ratio combining: Signals from individual paths are combined in such a way that the signals from stronger paths are given more weightage than the ones from weaker paths.

The RAKE–combiner discussed here is a maximal ratio combiner. The maximal ratio combiner uses the estimate of the complex path weights $\hat{\bar{\beta}}_l$ given by the channel estimator to compute the coherent sum of the weighted peaks R_i. The output of the RAKE–combiner, $\bar{z}$, is given by,

$$\bar{z} = \sum_{l=1}^{L} R_l \cdot B_l^* \,, \tag{4.12}$$

where $B_l = \hat{\bar{\beta}}_l$ and R_l is given by Equation 4.17.

The RAKE receiver implementation is characteristic of a spread spectrum communication system, where the transmission bandwidth is much larger than the coherence bandwidth and the chip duration smaller than the multipath delay spread.

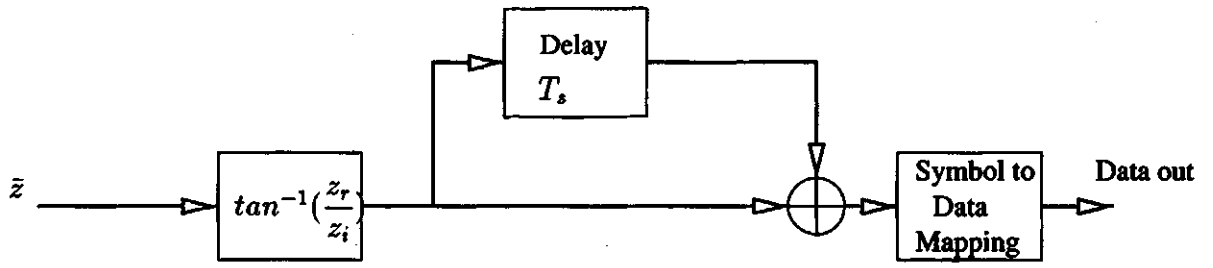

Figure 4.4: Differential demodulator

4.1.2.3 Demodulator

The output of the RAKE receiver $\bar{z}$ is differentially demodulated by the DQPSK demodulator. The demodulator performs the difference between consecutive estimates of the information signal $\bar{z}$:

$$\Delta\theta_n = \theta_n - \theta_{n-1} \ , \tag{4.13}$$

where, θ is the phase of $\bar{z}$ which is given by,

$$\theta = tan^{-1}(\frac{z_r}{z_i}) \ .$$

The phase $\Delta\theta_n$ is then decoded into bits using the symbol to data mapping as shown in Table 3.1.1. The differential demodulator is shown in Figure 4.4. The regenerated data packet is checked for errors using the CRC (cyclic redundancy check), and acknowledgement is sent if the packet was received without errors. If the packet contained uncorrectable errors, the packet is asked to be resent.

In the following section, the bit error rate (BER) analysis of the wireless modem is described.

4.2 BER Analysis of the Wireless Modem

This section deals with the bit error rate performance analysis for the wireless modem discussed in the previous section. The mathematical model of the wireless modem follows the one described in Proakis [26].

The transmit signal for M–phase signalling waveforms is given by

$$s_n(t) = \sqrt{2P} \cdot Re\left\{u_n(t)g(t)e^{j2\pi f_c t}\right\} \ , \tag{4.14}$$

where $u_n(t)$ is given by

$$u_n(t) = P_s(t - nT_s)exp\left\{\jmath\frac{2\pi}{M}(n-1)\right\} \qquad n = 1, 2, \cdots, M\ , \tag{4.15}$$

where for 4–phase signalling, $M = 4$ and $P_s(t)$ denotes the rectangular pulse of unit height, T_s, which denotes the symbol period of the transmitted information and $g(t)$ is the spreading code waveform, which is given by Equation 4.3.

Consider the case in which one of the four phase waveforms is transmitted for the duration of the signalling interval T_s. The received signal will then be

$$r_n(t) = s_n(t) \otimes h(t) + n(t)\ ,$$

where, $h(t)$ is the impulse response of the indoor channel as given by Equation 3.4 and $n(t)$ denotes the additive, white, complex Gaussian noise. In the wireless modem discussed, the transmitted bandwidth is larger than the coherence bandwidth and the multipath delay spread is larger than the chip duration. This allows for the multipath signals to be resolved. Let L be the total number of resolved paths. Then each of these paths will experience independent fading. Hence, the amplitude and phase of each of these paths are independent.

The matched filter, or the RAKE–correlator, consists of L arms, and for each of these L arms, the received signal, $r(t)$ is despread by multiplying by the delayed code signal $g(t - \tau_l)$. The output of each arm is integrated from $t = \tau_l$ to $t = T + \tau_l$.

Therefore, the output of each arm is

$$R_l = \int_{\tau_l}^{T+\tau_l} r_n(t) \cdot g(t - \tau_l)dt \tag{4.16}$$

$$= 2 \cdot E \cdot \bar{\gamma}_l \cdot u_n + \bar{N}_l\ , \tag{4.17}$$

where E is the transmitted signal energy, $\bar{N}_l$ is the sampled Gaussian noise component, and u_n is the sampled information signal. Note that, in $\bar{x}$ the bar is used to denote that x is complex. The introduced l–th coefficient, $\bar{\gamma}_l = \gamma_l \cdot e^{\jmath\theta_l}$, is given by

$$\bar{\gamma}_l = \int_{-\infty}^{\infty} R_{gg}(\xi - \tau_l) \cdot h(\xi) \cdot d\xi\ , \tag{4.18}$$

where $h(\xi)$ is the channel impulse response, and it has been assumed that there is no ISI, since the symbol duration T_s is much larger than the maximum multipath

delay spread. $R_{gg}(\xi)$ is the autocorrelation function of the spreading code $g(t)$. If $R_{gg}(\xi)$ has very good autocorrelation properties, then, $\bar{\gamma}_l$ will equal the complex path amplitude and phase given by, $\bar{\beta}_l = a_l \cdot e^{j\theta_l}$, where a_l is the path amplitude and θ_l, the path phase. Thus, the Equation 4.17 may be rewritten as,

$$R_l = 2 \cdot E \cdot \bar{\beta}_l \cdot exp\left\{ j\frac{2\pi}{M}(n-1) \right\} + \bar{N}_l \,, \tag{4.19}$$

where u_n has been substituted by Equation 4.15. As the noise samples, $\bar{N}_l$, and each of the path amplitudes and phase are statistically independent, the output of the matched filter consists of L statistically independent signals. In order for the demodulator to decide which of the M phases was transmitted in the signalling interval $0 \leq t \leq T_s$, it attempts to undo the phase shift introduced by each of the paths of the channel. In addition to correcting the phase, one would like to use a maximal ratio combiner in which each of the paths are weighted according to their path amplitudes. This operation is done by a RAKE–combiner. The RAKE–combiner, multiplies each of the L arms of the output of the matched filter, with the complex conjugate of an estimate $\hat{\bar{\beta}}_l$ of the actual path amplitude and phase, $\bar{\beta}_l$, provided by the channel estimator. The result is then added, and then is sent to the demodulator.

As the indoor channel has been shown to be quasi–stationary over the duration of the entire MPDU, the estimate of the channel path amplitude and phase can be done by using the information signals received in the previous signalling intervals. The estimate can be improved by extending the time interval over which it is formed to include several prior signalling intervals, as described in [25]. In general, where the estimation interval is the infinite past, the normalized estimate is given by,

$$\hat{\bar{\beta}}_l = \bar{\beta}_l + \frac{\sum_{i=1}^{\infty} c_i N_{ki}}{\sqrt{E_b}\left(\sum_{i=1}^{\infty} c_i\right)} \,, \tag{4.20}$$

where c_i is the weighting coefficient on the subestimate of $\hat{\bar{\beta}}_l$ derived from the ith prior signal interval and N_ki is the sample of additive Gaussian noise at the output of the filter matched to $u_i(t)$ in the ith prior signalling interval.

The demodulator input forms the sum of the product of $\hat{\bar{\beta}}_l$ and R_l over the L paths. The random variable that results is given by

$$\begin{aligned} \bar{z} &= \sum_{k=1}^{L} R_l \cdot B_l^* , \\ &= z_r + \jmath\, z_i , \end{aligned} \tag{4.21}$$

where $B_l^* = \hat{\bar{\beta}}_l^*$ and $*$ is used to denote complex conjugation, $z_r = Re\{z\}$ and $z_i = Im\{z\}$. The phase of $\bar{z}$ forms the decision variable, which is given as,

$$\theta = tan^{-1}\frac{z_r}{z_i} = tan^{-1}\frac{Im\left(\sum_{l=1}^{L} R_l \cdot B_l\right)}{Re\left(\sum_{l=1}^{L} R_l \cdot B_l\right)} . \tag{4.22}$$

The above expression for the decision variable is the same as given in Equation 7A.7, in Proakis [26]. The derivation that follows, takes a similar path as in the book.

In order to find the probability of a bit in error, it is necessary to find $p(\theta)$, which is the probability density function of θ, conditional on the transmitted signal phase. To simplify the analysis, the transmitted signal phase is assumed to be zero, i.e., $n = 1$. The pdf of θ, conditional on the other transmitted signal phases can be obtained by translating $p(\theta)$ by the angle $2\pi(n-1)/M$. Since the $\bar{\beta}_l$ are complex-valued numbers, which are statistically independent and identically distributed, complex, zero mean, Gaussian random variables, the random variables (R_l, B_l) are correlated, complex–valued, zero mean, Gaussian, and statistically independent and identically distributed with any other pair (R_i, B_i).

In evaluating the probability density function $p(\theta)$, first, the characteristic function of the joint probability distribution function of z_r and z_i, need to found. The density $p(z_r, z_i)$ is then found by performing a double Fourier transform on the characteristic function. The transformation,

$$\begin{aligned} r &= \sqrt{z_r^2 + z_i^2} , \\ \theta &= tan^{-1}\left(\frac{z_i}{z_r}\right) , \end{aligned}$$

yields the joint pdf of the envelope r and the phase θ. Finally, integration of this joint pdf over the random variable r yields the pdf of θ.

The pdf of θ, $p(\theta)$, is then of the form,

$$\begin{aligned} p(\theta) &= \frac{(-1)^{L-1}(1-|\mu|^2)^L}{2\pi(L-1)!} \\ &\times\left\{\frac{\delta^{L-1}}{\delta b^{L-1}}\left[\frac{1}{b-|\mu|^2\cos^2(\theta-\epsilon)}+\frac{|\mu|\cos(\theta-\epsilon)}{(b-|\mu|^2\cos^2(\theta-\epsilon))^{3/2}}\right.\right. \\ &\left.\left.\times\cos^{-1}\left(-\frac{|\mu|\cos(\theta--\epsilon)}{b^{1/2}}\right)\right]\right\}\Bigg|_{b=1} . \end{aligned} \tag{4.23}$$

In this equation, the notation

$$\frac{\delta^L}{\delta b^L} f(b,\mu)\Big|_{b=1} ,$$

denotes the *Lth* partial derivative of the function $f(b,\mu)$ evaluated at $b=1$

where μ is given by

$$\mu = \frac{m_{rb}}{\sqrt{m_{rr}m_{bb}}} = |\mu|e^{\varkappa} ,$$

where by definition,

$$\begin{aligned} m_{rr} &= E(|R_l|^2) , \quad for\ all\ l , \\ m_{bb} &= E(|B_l|^2) , \quad for\ all\ l , \\ m_{rb} &= E(R_l \cdot B_l^*) , \quad for\ all\ l . \end{aligned}$$

In order to evaluate the probability of error, it is necessary to evaluate the definite integral,

$$P(\theta_1 \le \theta \le \theta_2) = \int_{\theta_1}^{\theta_2} p(\theta)\, d\theta ,$$

where θ_1 and θ_2 are the limits of integration and $p(\theta)$ is defined in Equation 4.23. The μ used henceforth is a real-valued term, since a complex-valued μ will cause a shift of ϵ in the $p(\theta)$, which is simply a bias term. The limits of integration are assumed to be in the range of $0 \le \theta \le \pi$, as $p(\theta)$ is an even function.

$$\begin{aligned} \int_{\theta_1}^{\theta_2} p(\theta)\, d\theta &= \frac{(-1)^{L-1}(1-\mu^2)^L}{2\pi(L-1)!}\frac{\delta^{L-1}}{\delta b^{L-1}} \\ &\times\left(\frac{1}{b-\mu^2}\left\{\frac{\mu\sqrt{1-[(b/\mu^2)-1]x^2}}{b^{1/2}}\cot^{-1}x\right.\right. \end{aligned}$$

$$- \cot^{-1} \frac{x b^{1/2}}{\mu \sqrt{1 - [(b/\mu^2) - 1]x^2}} \Bigg\} \Bigg)_{x_1}^{x_2} \Bigg|_{b=1} , \qquad (4.24)$$

where, by definition,

$$x_i = \frac{-\mu \cos\theta_i}{\sqrt{b - \mu^2 \cos\theta_i}} , \qquad i = 1, 2 .$$

In four–phase signalling, a Gray code is used to map pairs of bits into phases. For the transmitted signal, $u_1(t)$, then a single bit is in error, if the received phase is $\pi/4 < \theta < 3\pi/4$, and both the bits are in error if the received phase is $3\pi/4 < \theta < 5\pi/4$.

Thus, the probability of a bit error is,

$$P_{4b} = \int_{\pi/4}^{3\pi/4} p(\theta)\, d\theta \; + \; 2 \int_{3\pi/4}^{5\pi/4} p(\theta)\, d\theta . \qquad (4.25)$$

Solving Equation 4.24, the probability of bit error for four–phase signalling is,

$$P_{4b} = \frac{1}{2}\left[1 - \frac{\mu}{\sqrt{2 - \mu^2}} \sum_{l=0}^{L-1} \binom{2l}{l} \left(\frac{1 + \mu^2}{4 - 2\mu^2}\right)^l \right] . \qquad (4.26)$$

The cross–correlation coefficient μ for the clairvoyant estimate in Equation 4.20 can be shown to be [26],

$$\mu = \frac{\sqrt{\nu}}{\sqrt{\left(\frac{1}{\hat{\gamma}_c} + 1\right)\left(\frac{1}{\hat{\gamma}_c} + \nu\right)}} , \qquad (4.27)$$

where by definition,

$$\nu = \frac{\left| \sum_{i=1}^{\infty} c_i \right|^2}{\sum_{i=1}^{\infty} |c_i|^2} ,$$

and,

$$\hat{\gamma}_c = \frac{E}{N_0} E\left(|\beta_l|^2\right) , \qquad l = 1, 2, \ldots, L . \qquad (4.28)$$

The parameter ν represents the effective number of signalling intervals over which the estimate is formed, and $\hat{\gamma}_c$ is the average SNR per path.

In case of differential signalling, the weighting coefficients are $c_1 = 1$, $c_i = 0$ for $i \neq 1$. Hence $\nu = 1$ and μ is given by

$$\mu = \frac{\hat{\gamma}_c}{1 + \hat{\gamma}_c} . \tag{4.29}$$

4.3 Summary

This chapter discussed the transmitter and the receiver design for a indoor wireless modem. The design of the wireless modem was based on the specifications provided by the IEEE 802.11 standard. The indoor channel for 2.4 GHz which impacts the design of the receiver was also discussed. The RAKE receiver using an optimal transversal filter diversity combiner was discussed. A theoretical analysis of the wireless modem with a optimal transversal filter diversity combiner was done to obtain a close form expression for the probability of bit error.

Chapter 5

System Design Alternatives

The indoor wireless modem was discussed in Chapter 4. In this chapter, improvements in the system design are considered which will deliver data at high speeds with an affordable retransmission rate.

Two well studied strategies for improvement of system performance are,

- Diversity reception and combining techniques, and
- Error correction techniques.

This thesis deals with improvements in the system using diversity reception and combining techniques [20].

5.1 Diversity reception

The signal conveyed through an indoor channel becomes impaired by long–term fading (shadowing) and short–term fading (Rayleigh). The shadowing is caused by a lack of power density, and this problem cannot be solved by diversity action at the stations alone. The macro-diversity action is accomplished by strategically placed base stations (action points). The simplest technique to maintain acceptable channel capacity (relative to the fading channel) is to increase the transmitted power. However, in doing so, the overall spectrum efficiency is reduced and the distance between frequency reuse transmitters must be greater to maintain acceptable interference levels. Moreover, there is a ceiling on the transmitted power level to be used by the stations as specified by the FCC standard and the IEEE 802.11 standard. Another technique often used is adaptive retransmission. A system operating in a time–variant indoor channel might generate too many ARQ (automatic retransmission requests) for reliable high speed reliable communications. Moreover, it was

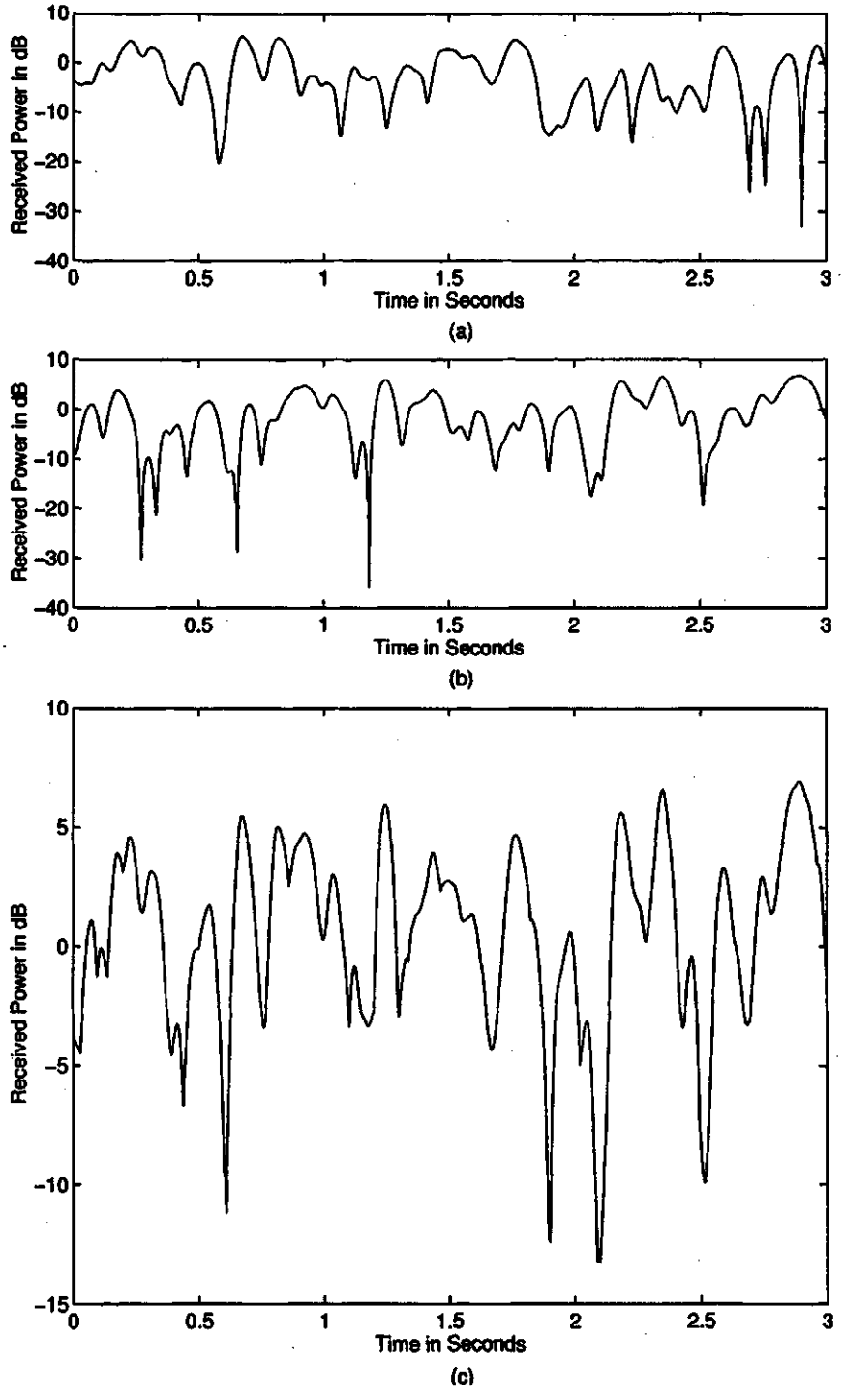

Figure 5.1: Diversity gain (a) and (b) shows two uncorrelated Rayleigh fading channels, and (c) shows selection diversity performed on them.

noted that the coherence–time of the channel is usually of the order of hundreds of milliseconds, which means the channel might be in a deep fade state for the duration of tens of packets. Alternative techniques to maintain channel capacity employ some kind of diversity scheme. The implementation of a diversity scheme and the obtainable improvement in signal statistics relies on the availability of two or more independently fading signals which have comparable mean signal levels [21] [6]. There are various methods of realizing independent signals for a diversity scheme: antenna diversity, time diversity and frequency diversity. In the design of the wireless modem, antenna and frequency diversity are used.

Frequency diversity is used by direct sequence spread spectrum to overcome multipath fading. It occurs when the signal appears to be received over distinct carriers. These carriers must be separated from each other by more than the coherence bandwidth of the channel so that each carrier experiences independent fading. The probability of then receiving a weak signal will be much reduced since fading will be independent for the distinct carriers. DSSS inherently uses frequency diversity when transmitting a signal with greater bandwidth than the channel's coherence bandwidth. Frequency diversity was discussed in the previous chapter with RAKE receiver implementation.

Antenna diversity [16] improves the channel capacity at the expense of adding extra equipment(antenna, combiner) at the receiver. The basic idea is to receive the same transmitted signals via independent channels. For example, while one channel is experiencing fading, the other might not. Figures 5.1(a) and 5.1(b) show uncorrelated Rayleigh fading channels with the same Doppler spread (4 Hz). Each of these figures show deep fades of upto -40 dB. Figure 5.1(c) shows the use of selection diversity on the two uncorrelated Rayleigh fading channels. It can be noted that the deep fades are about -15 dB. The diversity gain achieved supports the usage of diversity at the expense of adding extra equipment.

5.1.1 Antenna Diversity

Antenna diversity is realized by receiving the signal with multiple antennas separated by some distances (space diversity) and/or with different polarity (polarization diversity). Space diversity requires multiple antennas to receive signals through independent fading channels where an antenna separation of about one wavelength or less is required when the waves arrive at the antenna from all angles. Space diversity calls for a larger antenna separation for broadside–incidence, when the waves arrive

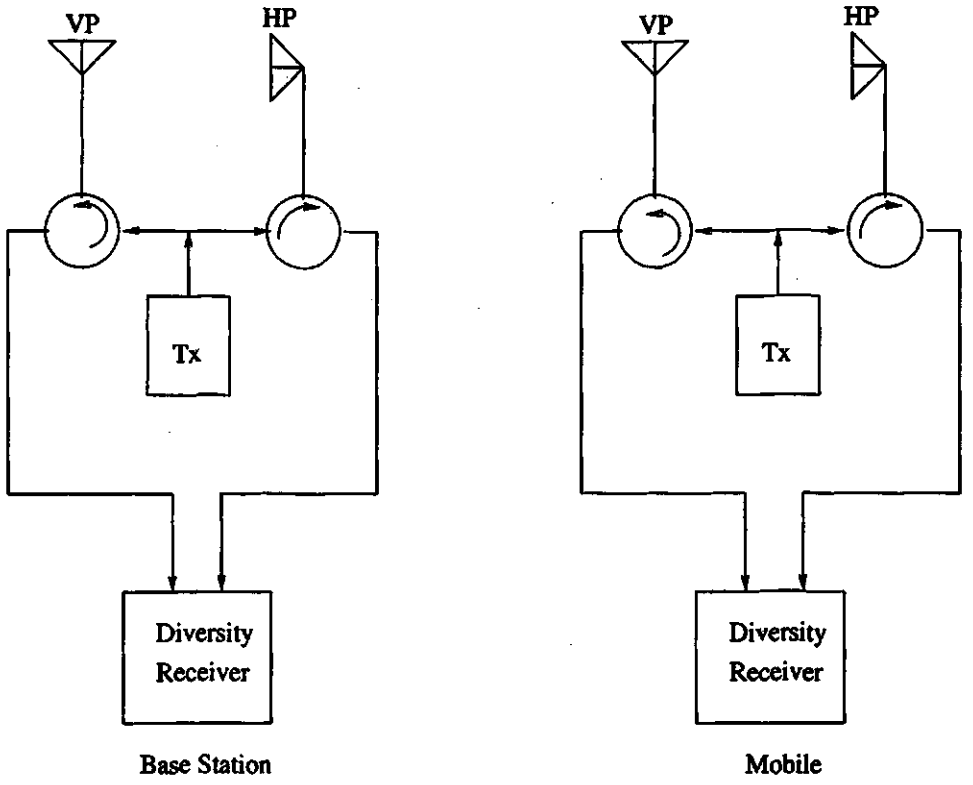

Figure 5.2: Polarization diversity system for outdoor mobile radio

through narrow angles as in the case of an elevated base station.

Considerable literature has dealt with the receiver antenna separation [12] [22] [34] needed to realize uncorrelated fading. Clarke [12] showed theoretically using electro-magnetic field components that the normalized correlation coefficient between spatially separated fields follows the squared Bessel function, in case of reception at the mobile where the waves arrive from all angles, in a Rayleigh fading environment. He showed that, for antenna separation of λ, $\lambda/2$ and $\lambda/4$, the correlation coefficients are 0.25, 0.06 and 0.03, respectively. Brennan [8] showed that a correlation coefficient of about 0.5 allows approximately the same diversity performance as in case of uncorrelated fading. Experimental evaluation of space diversity [16] [17] also corroborates the theoretical prediction. The indoor wireless LAN, will require smaller antenna spacing because, as in a typical office environment, the electro-magnetic waves arrive from all angles. For the 2.4 GHz ISM wireless communication, the spacing required for the spatial diversity branches is about 100 mm. Since the size of the modem is to be small, this allows for only a dual space diversity branch.

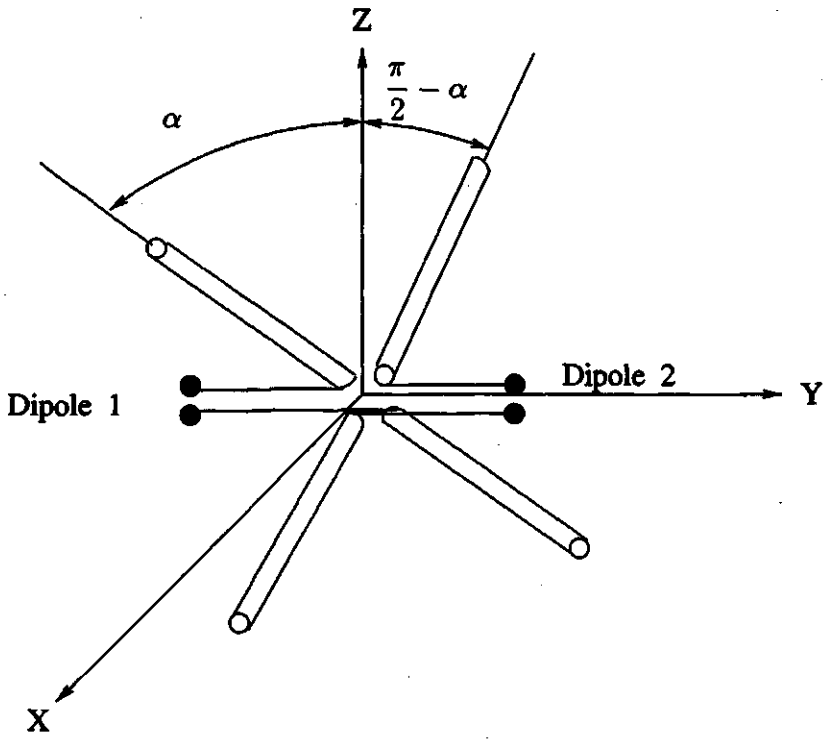

Figure 5.3: Cross–dipole antenna for polarization diversity

For further diversity reception, polarization diversity [32] is used. Polarization diversity provides a means of realizing independently fading signals without the need for physical separation of the antennas. It relies on the ability of scatterers in the path between the transmitter and the receiver to depolarize and decorrelate the signal giving rise to some coupling of energy into the orthogonal polarization. It was initially used as an alternative to the space diversity at the base station for mobile radio , where the implementation of space diversity will require spatial separation of antennas of over 30λ. For example, in the 900 MHz band, this will require a spatial separation of about 10 meters.

Polarization diversity for a mobile radio system is usually implemented with two antennas each, one vertically polarized (VP) and the other horizontally polarized (HP), for the transmitter and receiver, as shown in Figure 5.2. The spacing between the antennas is immaterial. This system performs the equivalent of a space diversity system, with the signals on the VP and HP arm of the receiver experiencing independent fading. The only drawback of this system is that the power requirement is increased by 3 dB. It was expected that because of the presence of reflectors and scatterers, a transmitter with a single antenna, say a VP antenna, will allow for cross–polarization coupling and polarization diversity could be implemented at the

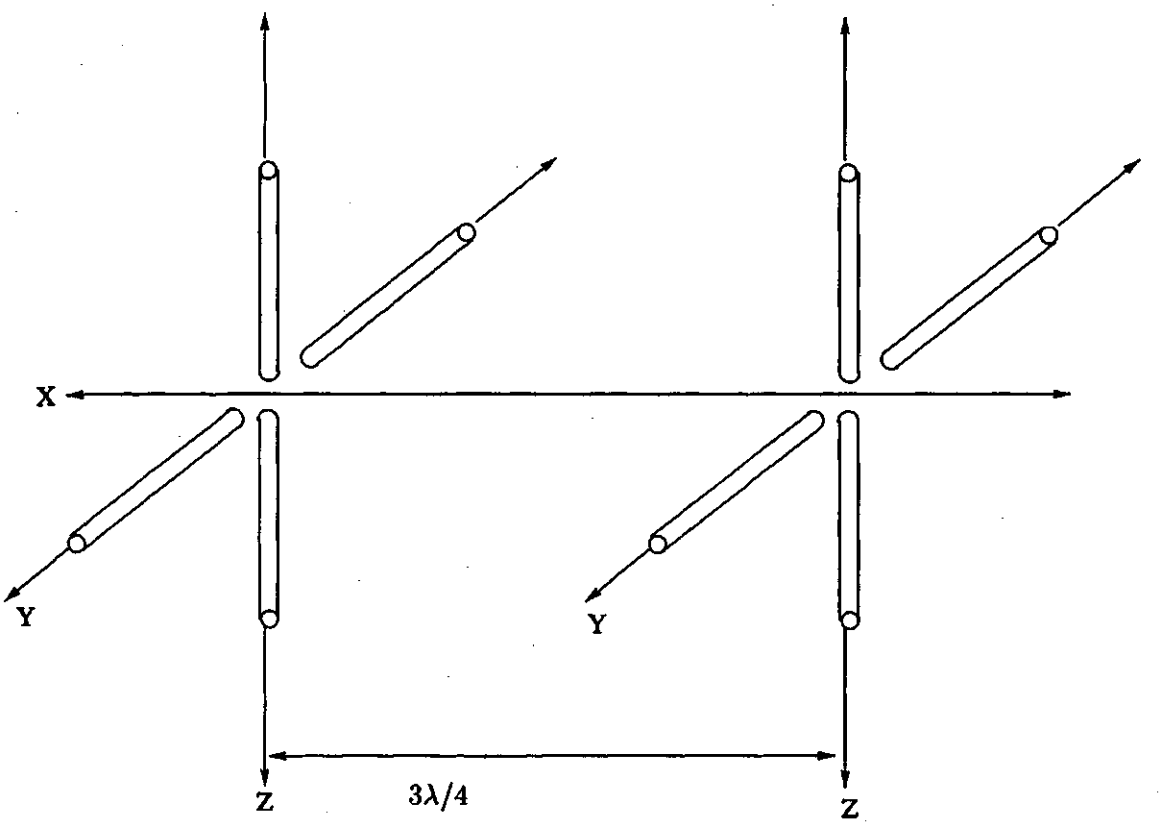

Figure 5.4: Antenna system for quad–diversity reception

receiver with a VP and a HP antenna. But experiments conducted in suburban areas [13] [33] showed a large difference in the mean signal level between the co–polarized and the cross–polarized branches, at about 6 dB. The cross–polarization discrimination (XPD), defined as the spread of the ratio of the two local means, was shown to be smaller for urban areas and in experiments conducted in indoor environments have yielded yet smaller XPD.

A considerable amount of literature has been focussed on the correlation properties of polarization diversity [4] [29] in the indoor mobile communication environments. Experiments with cross–dipole antenna diversity (shown in Figure 5.3 [29] has shown a low cross-correlation coefficient with the proper choice of the propagation parameters. When one dipole antenna is placed vertically and the other horizontally, i.e., $\alpha = 0°$, the branches are completely uncorrelated, since the vertical polarized radiation patterns of the antennas perpendicularly intersect each other in space. This zero correlation property is independent of the cross–polarization discrimination and the variation of the statistical distribution of the incident waves for other inclinations of the antenna system ($\alpha \neq 0$), the orthogonality of the antenna

pattern is not completely maintained and the correlation coefficient increases with the inclination angle α. In a mobile communications scenario, the portables could be inclined in at any angle, and hence the correlation coefficient will be a changing parameter. In the case of a wireless LAN, though mobility of the terminals is allowed by the IEEE 802.11 standard, in an indoor environment, the mobility of the computers is usually restricted to portability. Hence, the antenna pattern for the wireless modem discussed is the one with $\alpha = 0$, i.e., the correlation coefficient is assumed to be zero. Another reason for assuming uncorrelated VP and HP signals is because even non-zero but low cross-correlation coefficient (about 0.5), can yield diversity performances similar to uncorrelated branches.

The antenna system for the proposed wireless LAN is shown in Figure 5.4, where two cross-dipole antennas are shown separated by a spatial distance of $3\lambda/4$, which is about 10cm. Such an arrangement will provide quad-diversity branches at the receiver with uncorrelated (or low cross-correlation) fading.

5.2 Neural-Network based Diversity Combining

The aim of diversity combining is to use diversity reception such that it leads to an improvement in the performance of the system. The choice of the technique for diversity combining depends upon computational cost, cost of implementation and performance. In Chapter 4, RAKE combining was discussed for diversity combining of frequency diversity reception. Diversity combining techniques for quad-diversity branches are also based on similar principles:

- Selection combining: A quad-diversity system is shown in Figure 5.5. The logic used for combining differs for different implementations of diversity combining. For selection diversity, the receiver selects the best one of the quad-diversity branches for further demodulation and detection.

- Equal gain combining: In equal gain combining, the signals from each of the diversity branches are treated equally for further demodulation and detection.

- Maximal-ratio combining: The signals from the diversity branches are treated according to their merit. For example, if one of the branches experiences fading, it will be given lesser weighting. That is, each of the quad-branches are co-phased and added with appropriate branch weighting factors. The weighting factor are usually an estimate of the channel parameters.

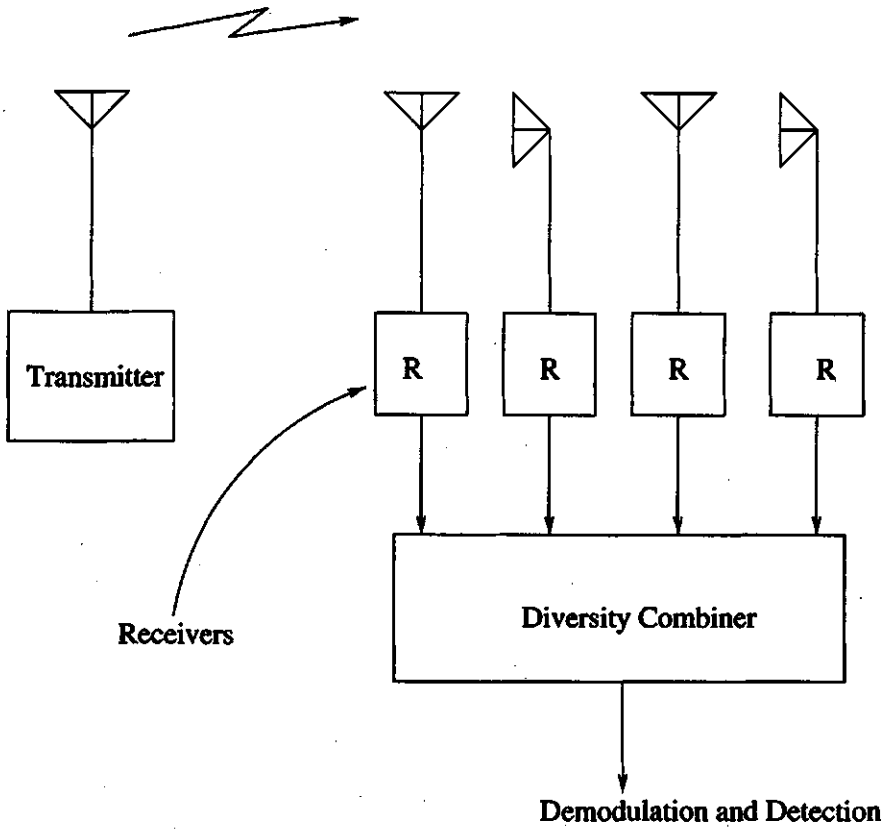

Figure 5.5: Quad–diversity branch with a diversity combiner

Of the above diversity combining techniques, the first two are simple and easy to implement, but the use to maximal–ratio combining needs sophisticated techniques where, an estimation of the channel parameters in needed. A number of algorithms have been proposed and studied, but they require that the received SNR be reasonably high for an acceptable estimate of the channel parameters. In a typical indoor wireless communication scenario, fading might last for as long as tens or even hundreds of MAC packets, and it might be that the wireless modem needs to work in an area were shadowing is inescapable. Hence, there is a need to study and investigate alternative diversity combining techniques which will allow the combiner to estimate acceptable channel parameters in low SNR conditions.

In this thesis, a novel approach to diversity combining using a neural network is proposed and its implementation investigated. The motivation for the use of neural networks for diversity combining arises from their ability to learn from the relationship between input and desired output variables with proper training [41] as well as to produce accurate outputs even when confronted with new data. This use of neural networks has led to its application to functional approximation, pattern recognition, adaptive signal processing, robotics, and they have recently been used in high speed networks for call routing. The application of neural networks to spread spectrum systems has been studied in various works [36] [38] [37] [39] [40]. In communication, neural networks have been used in channel equalisation [5] [38]. The application of a neural network to a class of channel equalisation problems for a high speed network [5] shows that the neural network performs better even under adverse SNR conditions, and when the channel is non–minimum phase, i.e., the poles and zeros lie outside the unit circle of the complex Z–plane. In this thesis, neural networks were used for diversity combining, where there is a need to characterise (learn) and to adapt to the time-variant fading indoor channel, even under adverse SNR conditions. Traditional digital signal processing has been used for this purpose but does not perform well under low SNR conditions. Through the experience gained in channel equalisation [5], it was prudent to investigate the application of a neural network for diversity combining. In the subsequent sections, the basics of neural networks are reviewed and receiver models using neural network diversity combining are studied.

5.2.1 The Multilayer Feedforward Neural Network

A neural network is generally a multiple–input multiple–output nonlinear mapping circuit, which can learn an unknown input–output relationship from a set of ex-

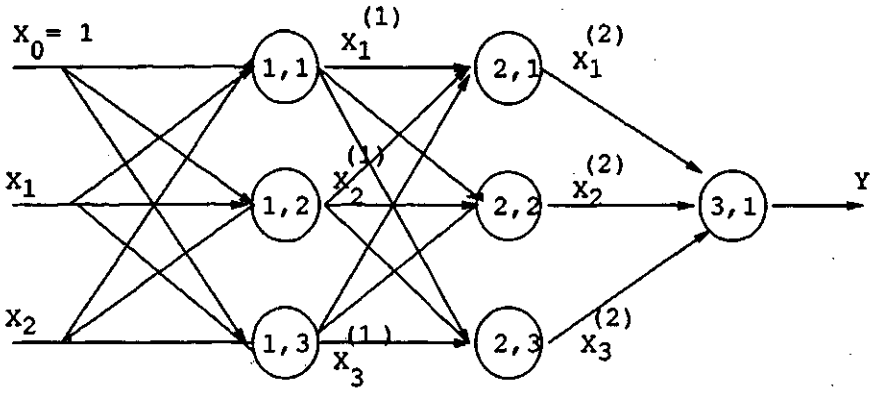

Figure 5.6: Multilayer Feed-forward Neural Network

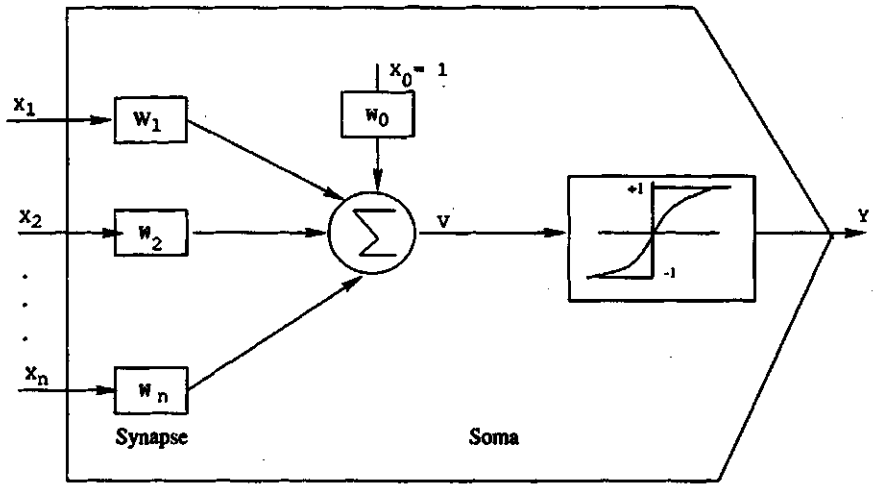

Figure 5.7: Neuron (processing element)

amples [41]. A neural network consists of many neurons connected to each other, each of which is a multiple–input single–output nonlinear circuit. Neural networks can be broadly divided into dynamic and static neural networks, where dynamic networks have feedback as compared to the static networks where the connection is feedforward only. The multilayer feed–forward neural network (MFNN) shown in Figure 5.6, is a three–layer neural network. The three layers are termed the input, the hidden and the output layer. The outputs of the each of the neurons of a layer are connected to the input of each of the neurons of the next layer.

The basic building block of a MFNN is a neuron (also called a processing element) as shown in Figure 5.7. The synapse shown in the Figure 5.7 is the process of multiplication of the inputs by their corressponding weights. The soma as shown in the Figure 5.7 is the process of summation and application of the non-linearity. For the i–th neuron, the net input y_i is given by

$$y_i = \sum_{j=1}^{n} W_{ij} x_j + w_0 x_0 \tag{5.1}$$

where W_{ik} is a connection weigth between the i–th neuron and the j–th neuron, x_j is the output of the j–th neuron, and x_0 is the bias. The relationship between the net input x_i and the output y_i is characterised by a transfer function, which is typically a nonlinear, continuous, nondecreasing and differentiable function. The sigmoidal function as given below is widely used,

$$x_i = \frac{exp(\lambda x) - exp(-\lambda x)}{exp(\lambda x) + exp(-\lambda x)} \tag{5.2}$$

where λ is the gain parameter. The above sigmoidal output, ranges from -1 to 1.

A neuron is a nonlinear mapping from *n−dimensional* input to *one−dimensional* output.

5.2.2 Back–propagation Algorithm

The neural network input–output relation can be modified by changing the set of weights values (vector). The back–propagation algorithm is widely used for adjusting the weight vector according to a set of input–output examples. The basic idea of this algorithm is a steepest descent gradient method in which the weight vector is updated by the gradient of the error function. The algorithm can be summarized as follows.

Let D be the training data set of m examples, represented as

$$D = \{(X_1, Y_1), (X_2, Y_2), \ldots (X_m, Y_m)\}$$

where X_i is the input vector to the neural network, and Y_i is the corresponding target output vector. For each input vector X_i, the weights are modified by the backward error corrections according to the following learning equation

$$W(t+1) = W(t) - \alpha \cdot \frac{\delta(Y_i - F(X_i))^2}{\delta W} \tag{5.3}$$

where, $W(\cdot)$ represents the connection weights, t indicates the number of weight updates, and α represents the learning rate, whose value is found empirically. $F(X_i)$ represents the neural network output values for the input X_i. This equation allows the connection weights to adjust so that the mean square error between the neural

network output and the desired output is minimized. The weight updating is repeated over the entire set of D training data set till an error goal is reached. After the neural network is trained, the neural network will produce the correct output for a given input vector. Even if the inputs are outside the training data set, the neural network gives outputs that are generalized and best fitted for the inputs.

5.2.3 MFNN Diversity Combiner (NNDC)

The need and motivation for a neural network based diversity combiner was discussed in the preceding sections. The design of the neural network diversity combiner is discussed in this section.

It is obvious that the neural network model discussed needs the knowledge of a desired output, when in the learning mode, or when updating its weights. The learning mode or the training mode is done by either of the two approaches: off–line learning and real–time learning. In off-line learning, a model of the real system is used and the neural network learns the statistics of the input to the neural network and adapts to it. Real–time learning is done during the operation of the system in a real life situation. The advantage of using off–line learning is that weight updating is not needed during the operation of the system and hence is faster, computationally. Real–time learning on the other hand requires weight updating during the operation and hence is computationally costly.

5.2.3.1 Off–line Learning

The use of off–line learning is done by training the neural network using a set of data already sampled, or data obtained from computer simulations. This is possible only for a good training data set, or when a good model of the entire system is available. The models used to train the neural network, should be supported by measurements made in the frequency band of use and subsequent studies on the models which fit the measurements in a statistical sense.

A neural network diversity combiner (NNDC) is shown in Figure 5.8. The output of the RAKE–correlator is given to the neural network. The input to the neural network is complex and since the neural network uses real input, the complex input is split into real and imaginary parts. The output of the neural network is a two–dimensional one, one for the real and the other for the imaginary part. The characteristics of the indoor channel was discussed in Chapter 4, with regards to

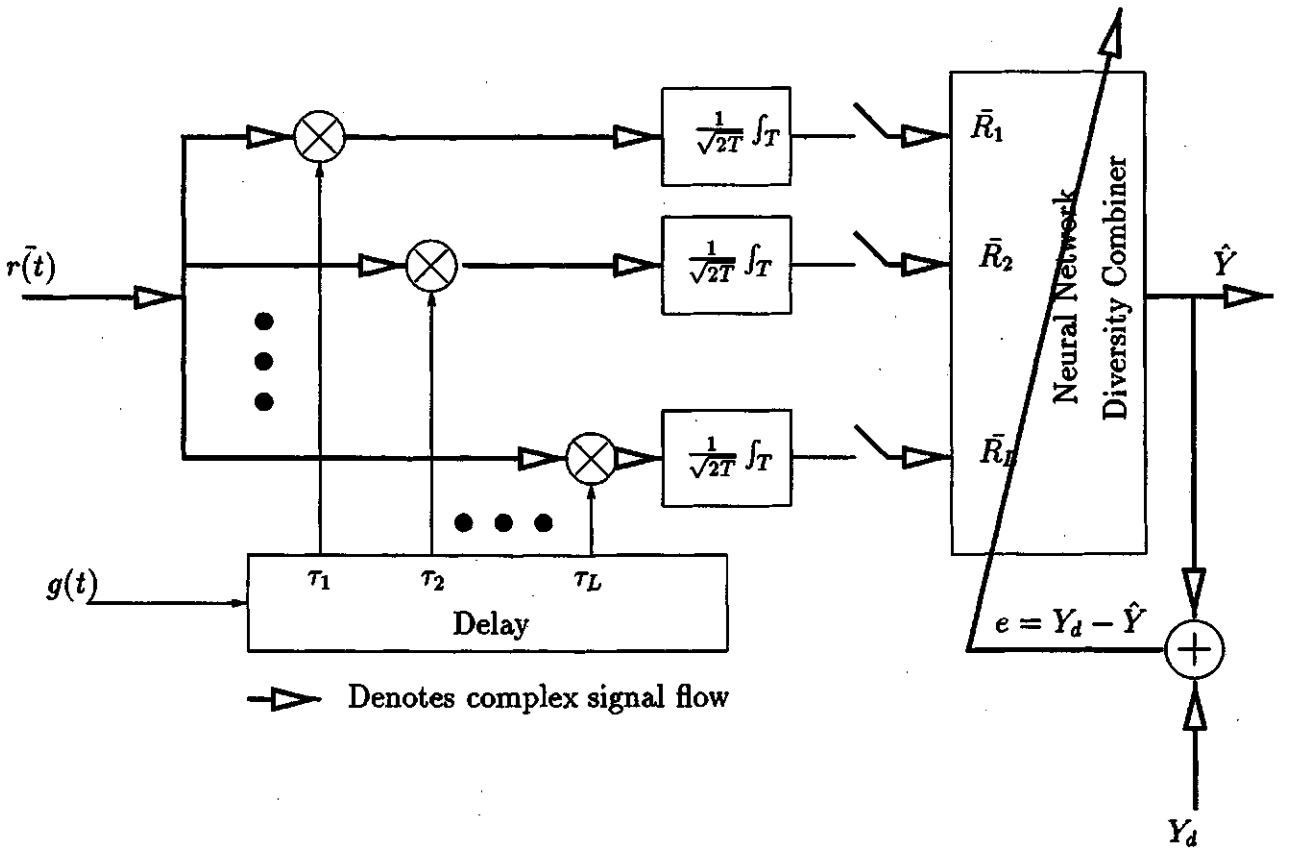

Figure 5.8: Neural Network Diversity Combiner

the 2.4 GHz ISM band. The number of resolvable paths was shown to be 2, for a non–diversity branch receiver. The path amplitudes for the 2.4 GHz band has been shown to follow various distributions like, Rayleigh, lognormal, Rice, or Nakagami, depending upon the indoor environment. In this thesis, it has been assumed to be a Rayleigh distribution, which has been found to be the case in many indoor environments. Learning by the NNDC is performed by updating the weights such that the output of the neural network approaches the desired output. The desired output is the complex differentially encoded information signal. The learning algorithm used is the back-propagation algorithm.

The NNDC with off–line learning is an attractive method, when there is good knowledge of the indoor environment. The NNDC does not need to adapt its weights when in operation, and hence is faster, but any deviation away from the statistical model may lead to potential pitfalls.

5.2.3.2 Real–time Learning

Real–time learning uses the same system as shown in Figure 5.8 but uses training data monitored in real time from a running system. Usually in a communication system, this means that the receiver needs to know the pattern which is being transmitted. But the IEEE 802.11 specifications allow the receiver to have knowledge of the desired (target) output. The IEEE 802.11 standard specifies a 128 bit synchronisation field in the front end of the packet. The synchronisation pattern can be preset such that all the wireless modems have the knowledge of it. Since the channel impulse response profile was shown to be constant for the duration of the entire packet, the NNDC can learn the channel conditions during synchronisation and it can be used to give the estimated output for the rest of the packet.

Real–time learning does not put any constraint on the distributions of the channel parameters, and hence can be used without any prior assumptions on the distributions of the path parameters. But the price paid comes in terms of computational cost, since weight updatng is required for every packet. In this thesis, we consider the real–time learning for the NNDC.

5.3 Improved Wireless Modem Receiver

The proposed wireless modem receiver is to have a four–diversity branch, two each for polarization and space. The diversity combining is to be performed by a neural

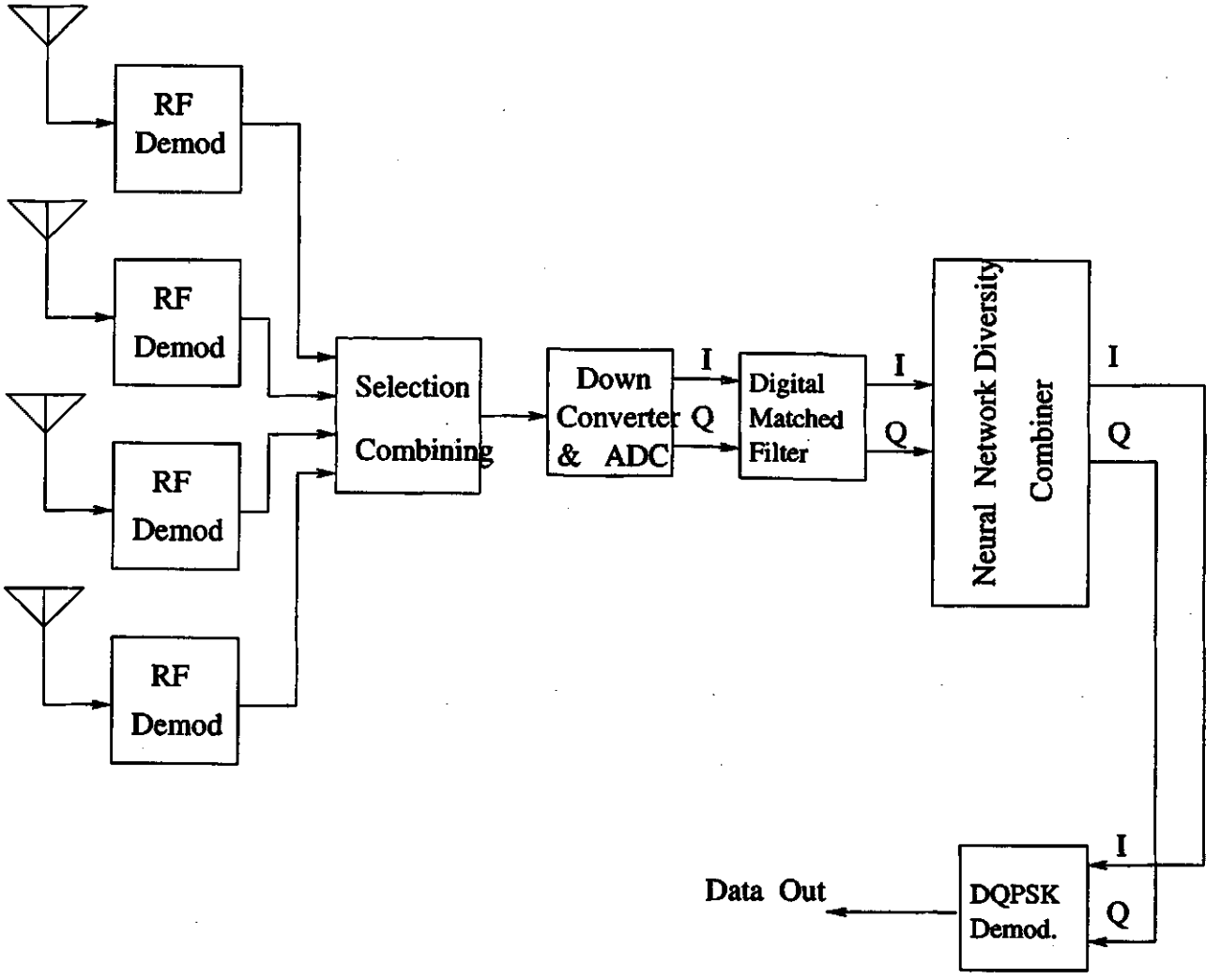

Figure 5.9: NNDC with selection combining (NNDC_SEL)

network. The NNDC can be operated in several ways for performance enhancement. This thesis studies different models and evaluates them by doing performance evaluation studies in terms of bit error rate with respect to SNR. The following models were used for performance evaluation studies.

5.3.1 NNDC with Selection Combining (NNDC_SEL)

The NNDC_SEL receiver model is shown in Figure 5.9. Selection diversity is used on the quad–diversity branch, and the signal from the selected branch is sent for further processing. The RAKE correlation is performed on the down converted and digitized signal from the selected branch. The delay spread for the indoor channel in the 2.4 GHz band is such that it allows two resolvable paths. Differential demodulation is done before the NNDC so that the diversity combiner doesn't need to do phase estimation. The output of the NNDC is fed to a data regeneration unit, which is a mapping from the phase state (symbol) to the data bits.

The number of neurons in the neural network should be low so as to keep the number of computations low. Experimentally, the number of inputs to the neural network was found to be 4, two neurons for each of the resolvable paths. This model will be computationally inexpensive since, lesser the number of neurons, lesser the number of weight updates.

5.3.2 NNDC with Dual–selection and Dual–full Diversity Combining (NNDC_2DSEL)

The NNDC_2DSEL receiver model is shown in Figure 5.10. Selection combining is performed on the dual space and the dual polarization diversity branches. The two selected branches are fed to the NNDC for diversity combining. The input to the NNDC is the differentially demodulated complex signal.

The requirement on the number of neurons in the neural network is expected to be more than that of the neural network used in NNDC_SEL. The number of inputs to the neural network is 8, four each for the two diversity branches. The computational complexity is more than that of NNDC_SEL.

5.3.3 NNDC with Quad–full Diversity Combining (NNDC_4D)

The NNDC_4D receiver model is shown in Figure 5.11. The signal from all the diversity branches is fed into the NNDC after they are differentially demodulated.

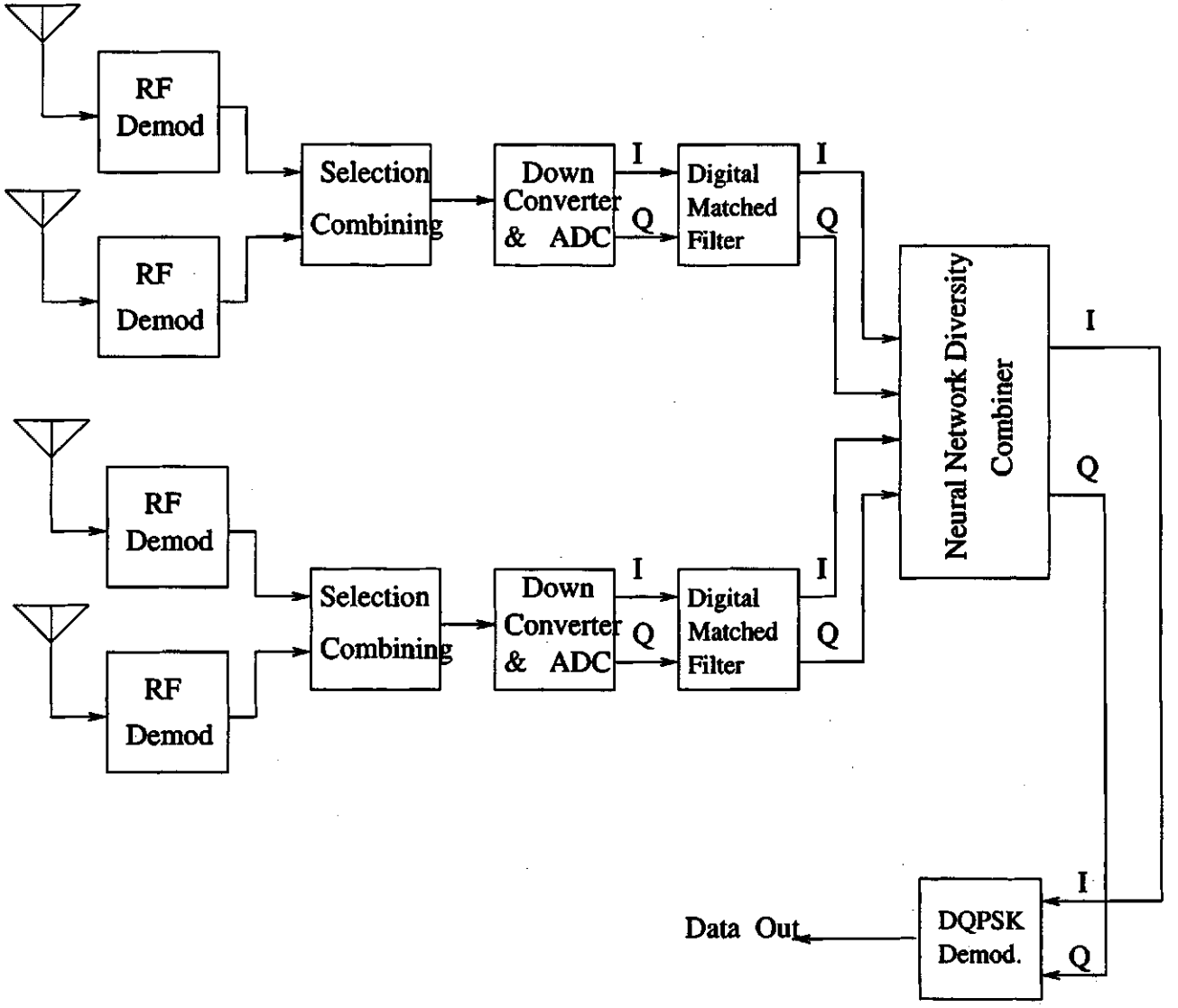

Figure 5.10: NNDC with dual-selection and dual-full diversity combining (NNDC_2DSEL)

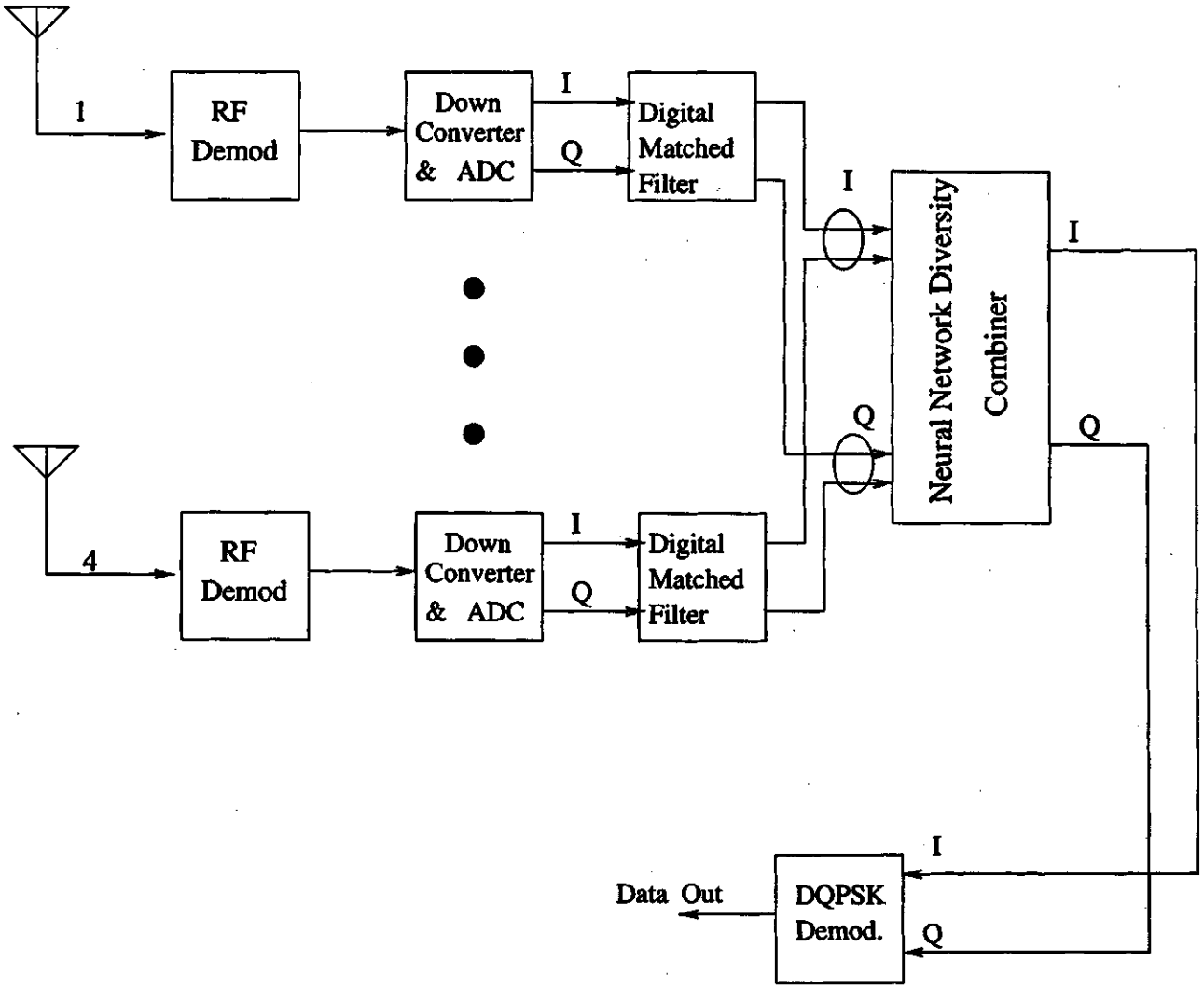

Figure 5.11: NNDC with quad-full diversity combining (NNDC_4D)

The number of inputs to the neural network is the highest: 16, four each for the four diversity branches. This will require the number of neurons to be more than NNDC_SEL and NNDC_2DSEL. The computational complexity will be the highest due to the large number of weight updates.

5.4 Summary

This chapter considered system design alternatives to the wireless modem discussed in Chapter 4. Diversity reception was used for improvement of the performance of the wireless modem, in terms of polarization and space diversity. The quad diversity branches were combined using a multilayer–feed-forward neural network, which is trained using a back-propagation algorithm. Two types of learning were considered: off–line learning and real–time learning. Different models for the wireless modem receiver were suggested for further performance evaluation studies, using a combination of selection and maximal ratio combining.

Chapter 6

Performance Evaluation Studies

In the previous chapter, various models of the wireless modem receivers were considered, using quad-diversity reception and a novel diversity combiner using a multilayer feed-forward neural network (NNDC). In this chapter, the simulation model used for the performance evaluation experiment is discussed for both optimal transversal filter diversity combiner (OTFDC) and NNDC. The BER performance studies of the various NNDC models discussed in Chapter 5, are evaluated against the wireless modem receiver using an OTFDC discussed in Chapter 4.

6.1 Simulation Model

The major components used for the computer simulation of the wireless modem are: DSSS transmitter, indoor channel, and the receiver. The simulation of the system is performed on the low-pass equivalent of the system. Simulation is based on samples picked from the various probability distributions that model the random processes in the wireless modem. This is performed a number of times to obtain BER estimates within a specified confidence interval.

6.1.1 Transmitter

The transmitter functions in a wireless modem are represented by appropriate models for the data source, digital modulation, and spread spectrum impulse response (spreading code). The signal waveform is denoted as,

$$u(t) = \sum_n I_n . P_s(t - nT_s) \tag{6.1}$$

where, T_s is the symbol period of the transmitted information, $P_s(t)$ denotes a rectangular pulse of unit height and duration T_s, and I_n denotes the information

vector, $exp(j\theta_n)$, with four phase states: $(\pi/4, -\pi/4, 3\pi/4, or -3\pi/4)$. The spread spectrum waveform is denoted as,

$$g(t) = \sum_m g_k P_c(t - mT_c) \tag{6.2}$$

where g_k is the spread spectrum impulse response, T_c is the chip duration, and $P_c(t)$ denotes a rectangular pulse of unit height and duration T_c.

The spreading code used is a 11–length Barker sequence. The data transmission is 2 Mbps, and the DQPSK modulation scheme, converts that to 1 Msymbols/s, which results in a symbol period, $T_s = 1\ \mu s$. Starting from bit 1, all odd numbered bits form one stream X_k, and all even numbered bits form the other stream Y_k. The bit pair (X_k, Y_k), is mapped onto differentially encoded signal phase using a Gray code as shown in the following table

1	1	$\frac{\pi}{4}$
1	1	$\frac{\pi}{4}$
1	1	$\frac{\pi}{4}$
1	1	$\frac{\pi}{4}$
1	1	$\frac{\pi}{4}$
1	1	$\frac{\pi}{4}$
1	1	$\frac{\pi}{4}$
1	1	$\frac{\pi}{4}$
1	1	$\frac{\pi}{4}$
1	1	$\frac{-3\pi}{4}$
1	0	$\frac{-\pi}{4}$

From the differential phase, $\Delta\phi_k$, the absolute phase angle for the k-th symbol, ϕ_k is given by:

$$\phi_k = \phi_{k-1} + \Delta\phi_k \tag{6.3}$$

The in-phase and quadrature components of the $\pi/4$ DQPSK signal corresponding to the k-th symbol are given by:

$$I_k = \cos\phi_k \tag{6.4}$$

$$Q_k = \sin\phi_k \tag{6.5}$$

The in-phase and quadrature phase components are spread using the 11–length Barker sequence. In an actual transmitter, the in-phase and quadrature components are passed through a filter to substantially limit the spectral power in the sidelobe outside the main lobe. The signal is then placed on a carrier and passed through a power amplifier. In simulation, we avoid the final two steps. The received symbol is obtained by passing the in-phase and quadrature components of the transmitted symbol through the lowpass equivalent of the indoor channel model.

6.1.2 Channel Model

The channel impulse response is assumed to be constant for the duration of the data packet. The quasi–stationary property of the channel is due to the large coherence time of the indoor channel. The complex low–pass equivalent impulse response of the bandpass channel for the link between the transmitter and the receiver is given by,

$$h(t) = \sum_{l=0}^{L-1} a_l \delta(t - t_l) e^{j\theta_l} \tag{6.6}$$

where a_l, t_l and θ_l are the path amplitude, time delay and the phase of the l-th path. Since the delay spread (from measurements) for the indoor channel is less than 200 nanoseconds and the chip period is 90.9 nanoseconds, the number of resolvable paths is 2, and hence $L = 2$. The path amplitude a_l is a Rayleigh distributed random variable, and θ_l is uniformly distributed in $0, 2\pi$. The Rayleigh distributed path amplitude is generated by the following method.

Let X be a uniformly distributed $0, 1$ random variable. An exponentially distributed random variable can be generated by using the following equation

$$Y = -ln(X) \tag{6.7}$$

where, Y has the probability distribution function as

$$f_Y(y) = \frac{1}{2\sigma^2} exp(-\frac{y}{2\sigma^2}) \tag{6.8}$$

To generate a Rayleigh random variable Z, the following equation is used,

$$Z = \sqrt{Y} \tag{6.9}$$

where, Z has the probability distribution function as

$$f_Z(z) = \frac{z}{\sigma^2} exp(-\frac{z^2}{2\sigma^2}) \tag{6.10}$$

with a variance $\sigma^2 = \frac{1}{2}$. The random variable Z represents the path amplitude.

The channel impulse response is changed for every data frame (packet) to take into account the time–variant nature of the indoor channel. Complex Gaussian noise is added to the output of the channel.

6.1.3 Receiver

The wireless modem receiver is a correlator type receiver. The receiver model consists of the RAKE correlator, differential detection, diversity combiner, the decision stage, and the symbol to data mapping.

The function of the correlator is implemented by multiplying the low–pass received signal with a spreading code aligned with the first path signal. This is followed by a summation which is equivalent to integration. Hence, the matched filter is a bank of correlators with each correlator aligned to a particular path signal. In case of a single branch receiver with no diversity, there will be two outputs for each of the resolvable paths. These are then fed to the diversity combiner.

- **Optimal transversal filter diversity combiner (OTFDC):** The OTFDC is a maximal ratio combiner. The transversal filter effectively weights each of the path signals by the respective path amplitude. The signals are then summed which forms the estimated information signal.

- **MFNN based diversity combiner:** In case of a neural network diversity combiner (NNDC), the in-phase and quadrature components of the outputs from the differential demodulator are given as the input to the NNDC. The weights of the NNDC are updated at the beginning of each data frame, where it uses the synchronisation bit pattern (128 bits long) to learn the channel conditions and uses the weights for the remainder of the data frame. The data is then regenerated by performing the inverse mapping, symbol to data.

To evaluate the bit error rate performance of the receiver, the variance of the complex Gaussian noise is changed. The above receiver model was discussed for a single branch receiver. The simulation flow chart for the quad–diversity receiver models is presented later.

6.2 Optimal Transversal Filter Diversity Combining (OTFDC)

The program construction for the OTFDC (or NO_NNDC) is shown in flow chart in three section of transmitter (Figure 6.1), the channel (Figure 6.2), and the receiver (Figure 6.3). The initialisation procedure includes frame length definition in number of bits, the number of frames to processed for obtaining BER estimates with sufficient confidence, and the 11–chip length Barker sequence. In the second step,

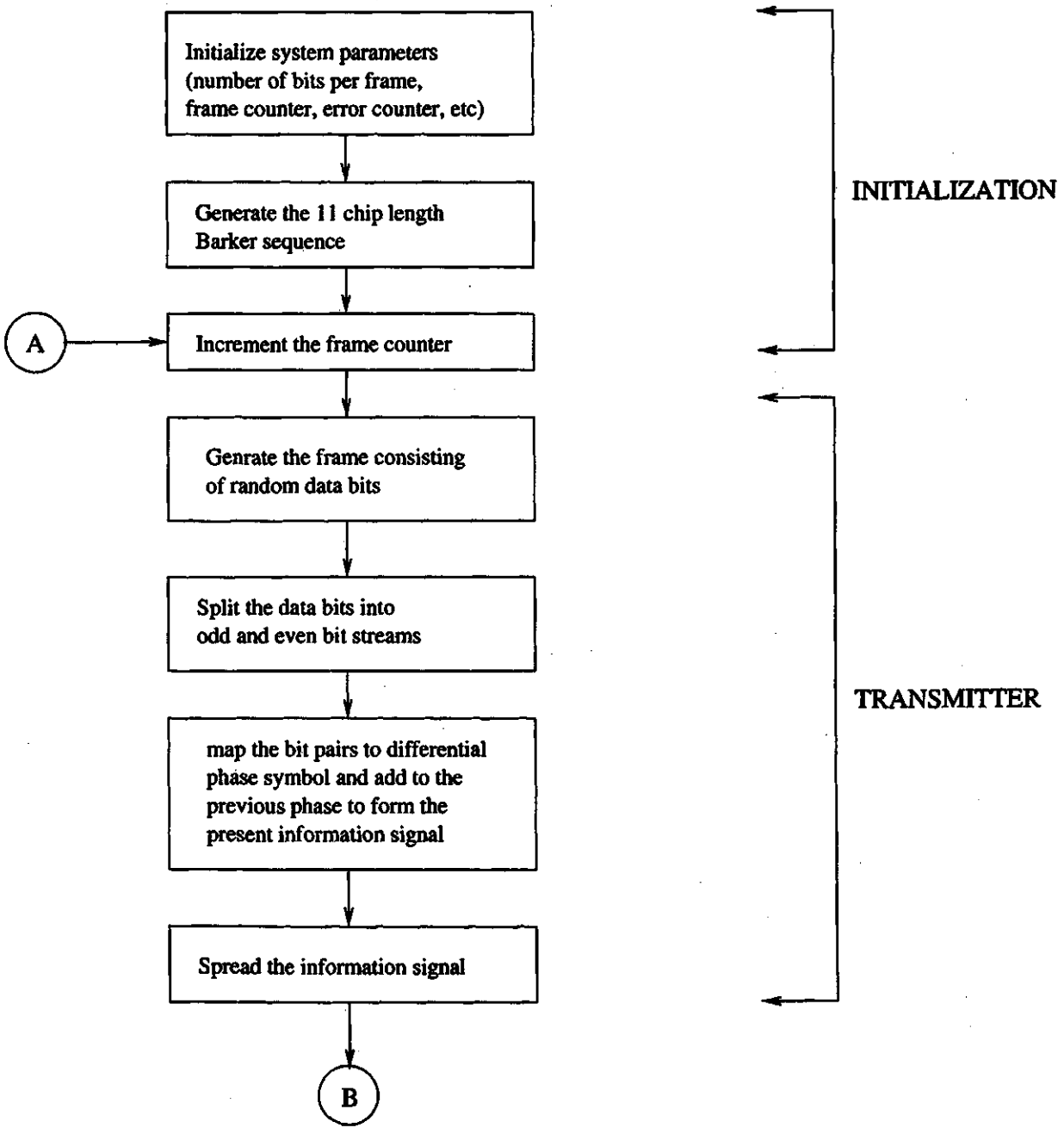

Figure 6.1: Flow chart of the transmitter section of the simulation program for BER performance evaluation of a OTFDC based receiver

the loop is repeated 20000 times. This loop consists of the transmitter, channel and the receiver section. An error detector and counter stage after the receiver section counts the number of bits in error.

For each iteration loop, a new data frame is generated consisting of random bits. The data frame is converted to the information signal (packet) by the DQPSK encoding scheme. The information signal is then spread using the 11–chip length Barker sequence spreading code.

In the channel section, D sets of channel impulse response are generated using uniformly distributed path phases, Rayleigh distributed path amplitudes and uniformly distributed path delays for the L resolvable paths, where D is the number of diversity branches at the receiver. The information signal is convolved with each of the channel impulse responses, and the output is added with independent, white, Gaussian noise for each of the D channels.

In the receiver section, the received signal in each of the D diversity branches is passed through a correlator or a RAKE receiver. The despreading in the correlator receiver is done with the spreading code aligned to the first path signal. The path signals at the matched filter output are maximal ratio combined using the OTFDC which is provided with the path amplitudes and phases of the D channels. The output of the combiner is summed and passed through the DQPSK demodulator. The demodulator outputs the estimated data bits.

6.2.1 Simulation Studies for OTFDC

The complete indoor wireless modem with the receiver based on the OTFDC was simulated and the BER performance evaluated using Monte Carlo techniques. Typically, to obtain a BER p, the symbol size required will be $\frac{10}{p}$. Such a choice will give a BER estimate in the confidence interval $[1.8p, 0.55p]$, at a confidence level of 0.95. In this case, the basic limit will be the minimum symbol size dictated by the BER, p, where p can found from the theoretical probability of bit error discussed in Chapter 4.

For each simulation run, the initial SNR was fixed and then modified at the end of the run when averaged after taking the channel path amplitudes into consideration. For each SNR, the simulation was rerun with different initial seeds. The simulated BER versus $\frac{E_b}{N_o}$ performance results are shown in Figures 6.4 and 6.5. Figure 6.4 shows the performance of a single branch receiver with no diversity

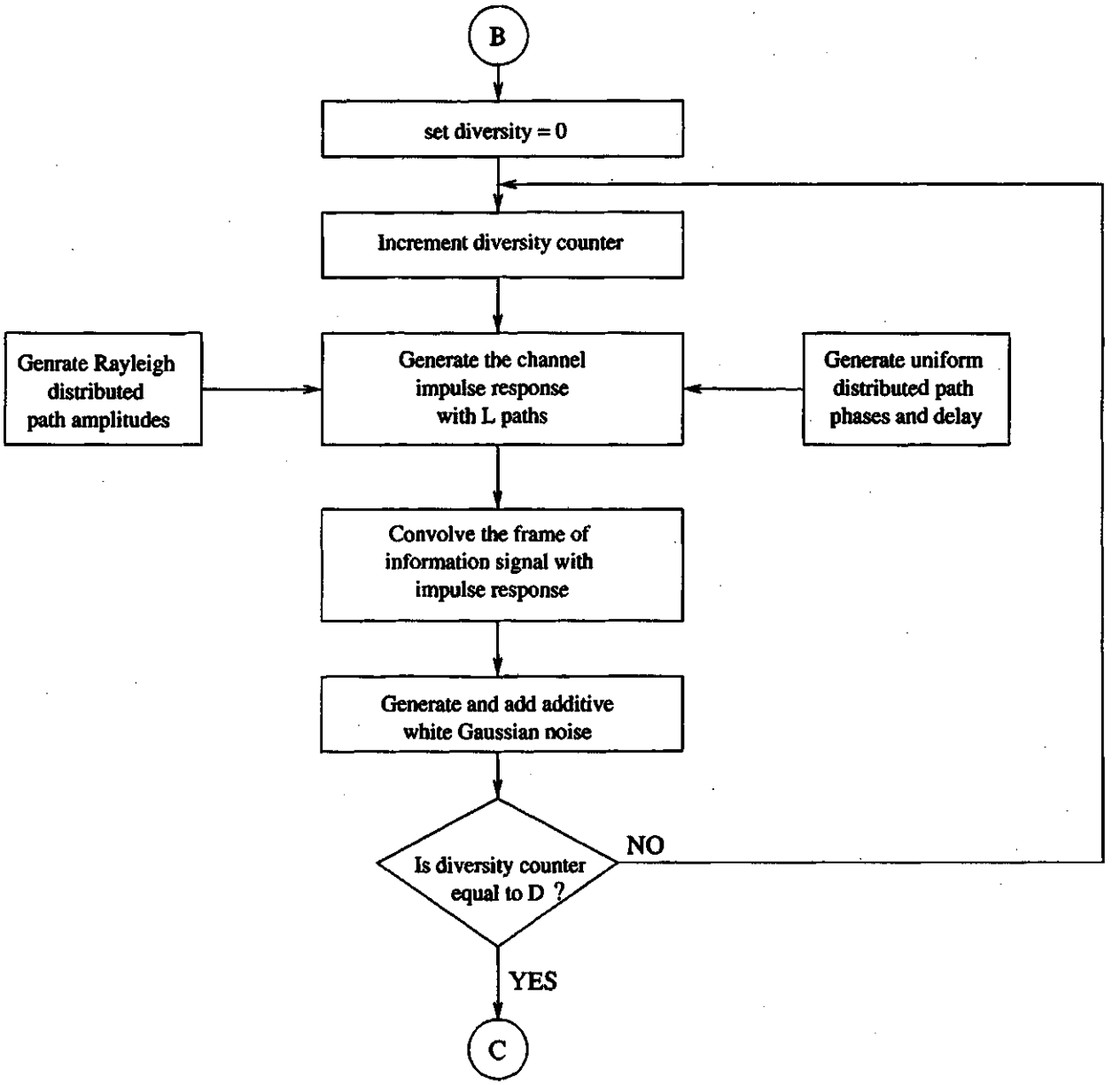

Figure 6.2: Flow chart of the channel section of the simulation program for BER performance evaluation of a OTFDC based receiver

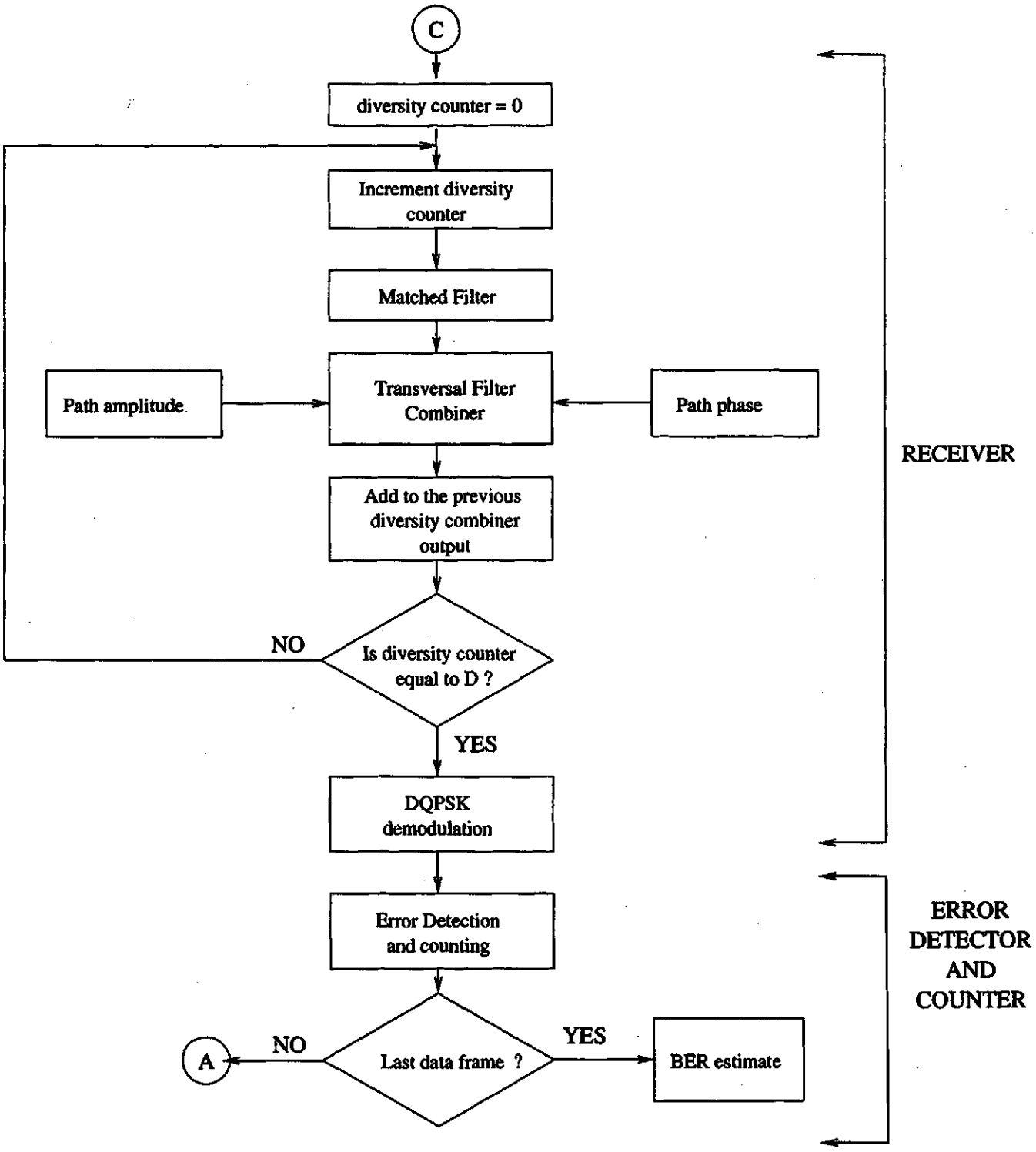

Figure 6.3: Flow chart of the receiver section of the simulation program for BER performance evaluation of a OTFDC based receiver

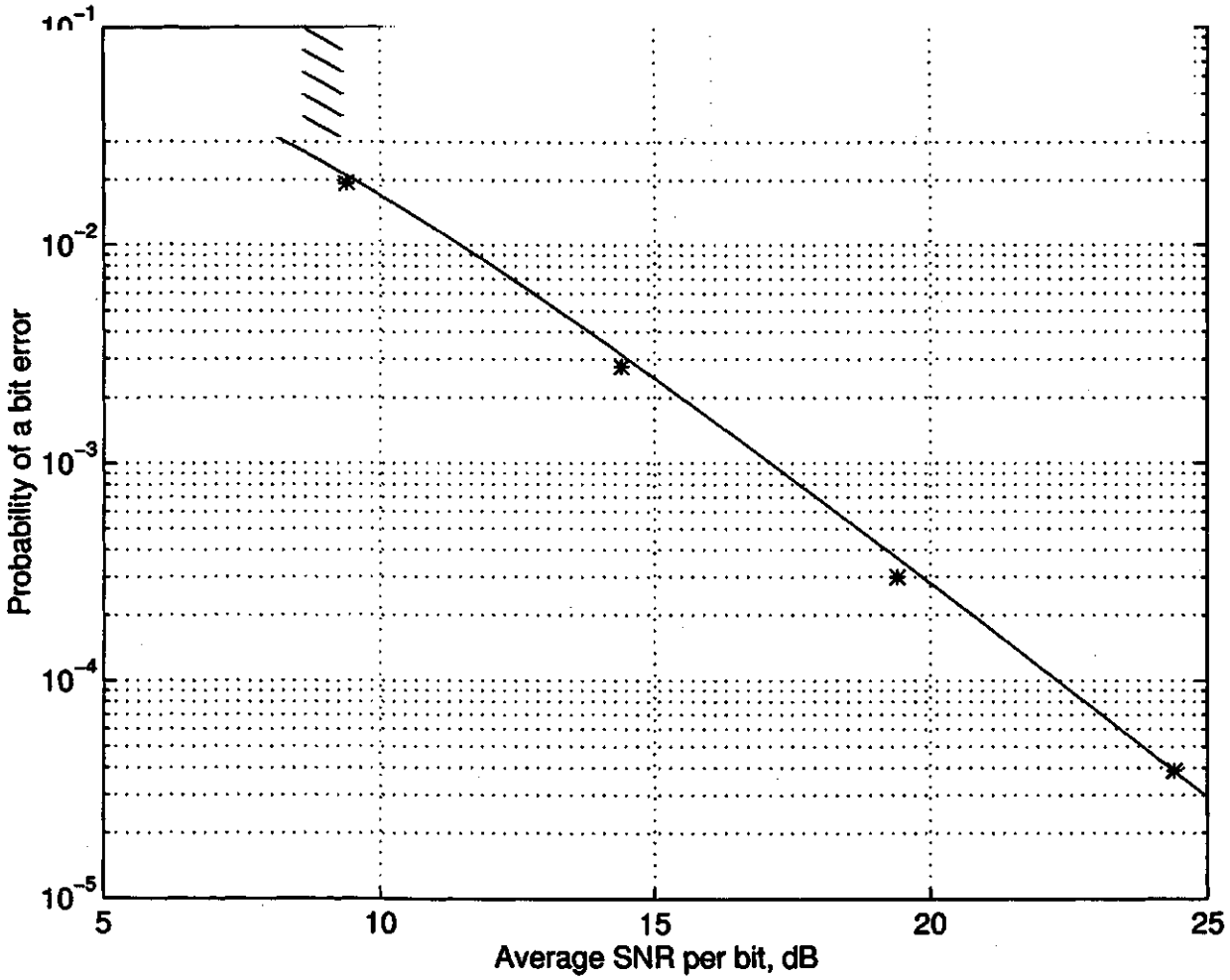

Figure 6.4: BER versus $\frac{E_b}{N_o}$ (analytical and simulated) for a single branch no diversity reception, OTFDC based receiver. The number of resolvable paths, L =2

reception, against the theoretical BER performance. The simulated BER results and theoretical performance agree well. Figure 6.5 shows the performance of the simulated quad–diversity receiver.

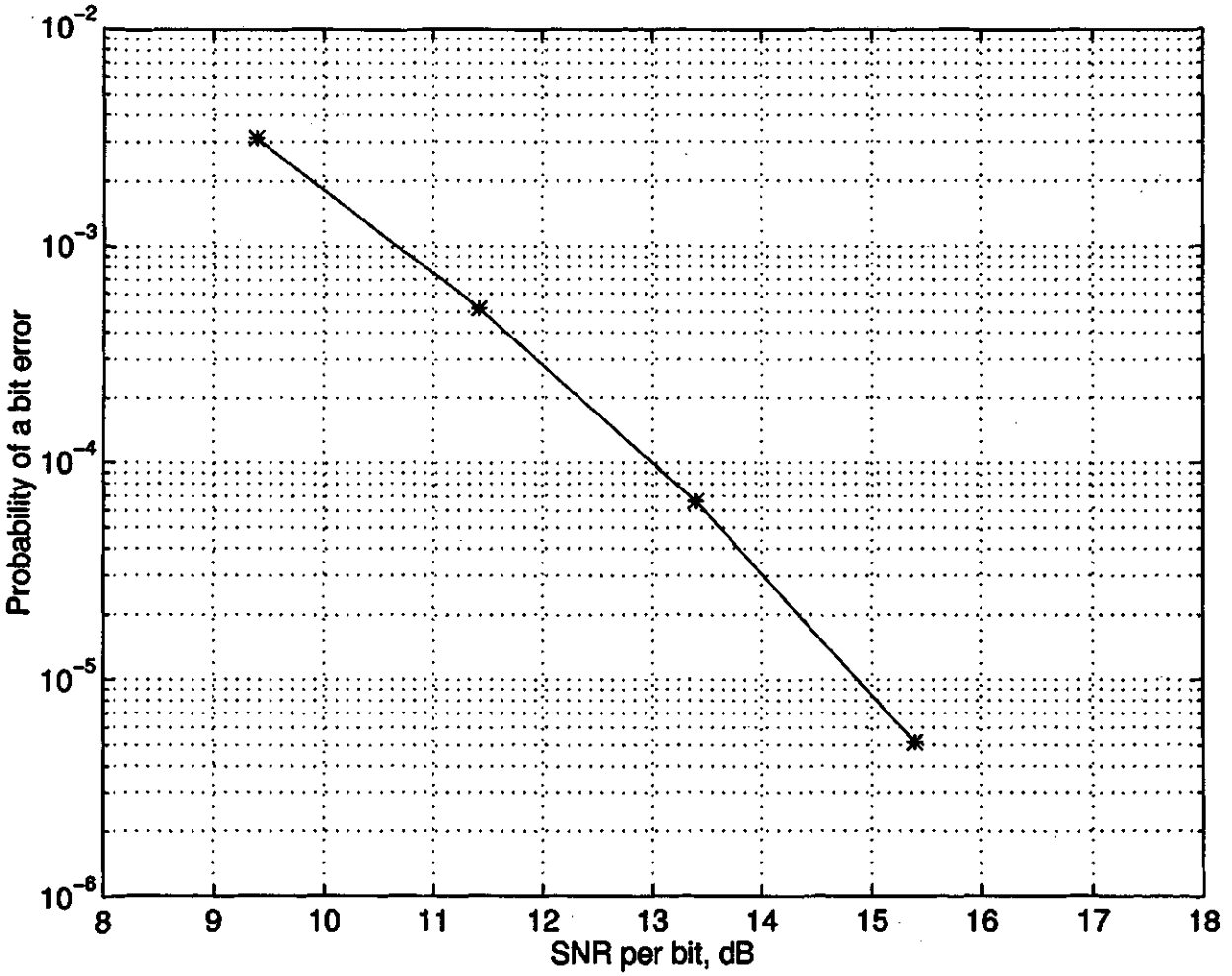

Figure 6.5: BER versus $\frac{E_b}{N_o}$ (simulation) for a quad diversity reception, OTFDC based receiver. The number resolvable paths, L =2

6.3 Neural Network Diversity Combiner

The program construction for MFNN based diversity combiner (NNDC) is shown in flow chart for the various receiver models. The initialisation, transmitter and the channel section is the same for all the three receiver models discussed in Chapter 5. The initialisation procedure includes, frame length definition in number of bits, the number of frames to processed for obtaining BER estimates with sufficient confidence, and the 11–chip length Barker sequence. The number of neurons per stage is also defined in the initialisation procedure. In the second step, the loop is repeated 20000 times. This loop consists of the transmitter, channel and the receiver section. An error detector and counter stage shown in Figure 6.10 after the receiver section counts the number of bits in error.

For each iteration loop, in the transmitter section (shown in Figure 6.6), a new data frame is generated consisting of random bits. The data frame is converted to the information signal (packet) by the DQPSK encoding scheme. The information signal is then spread using the 11–chip length Barker sequence spreading code.

The channel section for the simulation of the wireless modem using the NNDC is the same as that used for OTFDC, as shown in Figure 6.2.

The simulation of the various receiver models based on NNDC differ only in the receiver section.

1. **NNDC with full diversity combining (NNDC_4D)**: The flow chart for the simulation of the NNDC with full diversity combining (NNDC_4D), is shown in Figure 6.7. The received signal in each of the D diversity branches is passed through a correlator or a RAKE receiver. The despreading in the correlator receiver is done with the spreading code aligned to the first path signal. The path signals at the matched filter output are passed onto the NNDC. Since each symbol is complex, and the NNDC is real, the complex information signal is split into real and imaginary components and fed separately. The input to the NNDC hence forms a $2 \cdot D \cdot L$ length vector for each transmitted information signal. The NNDC learns the channel conditions during the 128 bit sync patterns in the beginning of a data frame, using the back–propagation algorithm. The 128 bit pattern or the 64 symbol information signal is given to the neural network P times. Such a procedure has shown to allow the neural network to monotonically reach the global minima. The remaining data frame is then fed to the NNDC, and its output is fed to the DQPSK demodulator.

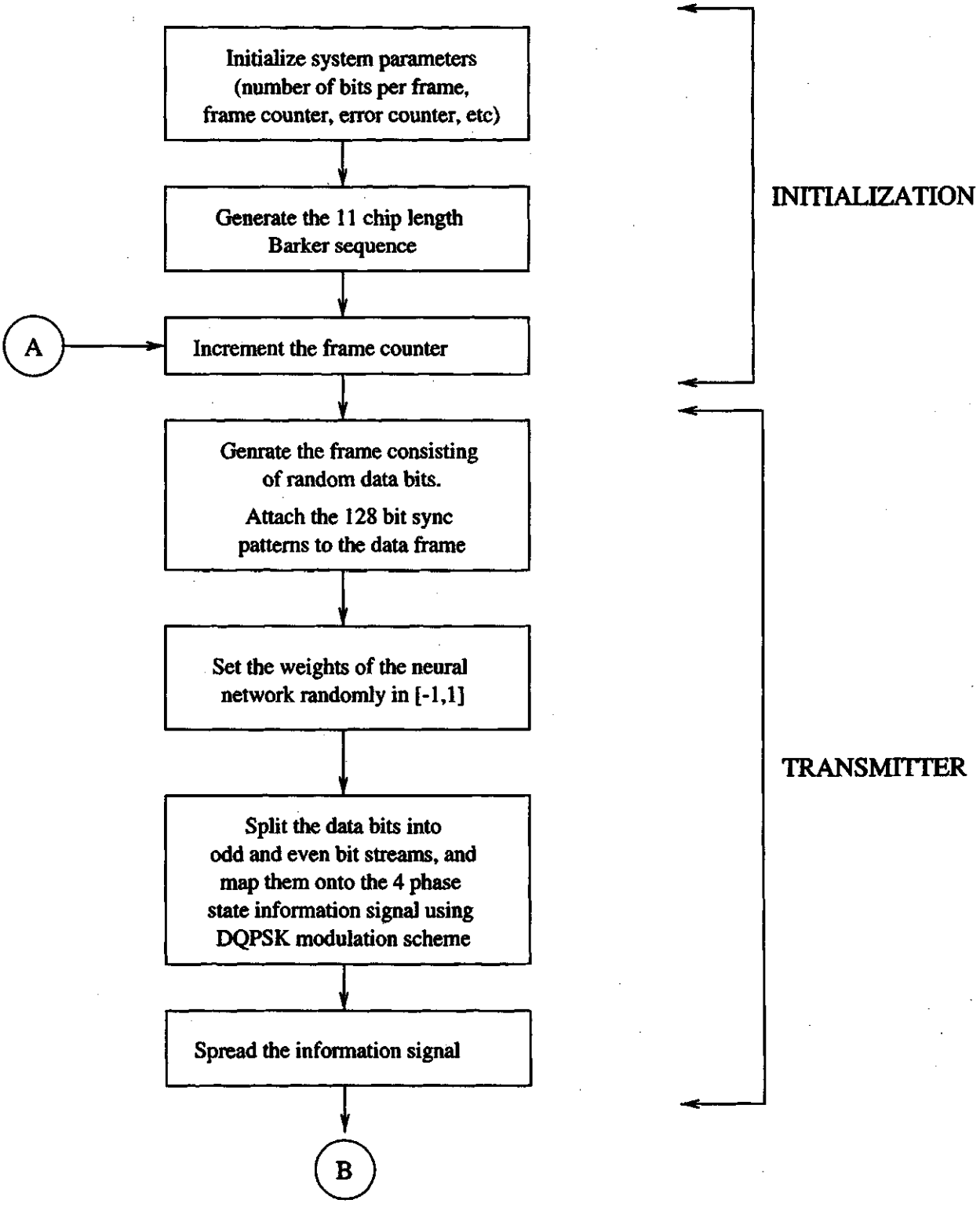

Figure 6.6: Flow chart of the transmitter section of the simulation program for BER performance evaluation of a neural network diversity combiner (NNDC) based receiver

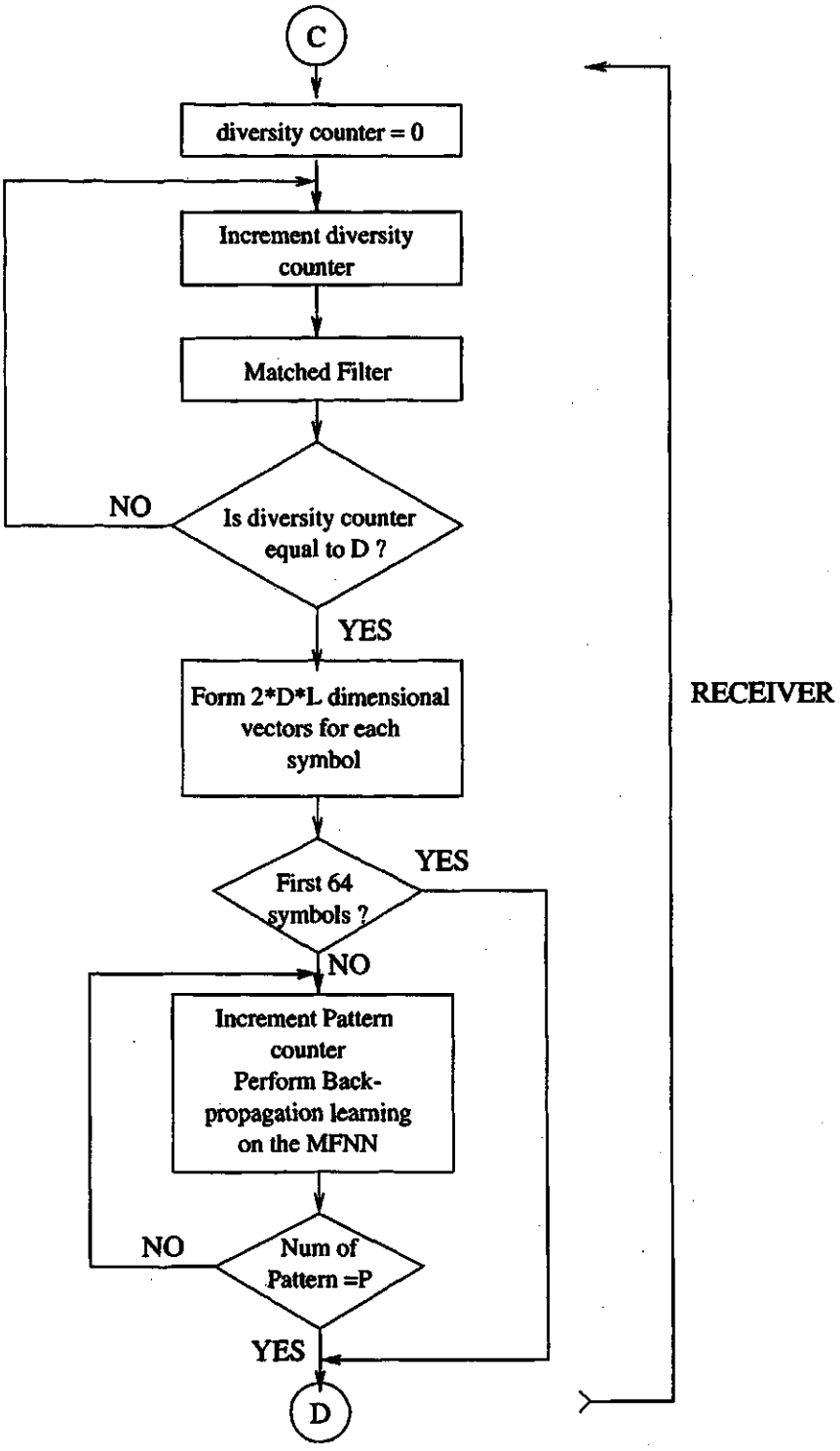

Figure 6.7: Flow chart of the receiver section of the simulation program for BER performance evaluation of NNDC_4D receiver

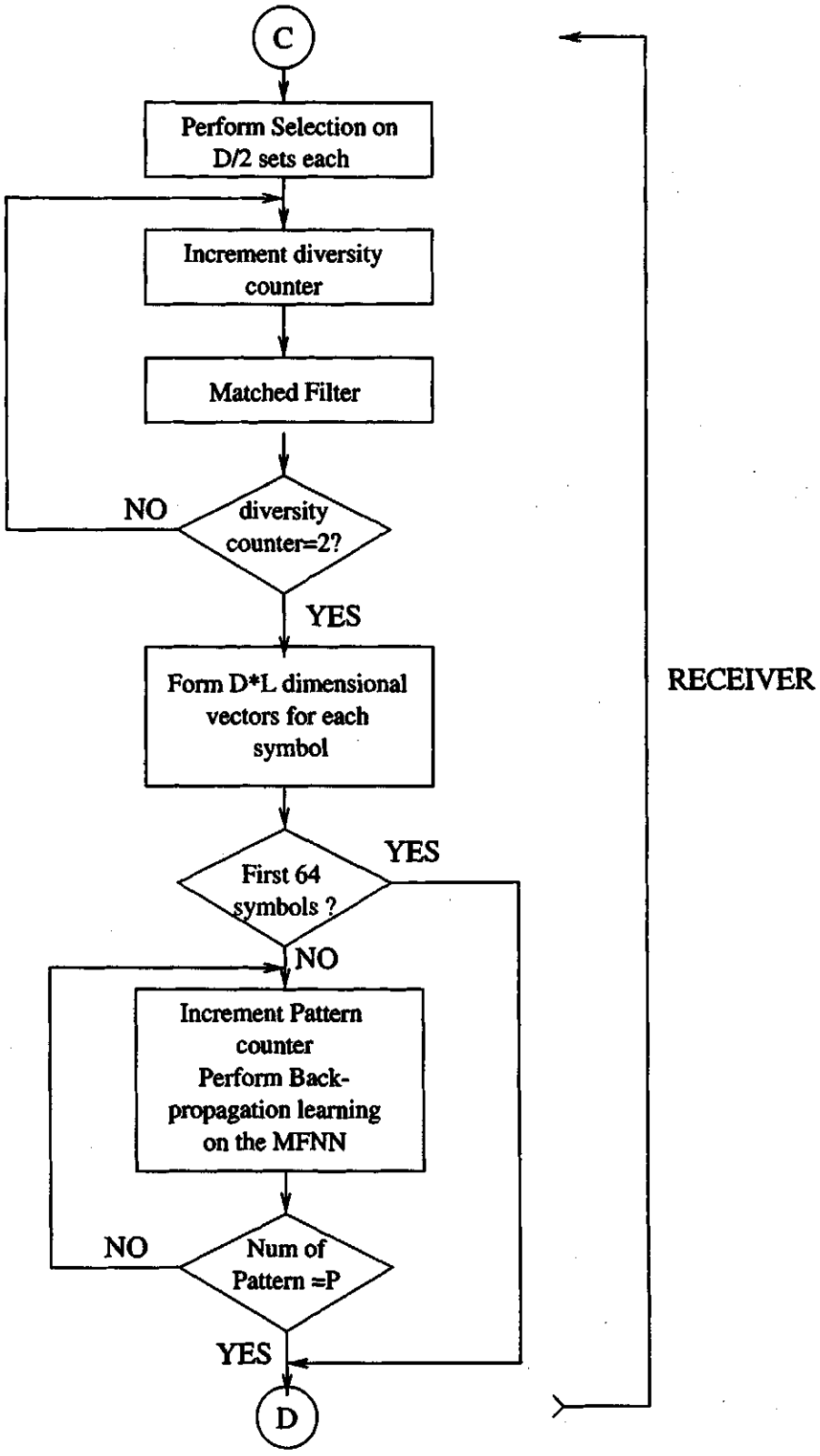

Figure 6.8: Flow chart of the receiver section of the simulation program for BER performance evaluation of NNDC_2DSEL receiver

The demodulator outputs the estimated data bits.

2. **NNDC with dual selection combining (NNDC_2DSEL)**: The flow chart for the simulation of the NNDC with dual selection combining and dual full diversity combining (NNDC_2DSEL), is shown in Figure 6.8. The selection combining is performed on $D/2$ of the diversity branches and hence received signals from two diversity branches are selected for further processing. The two sets of received signal is then passed through a correlator or a RAKE receiver. The despreading in the correlator receiver is done with the spreading code. The L path signals at each of the two matched filter outputs are passed onto the NNDC. The input to the NNDC hence forms a $D \cdot L$ length vector for each transmitted information signal. The NNDC learns the channel conditions during the 128 bit sync patterns in the beginning of a data frame, using the back–propagation algorithm. The 128 bit pattern or the 64 symbol information signal is given to the neural network P number of times. The remaining data frame is then fed to the NNDC and its output is fed to the DQPSK demodulator. The demodulator outputs the estimated data bits.

3. **NNDC with selection combining (NNDC_SEL)**: The flow chart for the simulation of the NNDC with selection combining (NNDC_SEL), is shown in Figure 6.9. The selection combining is performed on the D diversity branches and hence received signals from one of the diversity branch is selected for further processing. The received signal are then passed through a correlator or a RAKE receiver. The despreading in the correlator receiver is done with the spreading code. The L path signals at the matched filter outputs are passed onto the NNDC. The input to the NNDC hence forms a L length vector for each transmitted information signal. The NNDC learns the channel conditions during the 128 bit sync patterns in the beginning of a data frame, using the back–propagation algorithm. The 128 bit pattern or the 64 symbol information signal is given to the neural network P times. The remaining data frame is then fed to the NNDC and its output is fed to the DQPSK demodulator. The demodulator outputs the estimated data bits.

6.3.1 Simulation Studies for NNDC receiver models

The complete indoor wireless LAN was simulated and the BER performance evaluated for the various receiver models with NNDC using Monte Carlo techniques. Importance sampling was not used since performance of the NNDC in effect was being studied with respect to the time–variant random indoor channel, and reduc-

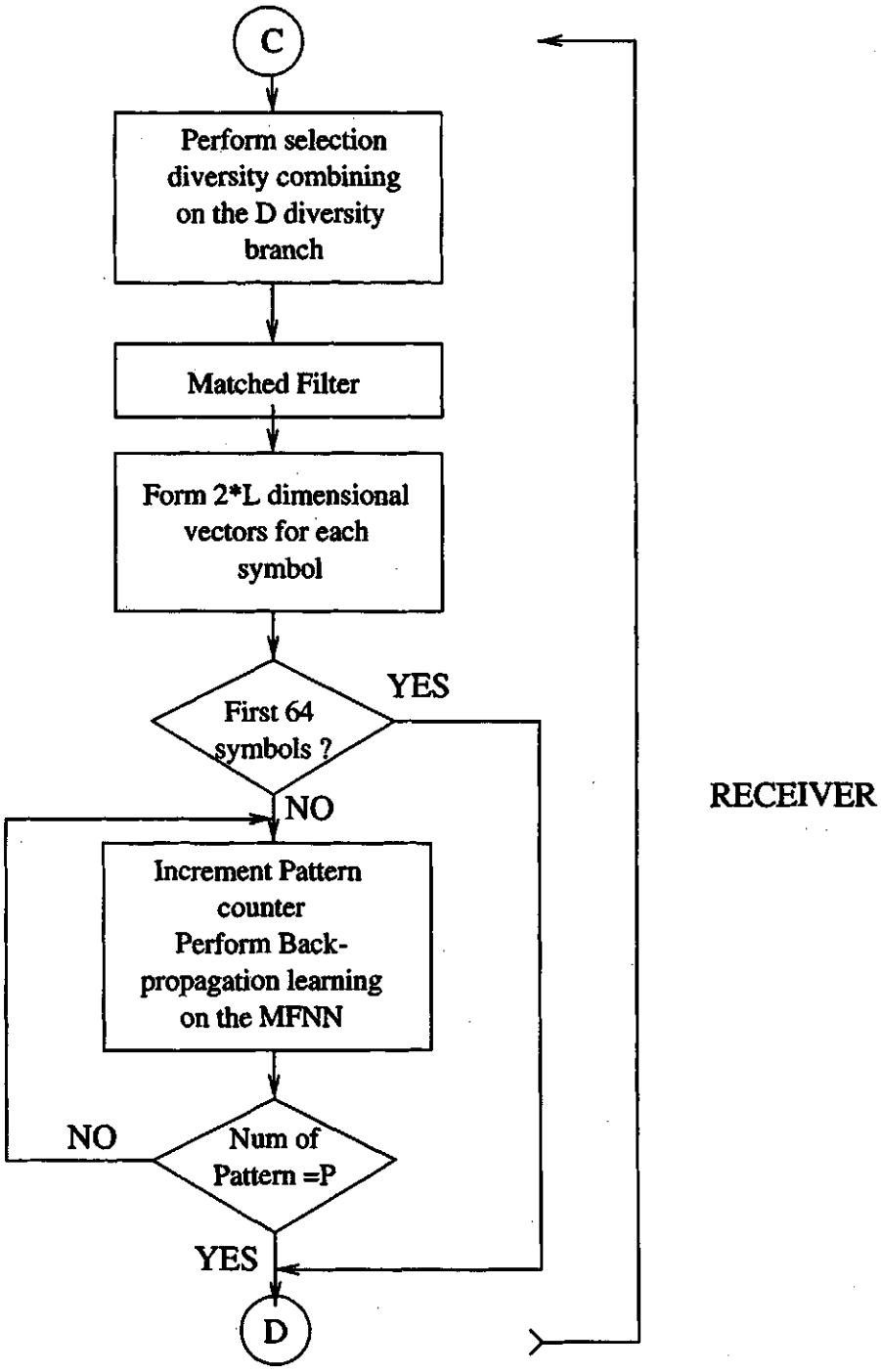

Figure 6.9: Flow chart of the receiver section of the simulation program for BER performance evaluation of NNDC_SEL receiver

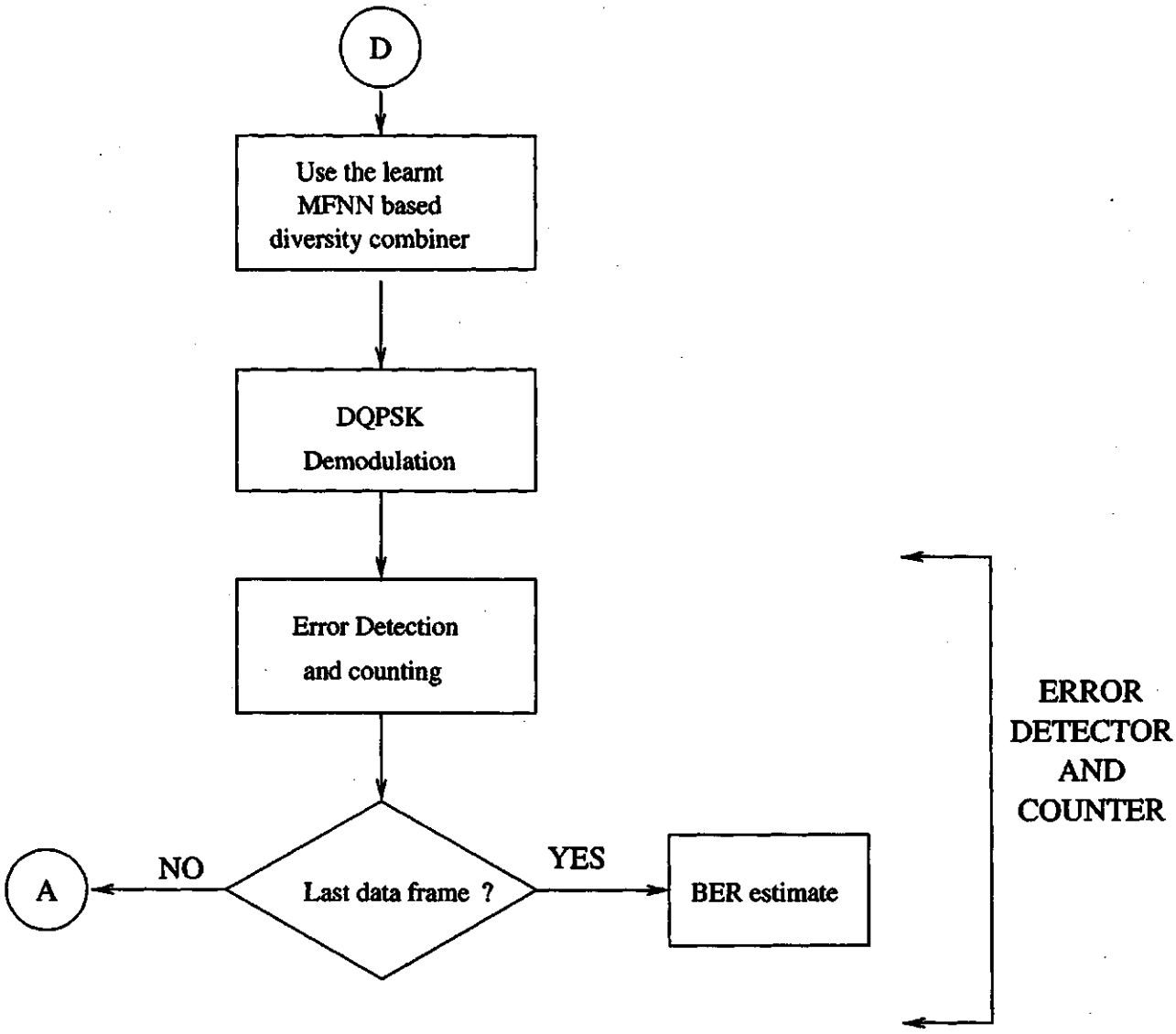

Figure 6.10: Flow chart of the error detection and counting of the simulation program for BER performance evaluation of the various NNDC receiver based wireless modem

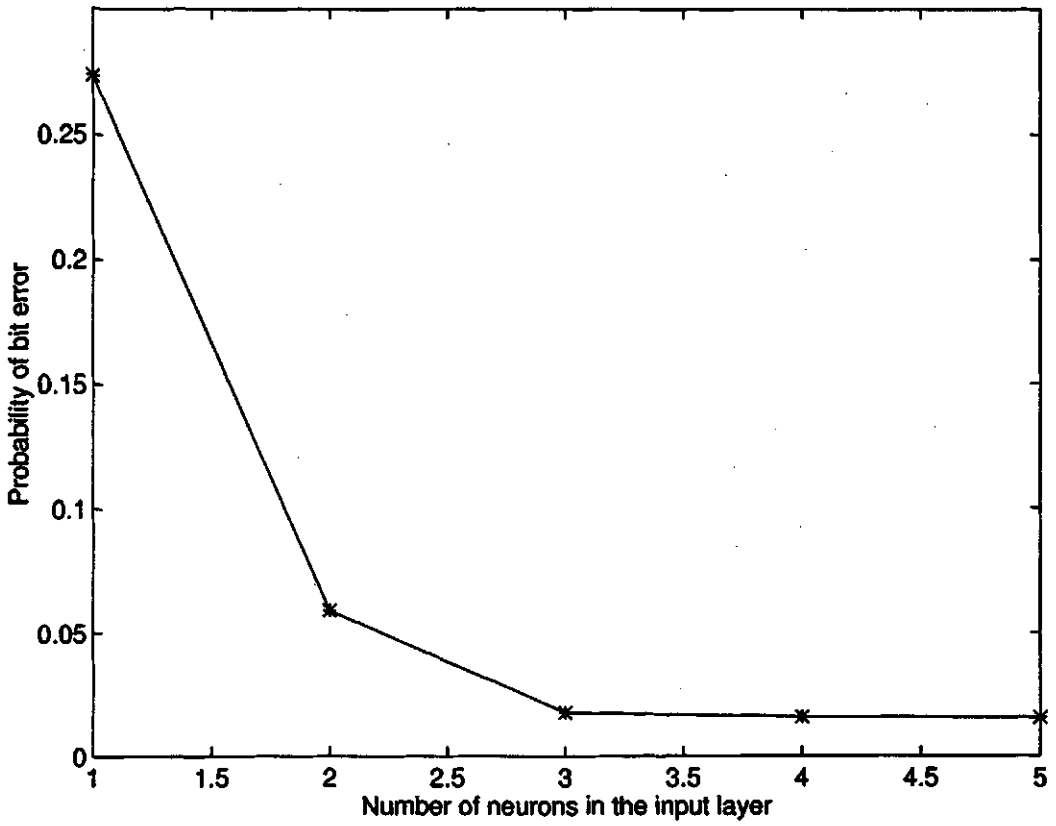

Figure 6.11: Number of neurons required in the input layer of the neural network versus the BER performance of a single branch receiver at an approximate $\frac{E_b}{N_o} = 9.8dB$.

ing the number of packets by using importance sampling will not give an acceptable result from a statistical standpoint. Typically, to obtain a BER p, the symbol size required will be $\frac{10}{p}$. Such a choice will give a BER estimate in the confidence interval $[1.8p, 0.55p]$, at a confidence level of 0.95. In this case, the basic limit will be the minimum symbol size dictated by the BER, p, but to see the effect of NNDC, the number of packets used is 20000. Each packet or data frame is assumed to consist of a 128 bit sync pattern and a 1024 bit data field. In an actual scenario, the MAC level packet varies from 98 bytes to 2410 bytes, excluding the 128 bit sync pattern. 1024 bits for the data field was used for simulation studies because of smaller computational loads, though it was noted that there was no difference in using a 1024 bit data field or a 2410 byte field as far as the BER was concerned.

For each simulation run, the initial SNR was fixed and then modified at the end of the run when averaged after taking the channel path amplitudes into consideration. For each SNR, the simulation was rerun with different initial seeds.

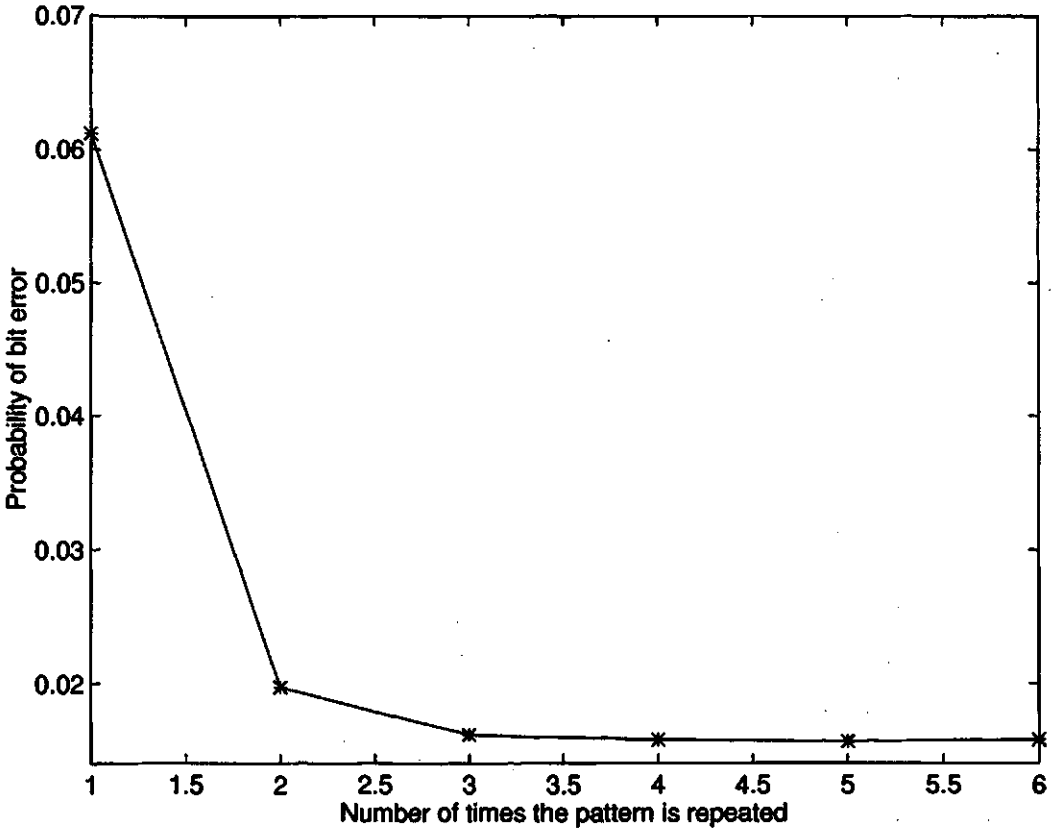

Figure 6.12: Number of times the learning pattern is given to the neural network versus BER performance for a single branch receiver, at an approximate $\frac{E_b}{N_o} = 9.8$ dB

The neural network used in this thesis was a three layer neural network with a input layer, hidden layer and an output layer, as discussed in Chapter 5. One of the major parameters in the design of the neural network is the choice of the number of neurons. Each layer of the neural network has a specific number of neurons. The number of neurons in the output layer is usually chosen as the output dimension. In this case, since a complex output is required, the number of neurons required will be 2. Since there has not been a proper mathematical study on the number of neurons required for a particular application, it is left to the designer to choose from trial and error. Such experiments were performed with the number of neurons as a variable. Experiments showed that the input layer has the most drastic impact on the performance of the neural network. Figure 6.11 shows an experiment with the number of neurons in the input layer for a N:4:2 (N neuron in the input layer, 4 in the hidden layer and 2 in the output layer) versus the BER performance, in the case of a single branch receiver (no diversity reception) with two resolvable paths at an $\frac{E_b}{N_o}$. Figure 6.11 shows that the BER performance decreases exponentially with increase in the number of neurons in the input layer. It can be seen that, for an input of dimension N, it is a good rule of thumb to choose the number of neurons in the input layer as N. Experiments with a N:M:2 neural network, where M is greater than 4 showed no impact on the BER performance even in case of the quad–diversity branch receivers.

The slope λ of the sigmoidal function non–linearity, used in the output stage of each neuron, and the learning gain σ are also important considerations in the design of the neural network. The learning gain specifies the amount of updating used. A larger learning gain will mean faster learning but it could also lead to an overshoot of the global minimum. A smaller learning gain on the other hand is slower in learning but has a better chance of reaching the global minimum. The slope of the sigmoidal function of each neuron and the learning gain can also be updated along with the weights, but could be made constants without much effect on the performance, if chosen properly. Through extensive simulation studies, the learning gain and slope of the sigmoidal functions are made constants. The slope λ was fixed at 0.2 and the learning gain, σ was fixed at 0.8. The output from the non–linearity stage of each neuron was multiplied by a gain equal to 1.2 (fixed empirically).

The initial weights of the neural network for each data frame were chosen according to the uniform distributed random variable, defined in $-1, 1$. The neural network was in the learning mode during the 64 symbol information signal at the start of each data frame. The learning algorithm was the back–propagation algo-

rithm. It was seen that when the 64 symbol information signal is repeated P number of times, the performance of the NNDC improves drastically initially and then slows down. This is shown in Figure 6.12. The number times the patterns is repeated to the neural network was chosen to be 3.

Before using neural network for diversity combining, investigative studies were required to show that such an experiment is worthwhile. The single branch receiver was chosen for such a study. For investigative purposes, the 128 bit sync pattern was chosen to be random, and the data frame was chosen to contain the same information signal (for data bit pattern ...00110011...), with phase state $3\pi/4$. Figure 6.13 and 6.14, shows the output of a NNDC and the output of a OTFDC combiner for SNR 5.7 dB and 8.9 dB, for the same received data frame. Firstly, it can be noted that the outputs of the NNDC are more concentrated toward the actual phase state $3\pi/4$ than the OTFDC. Secondly, the NNDC outputs lead to fewer errors ($*$ outside the phase state boundary) than the OTFDC. The performance of the NNDC is not consistently better than the OTFDC, since that depends on how well the neural network has learnt, but on an average, it does perform marginally better than the OTFDC.

Figure 6.15 shows BER performance of the wireless modem with a single branch receiver using NNDC. This is compared to the performance curve of the OTFDC (for a single branch receiver, obtained analytically and through simulation). The NNDC based system performs consistently better than the OTFDC based system. This could be attributed to the learning ability of the neural network.

Figure 6.16 shows BER performance of the wireless modem with a quad–diversity receiver based on the NNDC_4D model. This is compared to the performance curve of the OTFDC (for quad–diversity reception, obtained through simulation). The NNDC based system performs consistently better than the OTFDC based system, albeit only marginally.

Figure 6.17 shows BER performance of the wireless modem with a quad–diversity receiver based on the NNDC_2DSEL model. This is compared to the BER performance of the wireless modem with a quad–diversity receiver based on the NNDC_4D model. The NNDC_2DSEL model performs poorly than the NNDC_4D model but requires lower complexity and needs lesser computations.

Figure 6.18 shows BER performance of the wireless modem with a quad–diversity receiver based on the NNDC_SEL model. This is compared to the BER performance

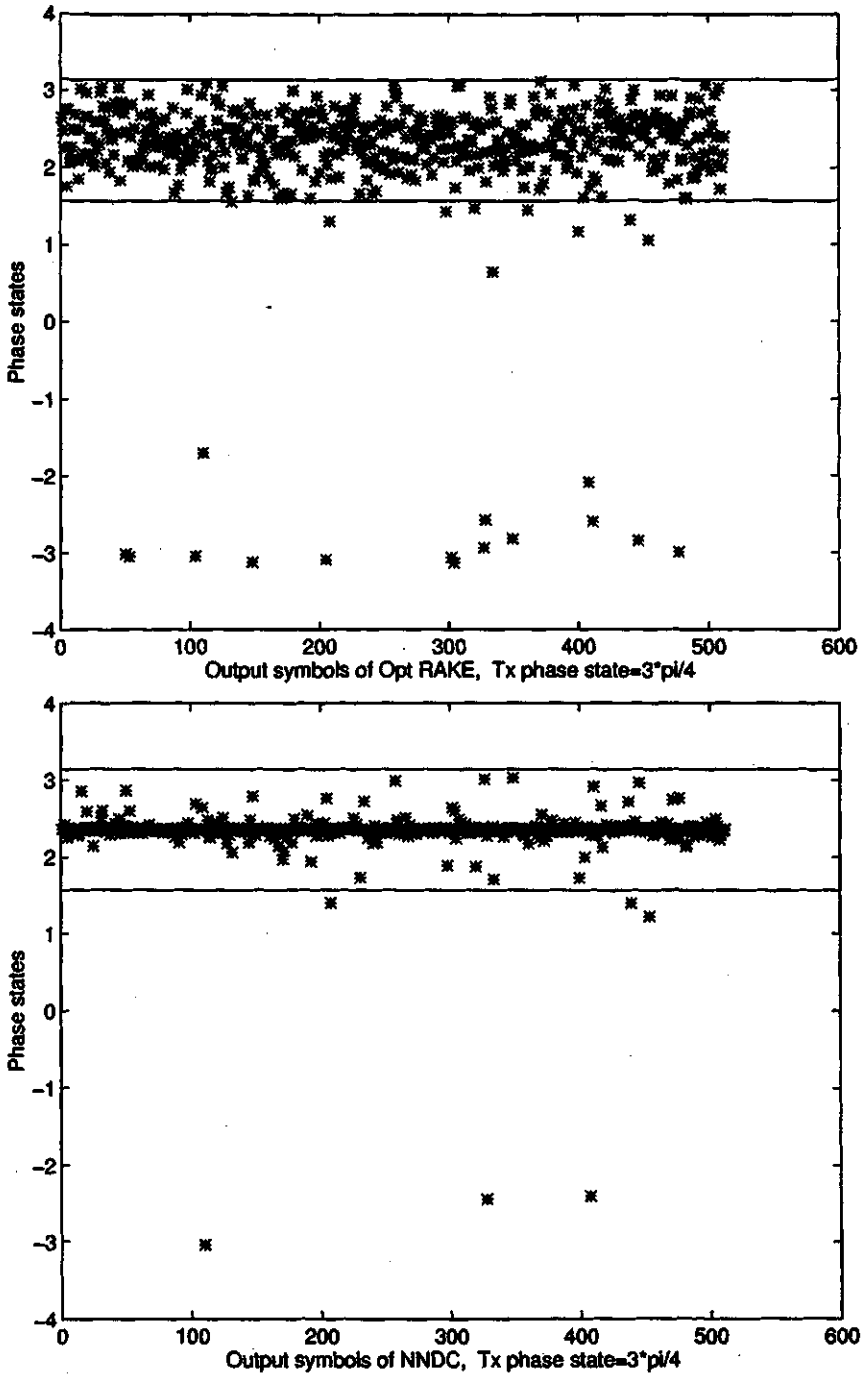

Figure 6.13: Output symbols with phase state $3\pi/4$ for OTFDC (top) and NNDC (bottom) respectively for SNR = 5.7dB

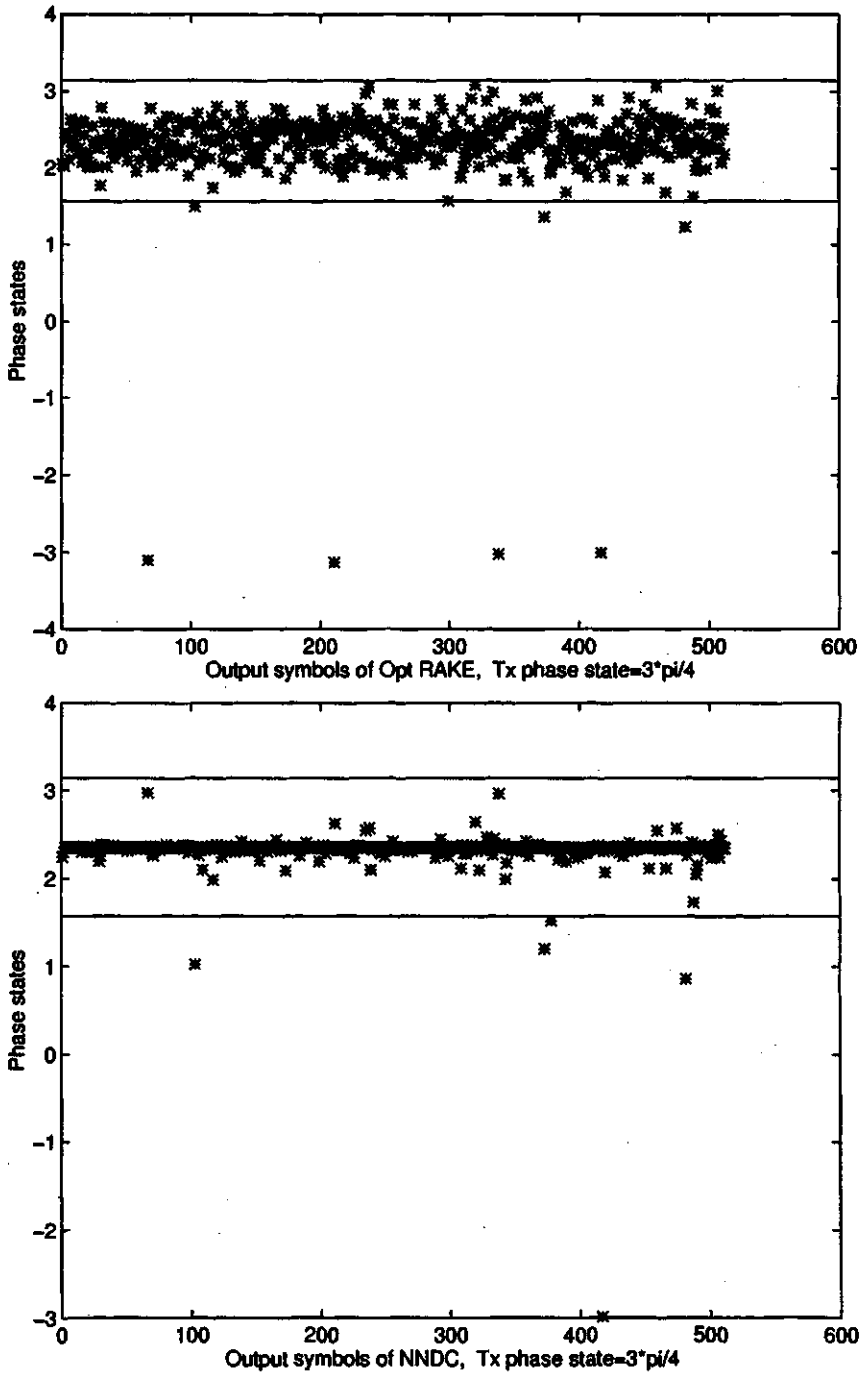

Figure 6.14: Output symbols with phase state $3\pi/4$ for OTFDC (top) and NNDC (bottom) respectively for SNR = 8.9dB

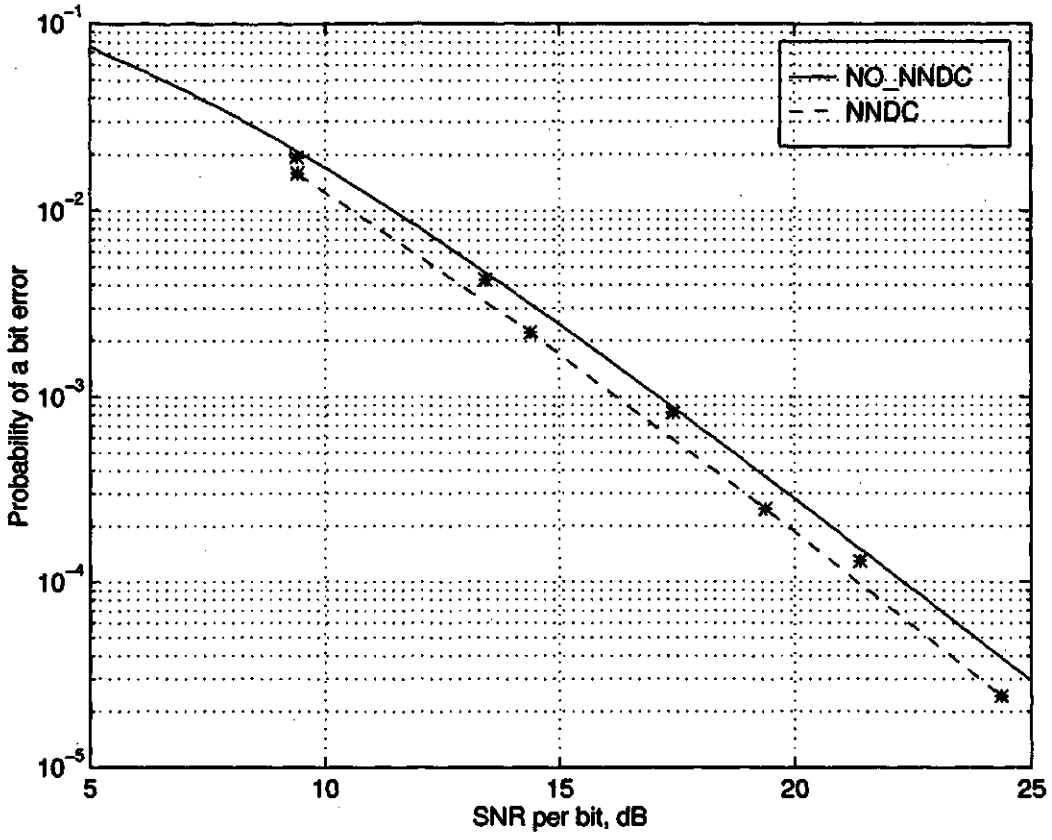

Figure 6.15: BER versus $\frac{E_b}{N_o}$ for a NNDC with single branch receiver compared to the BER performance of the OTFDC. The number of resolvable paths, L was chosen to be 2 and the neural network was used in $4:2:2$ combination

of the wireless modem with a quad–diversity receiver based on the NNDC_4D model. The NNDC_2DSEL model performs poorly than the NNDC_4D model but requires significantly lower complexity and needs lesser computations. The complexity of the NNDC_SEL model is the lowest among the three receiver models discussed.

Figure 6.19 shows the comparision of the various NNDC based receiver models against the OTFDC. It can be seen the NNDC_4D performs the best followed by NNDC_2DSEL and then NNDC_SEL.

6.4 Summary

The design of the NNDC was discussed with respect to the number of neurons required in the input layer, the number of times the learning pattern should be repeated, the learning gain and the slope of the sigmoidal function were discussed.

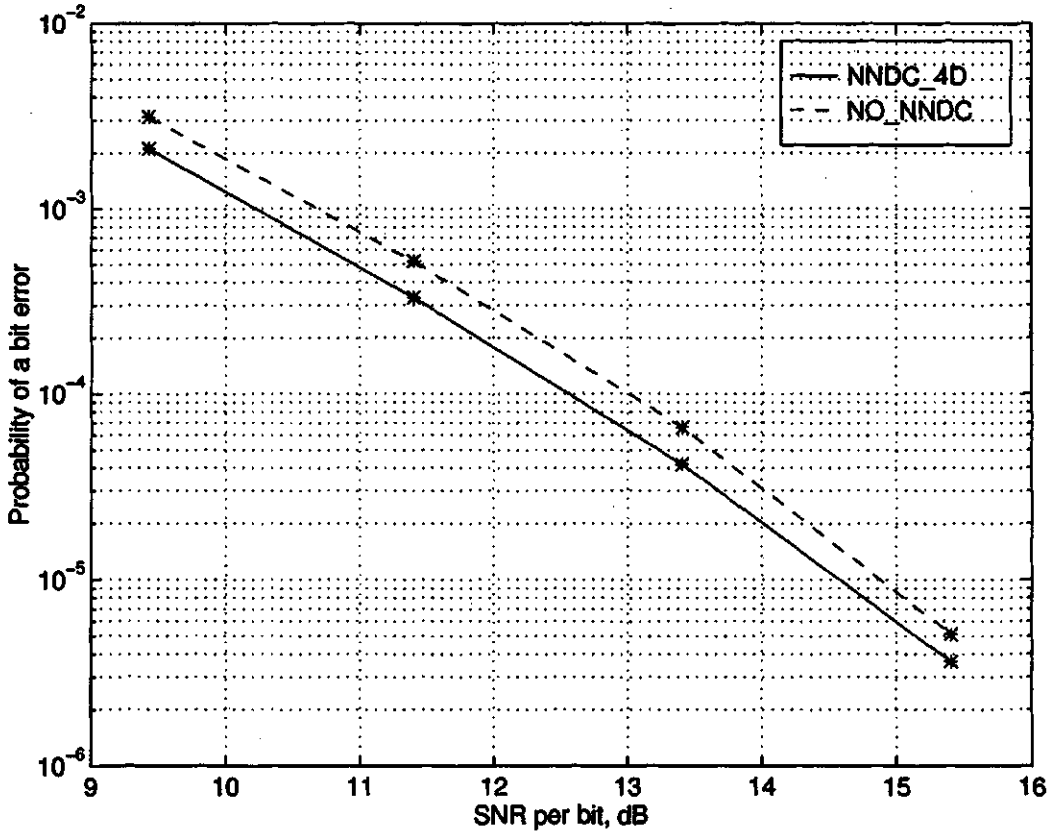

Figure 6.16: BER versus $\frac{E_b}{N_o}$ for a NNDC with quad–diversity branch receiver based on the NNDC_4D model, compared to the BER performance of the quad–diversity branch receiver based on OTFDC (obtained through simulation). The number of resolvable paths L was chosen to be 2 and the neural network was used in $16:4:2$ combination

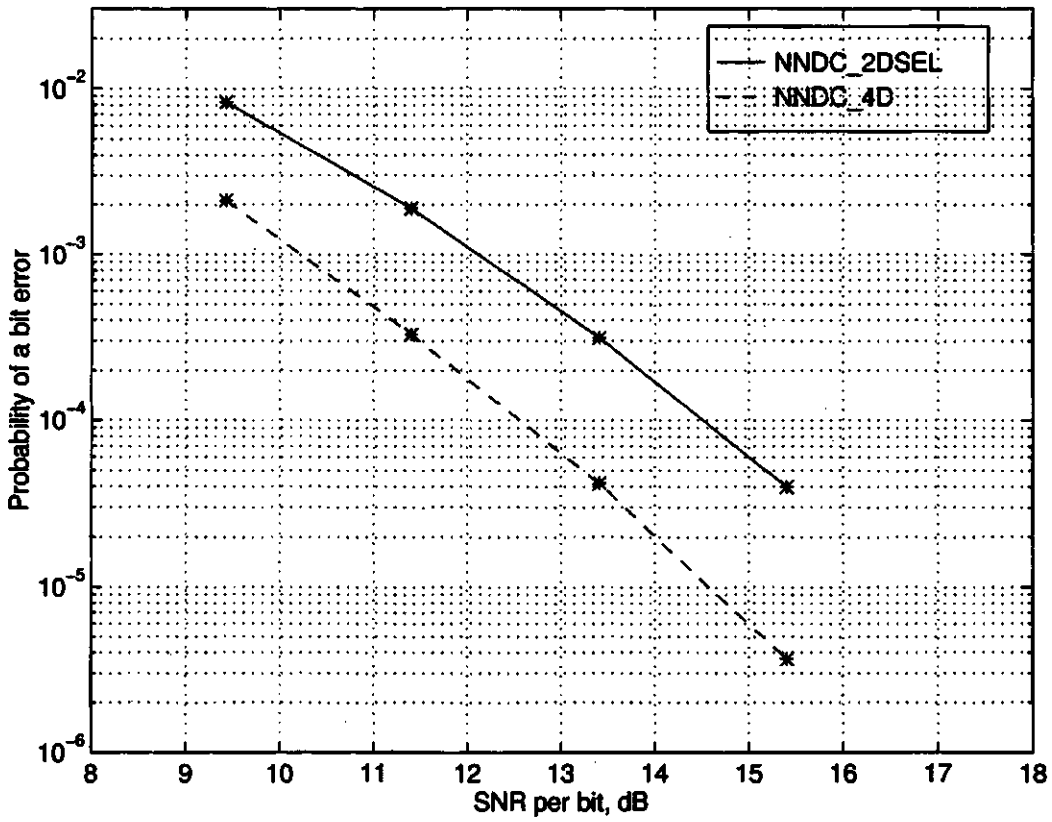

Figure 6.17: BER versus $\frac{E_b}{N_o}$ for a NNDC with quad–diversity branch receiver based on the NNDC_2DSEL model, compared to the BER performance of the quad–diversity branch receiver based on the NNDC_4D model. The number of resolvable paths L was chosen to be 2 and the neural network was used in $8:4:2$ combination

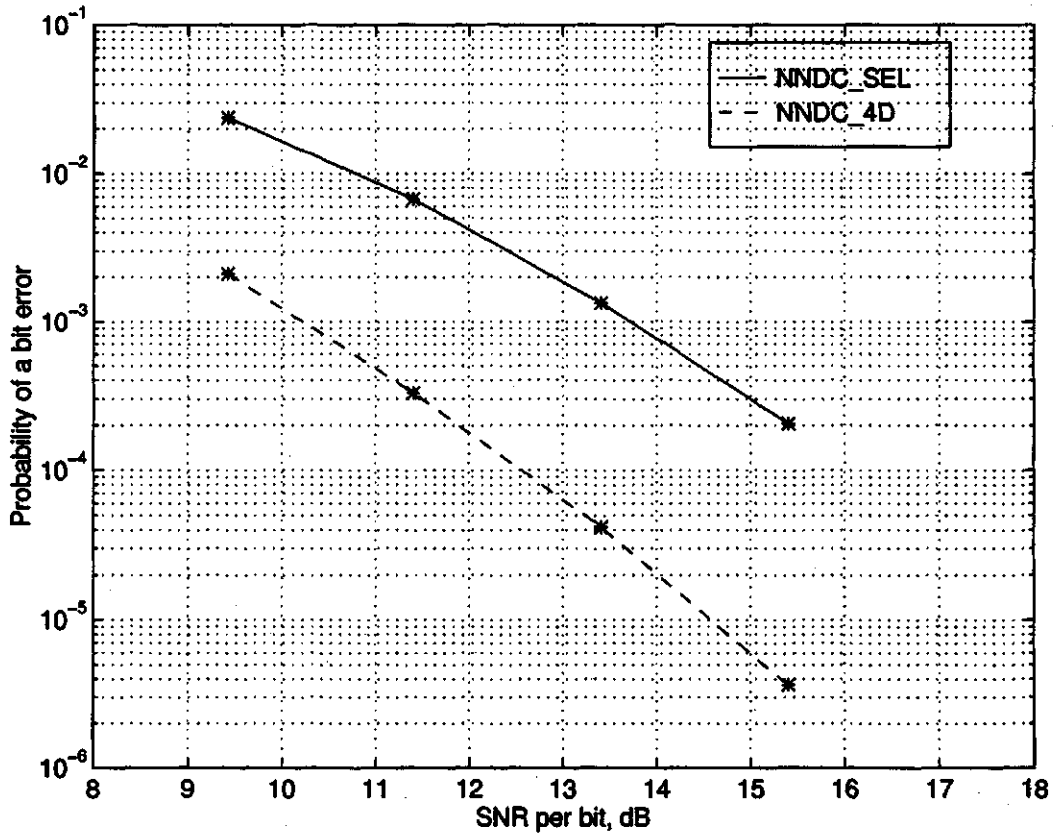

Figure 6.18: BER versus $\frac{E_b}{N_o}$ for a NNDC with quad–diversity branch receiver based on the NNDC_SEL model, compared to the BER performance of the quad–diversity branch receiver based on the NNDC_4D model. The number of resolvable paths L was chosen to be 2 and the neural network was used in $4:4:2$ combination

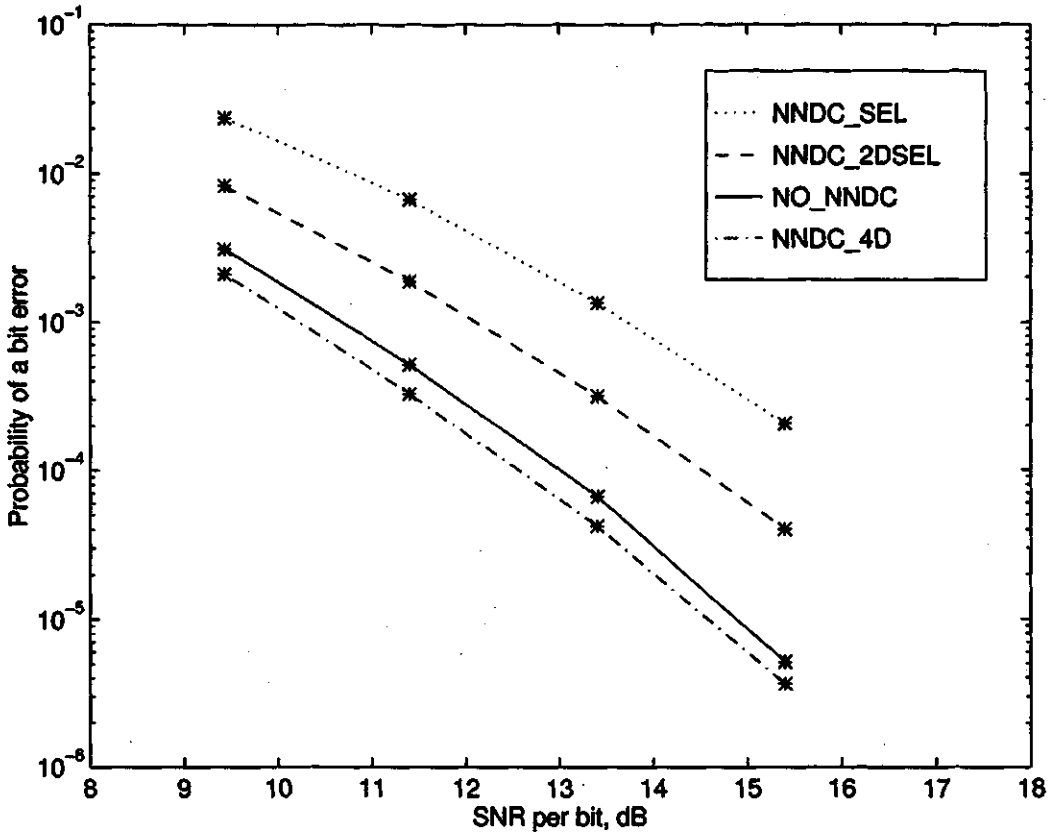

Figure 6.19: The BER versus $\frac{E_b}{N_o}$ for all the receiver models, NNDC_4D, NNDC_2DSEL, NNDC_SEL and NO_NNDC (OTFDC) for a quad-diversity branch receiver is compared. L =2.

Preliminary investigations on NNDC showed that it could work marginally better than the OTFDC. The BER performance of the OTFDC and the various NNDC based receiver models described in Chapter 5 were evaluated for a quad-diversity branch receiver. Simulation results show that the NNDC_4D works marginally better than the OTFDC for a quad-diversity branch receiver. The other two receiver models perform poorer, with the NNDC_SEL having the lowest performance.

Chapter 7

Summary and Future Research

7.1 Summary

The following objectives of the research work were stated in Chapter 1:

1. To study and investigate diversity reception which will improve the bit error rate performance of the wireless modem in a deleterious indoor channel.

2. To study and investigate the use of multilayer feed–forward neural network (MFNN) as a diversity combiner and compare it with the optimal transversal filter diversity combiner.

The wireless LAN was discussed in detail in Chapter 2. The IEEE 802.11 standards were reviewed for both the MAC layer and the physical layer. The overall functioning of the wireless LAN was discussed in brief to stress the differences which separate wireless and wired LANs. The specifications for a direct sequence spread spectrum based wireless modem for operation in 2.4 GHz range was discussed. The design of the wireless modem was considered in Chapter 4 after discussing the various constituents of the design in Chapter 3. A detailed study of the indoor channel in the 2.4 GHz ISM band was done, since it impacts the design of the receiver. A theoretical analysis of the wireless modem based on the optimal transversal filter diversity combiner (OTFDC) was performed to get a close form equation of the probability of bit error. This formed the goal that a practical diversity combiner receiver proposed in this thesis will be evaluated against.

Diversity reception was considered in Chapter 5, which take advantage of improved signal statistics by relying on the availability of two or more independently fading signals which have comparable mean signal levels. Of the various diversity techinques considered, space and polarization diversity were considered for the design. A quad–diversity reception technique based on both space and polarization

was proposed to improve signal reception in the deleterious indoor channel. The antenna system needed to achieve uncorrelated received signals was discussed.

A novel diversity combiner based on the multilayer feed-forward neural network was discussed in Chapter 5. The 128 bit synchronisation pattern was considered as the learning pattern for the neural network diversity combiner (NNDC). The 128 bit synchronisation pattern is present in the beginning of every packet sent on the network and hence is ideal for use by the neural network to learn the channel conditions. The design of the NNDC was considered and optimised for the wireless modem, by the choice of learning gain, slope of the sigmoidal function, number of neurons required in each of the layer, and the number of times the learning pattern is to be used. The neural network based diversity combiner was applied on the various quad–diversity branch receiver models discussed is Chapter 5 and the BER performance evaluation of these systems were evaluated in Chapter 6. The neural network diversity combiner with full diversity combining (NNDC_4D) system was shown to perform best among the three but is computationally expensive and of high complexity. The neural network diversity combiner with selection combining (NNDC_SEL) is lesser in complexity and has lower computational requirement.

7.2 Future Research

This thesis considered the design of the 2 Mbits/sec wireless LAN device using the direct sequence spread spectrum technology under the IEEE 802.11 standard. A quad-diversity technique was proposed using space and polarization. A multilayer feedforward neural network was used as the diversity combiner to combine both the multipath and the quad-diversity signals.

The neural network based diversity combiner proposed in this thesis involves a large number of neurons and hence is computationally expensive. Recurrent or dynamic neural network are known to require fewer number of neurons and fewer number of layers to achieve the same performance of a feedforward neural network. This is because of the additional feedback path associated with each of the neurons. A lower number of neurons will mean that the implementation of the receiver will be less complex and will require fewer computations to implement. This work can be extended to use dynamic neural networks.

References

[1] Victor O.K. Li and Xiaoxin Qiu, "Personal Communication Systems," *Procs. of IEEE*, 83(9):1210–1243, September 1995.

[2] P802.11 IEEE Draft Standard for Wireless LAN Medium Access Control (MAC) and Physical Layer (PHY) Specifications, IEEE Standards Department, 445 Hoes Lane, P.O. Box 1331, Piscataway, NJ, July 1995.

[3] A. Acampora and J. Winter, "A Wireless Network for Wide-band Indoor Communications," *IEEE J. Selected Areas Commun.*, SAC-5(5):796–805, June 1982.

[4] P.A.Jefford A.M.D.Turkmani, A.A.Arowojolu and C.J.Kellet, "An Experimental Evaluation of the Performance of Two-branch Space and Polarization Diversity Schemes at 1800 MHz," *IEEE Transactions on Vehicular Technology*, 44(2):318–326, May 1995.

[5] Kirupairaj Asirvatham and Nikhil Deshpande, "Communication Channel Equalization using Neural Network," Project for ME898.3, University of Saskatchewan, 1995.

[6] David F. Bantz and Frederic J. Bauchot, "Wireless LAN Design Alternatives," *IEEE Network*, pages 43–53, March 1994.

[7] K. E. Feher, *Advanced Digital Communications: Systems and Signal Processing Techniques*, Englewood Cliffs, New Jersey: Prentice Hall, 1987.

[8] D.G. Brennan, "Linear Diversity Combining Techniques," *Proc. IRE*, 47:957–1000, June 1959.

[9] Jr. Britton Sanderford, "New Markets Emerge as PCN Reduces Wireless Link Costs," *IEEE Communications Magazine*, pages 28–32, June 1992.

[10] K. Bronson, G. Pahlavan and H. Rotithor, "Performance Evaluation of Wireless LANs in the Indoor Environment," *Proceedings. 18th Conference on Local Computer Networks*, pages 452–60, 1993.

[11] Kwang-Cheng Chen, "Medium Access Control of Wireless LAN for Mobile Computing," *IEEE Network*, pages 50–63, September 1994.

[12] R.H. Clarke, "A Statistical Theory of Mobile Radio Reception," *Bell Syst. Tech. Jr*, 47:957–1000, July/Aug 1968.

[13] William C.Y.Lee and Yu S. Yeh, "Polarization Diversity System for Mobile Radio," *IEEE Transactions on Communications*, COM-20(5):912–922, October 1972.

[14] Mark Taylor Dale Buchholz, Paul Odlyzko and Richard White, "Wireless In-building Network Architecture and Protocols," *IEEE Network Magazine*, pages 31–38, November 1991.

[15] A.F. de Toledo and A.M.D. Turkmani, "Propagation into and Within Buildings at 900, 1800 and 2300 MHz," *IEEE*, pages 633–636, 1992.

[16] J.F. Lemieux; M.S. El-Tanany; and H.M. Hafez, "Experimental Evaluation of Space/Frequency/Polarization Diversity in the Indoor Wireless Channel," *IEEE Trans. Vehic. Technol.*, 40(3):569–574, 1991.

[17] S. R. Todd; M.S. El-Tanany and S.A. Mahmoud, "Space and Frequency Diversity Measurements of the 1.7 GHz Indoor Radio Channel using a Four-branch Receiver," *IEEE trans. Vehic. Technol.,*, 41(3):312–320, August 1991.

[18] K. Guo, Y.; Feher, "Modem/Radio IC Architectures for ISM Band Wireless Applications," *IEEE Transactions on Consumer Electronics*, 39(2):100–6, May 1993.

[19] Homayoun Hashemi, "The Indoor Radio Propagation Channel," *Proceedings of the IEEE*, 81(7):943–968, July 1993.

[20] M. Kavehrad and P. J. McLane, "Performance of Low-complexity Channel Coding and Diversity for Spread Spectrum in Indoor, Wireless Communications," *AT&T Technical Journal*, 64:1927–1965, October 1985.

[21] M. Kavehrad and P.J.Maclane, "Direct Sequence Spread Spectrum with DPSK Modulation and Diversity for Indoor Wireless Communication," *IEEE Trans. Commun.*, COM-35:224–236, February 1987.

[22] W.C.Y. Lee, "Antenna Spacing Requirements for a Mobile Radio Base Station Diversity," *Bell Syst. Tech. Jr.*, 50:1859–76, July/Aug 1971.

[23] James E. Mitzlaff, "Radio Propagation and Anti-multipath Techniques in the WIN Environment," *IEEE Network Magazine*, pages 21–26, 1991.

[24] H. Zaghbul; M. Fattouche; G. Morrison and D. Tholl, "Comparision of Indoor Propagation Channel Characteristics at Different Frequencies," *Electronics Letters*, 27(22):2077–9, October 1991.

[25] R. Price, "The Detection of Signals Perturbed by Scatter and Noise," *IRE Trans. Information Theory*, PGIT-4:163–170, September 1954.

[26] John G. Proakis, *Digital Communications.*, McGraw-Hill International Editions, 1989.

[27] Lawrence B. Milstein Raymond L. Pickholtz and Donald L. Schiling, "Spread Spectrum for Mobile Communications," *IEEE Transactions on Vehicular Technology*, 40(2):313–321, May 1991.

[28] Adel A.M. Saleh and Reinaldo A. Valenzuela, "A Statistical Model for Indoor Multipath Propagation," *IEEE Journal on Selected Areas in Communications*, SAC-5(2):128–137, February 1987.

[29] Kikuo Tsunoda Tokio Taga and Hiroyuki Imahori, "Correlation Properties of Antenna Diversity in Indoor Mobile Communication Environments," *IEEE*, pages 446–451, 1989.

[30] Bruce Tuch, "Development of WaveLAN an ISM Band Wireless LAN," *AT&T Technical Joural*, pages 27–37, July 1993.

[31] G. L. Turin, "Introduction to Spread Spectrum Antimultipath Techniques and their Application to Urban Digital Radio," *Proc. IEEE*, 68(3):328–353, March 1980.

[32] Rodney G. Vaughan, "Polarization Diversity in Mobile Communications," *IEEE Transaction on Vehicular Technology*, 39(3):177–186, August 1990.

[33] Rodney G. Vaughan and J. Bach Andersen, "Antenna Diversity in Mobile Communications," *IEEE Transactions on Vehicular Technology*, VT-36(4):149–172, November 1987.

[34] Jr. W.C.Jakes, "A Comparision of Specific Space Diversity Techniques for Reduction of Fast Fading in UHF Mobile Radio Systems," *IEEE Trans. Vehic. Tech.*, VT-20:81–92, November 1971.

[35] T.A. Wilkinson and S.K.Barton, "Receiver Techniques for Direct Sequence Spread Spectrum ISM Band Radio LANs," *IEEE*, pages 376–380, 1994.

[36] Wolfgang H. Gerstacker, Ralf R. Muller, and Johannes B. Huber, "Iterative Equalization with Adaptive Soft Feedback," *IEEE Trans. on Communicatipons*, 48(9):1462–1466, September 2000.

[37] P. R. Chang, and J. T. Hu, "Narrow-Band Interference Suppression in Spread–Spectrum CDMA Communications Using Pipelined Recurrent Neural Networks," *IEEE Trans. on Vehicular Technology*, 48(2):467–478, March 1999.

[38] G. Kechriotis, E. Zervas, and E. S. Manolakis, "Using Recurrent Neural Networks for Adaptive Communication Channel Equalization," *IEEE Trans. on Neural Networks*, 2(5):267–278, March 1994.

[39] S. E. El-khamy and H. M. Abdou, "Neural Network Matched Filter Receivers for CDMA Systems," *IEEE Fourth International Symposium on Spread Spectrum Techniques and Applications, ISSTA '96 Mainz, Germany*, September 1996.

[40] U. Mitra and H. V. Poor, "Neural Network Techniques for Adaptive Multiuser Demodulation," *IEEE J. Selected Areas in Communications*, 12(9):1460–1470, December 1994.

[41] Jacek M. Zurada, *Artificial Neural Systems*, West Publishing Company, 1992.

[42] Ning Zhang and S. W. Golomb, Sixty-phase generalized barker sequences, *IEEE Transactions on Information Theory*, 35(4), July 1989.

[43] R. L. Pickholtz; D. L. Schilling; and L. B. Milstein. Theory of spread spectrum communications - atutorial,. *IEEE Transactions on Communications*, COM-30(5):855–884, May 1982